CONTROLS ON THE ACCUMULATION OF HYDROCARBONS IN THE LOWER BRUSHY CANYON FORMATION, SOUTHEASTERN NEW MEXICO

by

Jason Lennane, B.S.

Submitted in Partial Fulfillment

of the Requirements for the Degree of

Masters of Science in Geology

Department of Earth and Environmental Sciences

New Mexico Institute of Mining and Technology

Socorro, New Mexico

December, 2002

ABSTRACT

The lower Brushy Canyon Formation (LBC) of southeastern New Mexico consists of fine- grained clastic material deposited by turbidity currents during sea level lowstands in the Delaware Basin. Hydrocarbon production from the LBC is often unpredictable and well logs offer little assurance of pay.

Detailed descriptions of several cores taken from the LBC show a very fine-grained siltstone, which is dominated by finely interbedded organic shale turbidities. The producing intervals are generally thicker, cleaner siltstones. Non-producing siltstones are generally darker in color indicating a high clay content. Further petrographic analysis of both producing and non-producing sandstones confirm observations from the core. The non-producing siltstones contain high amounts of clay and calcite cement. These components fill pore space and increase pore entry pressures, thereby reducing the ability of the rock to transmit hydrocarbons. The producing siltstones are generally clean with very low amounts of clay or calcite cement. Porosity in these productive rocks is very high and pores are interconnected. Further research shows that it is possible to calculate the amount of clay in a siltstone from the LBC based on its gamma ray curve. Clay content of sandstones can then be quantitatively mapped at the reservoir level and at the basinal level. This technique will help identify unproduced reservoirs as well as better explain current reservoirs and traps.

ACKNOWLEDGEMENTS

This study is part of a larger project that is funded by the Department of Energy: Risk Reduction with a Fuzzy Expert Tool (DE-AC-26-99BC15218). I would like to thank the New Mexico Bureau of Geology and Mineral Resources, for its records, cores and other resources. Thank you to Caprock Laboratories for the thin section preparation.

Thank you to my committee, Ron Broadhead, Dr. Peter Mozley, and Dr. Bruce Harrison for their guidance and assistance for the past two years. I would also like to than all of my family and friends who had the patience to stick with me through this time. Most importantly I would like to thank my parents Joe Lennane, Brenda Thigpen, Ruth Arnone, Jack Arnone, and of course my lovely wife Linda D. Lennane. I would also like to thank my grandma Fran for all of her support through the last 24 years.

TABLE OF CONTENTS

LIST OF FIGURES

LIST OF TABLES

1.0 INTRODUCTION

The lower Brushy Canyon Formation of southeastern New Mexico is a lowstand turbidite unit that was deposited during the Late Permian in the Delaware Basin (Beauboueff et al., 1999). The turbidites consist of siltstones and black shales. Hydrocarbon production from the lower Brushy Canyon is predominately oil, however some gas associated production exists as well. Previous workers have shown that hydrocarbon production in the lower Brushy Canyon is generally poor and reservoir tests often show little sign of economic pay. However, certain limited areas within the lower Brushy Canyon produce economic quantities of hydrocarbons. The greatest oil producing areas lie in the central and eastern parts of the basin, whereas the western areas tend to have very little production (Justman, 2001). Due to the high risk of drilling exploratory wells that target economic quantities of hydrocarbons within the Brushy Canyon, the majority of the production has come from secondary completions. The hydrocarbon system of the Brushy Canyon is poorly understood; therefore, production companies often overlook potentially economic plays. The goals of this research are to: (1) identify those areas likely to produce economic amounts of hydrocarbons, and (2) determine the factors that control the accumulation of hydrocarbons in the lower Brushy Canyon.

In order to attain these goals, a combination of well logs, cross-sections, mapping and thin section petrography was used to define productive areas.

1.1 GEOLOGIC SETTING

The Delaware Basin, located in southeastern New Mexico and western Texas, occupies the western portion of the Permian Basin. Basement uplifts, including the Marathon Fold and Thrust Belt, the Diablo Platform, and the Central Basin Platform bound the Delaware Basin on three sides. The Northwestern Shelf, which is a constructional feature, bounds the north side of the basin (Fig. 1.1). Within the Delaware Basin the Delaware Mountain Group (Guadalupian) was deposited over mostly Pennsylvanian structures. This group is composed of (ascending): the Brushy Canyon, the Cherry Canyon, and the Bell Canyon Formations (Montgomery et al., 1999). The Brushy Canyon Formation, at the base of the Delaware Mountain Group is composed of siltstones and sandstones that are believed to have been deposited by density and or turbidity flows (Harms and Brady, 1996). This formation is generally separated into three units, the upper, middle, and lower. The lower unit produces the most hydrocarbons and is the focus of this research. The Brushy Canyon is bounded by basinal sand and siltstones above, and below by the carbonates and siliciclastics of the Bone Spring Formation (Broadhead and Justman, 2000; Downing and Mazzullo, 2000).

1.2 BRUSHY CANYON DEPOSITION

The depositional environment of the Brushy Canyon Formation is not known with certainty. Harms and Brady (1996) reviewed several contrasting hypotheses. Deposition in a shallow water environment was first proposed by King (1948). This hypothesis was short lived because of negative evidence including the lack of biogenic structures, the lack of shoreline deposits, and the lowstand transition to carbonate facies along the

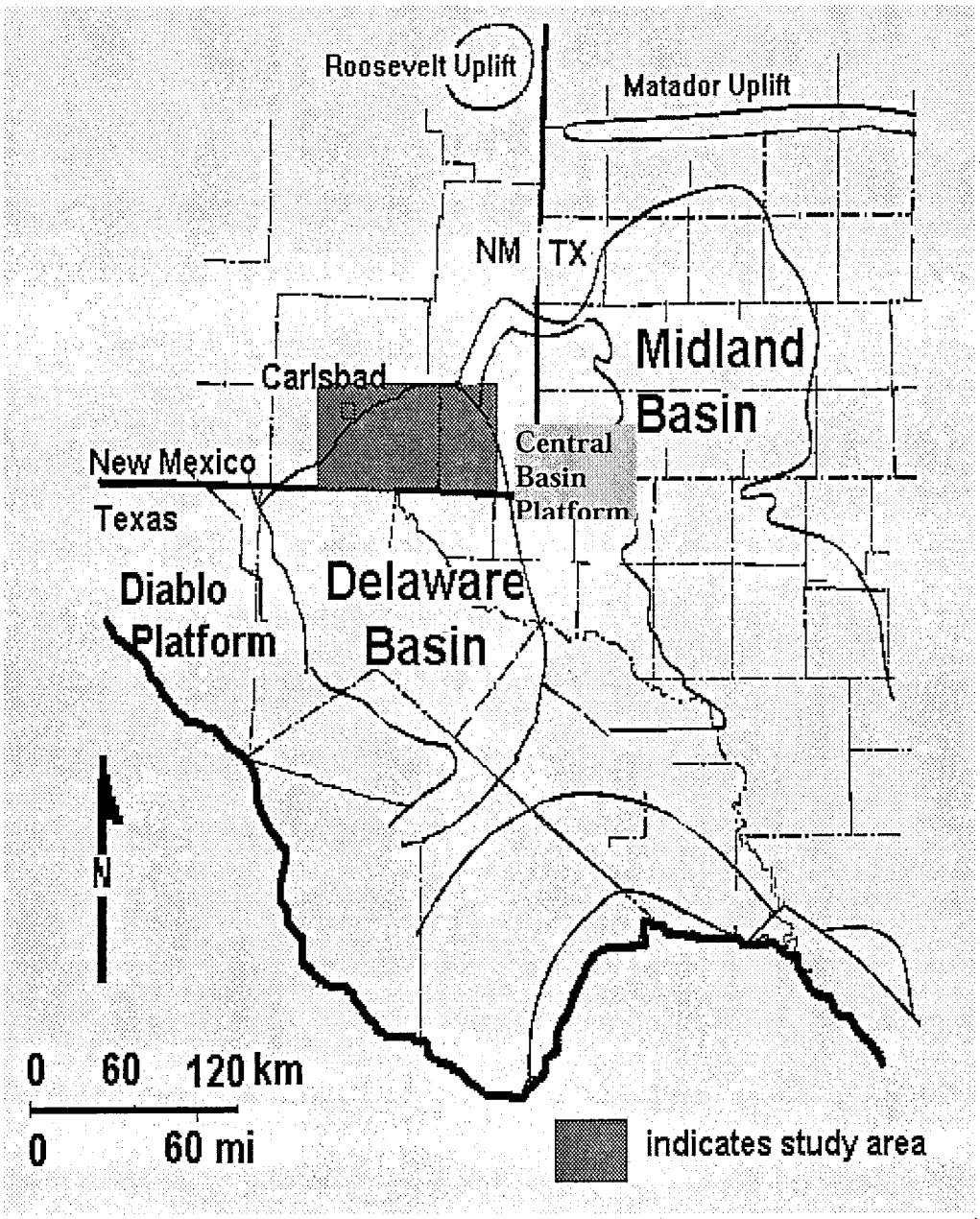

Figure 1.1: Map of Delaware Basin. Study area highlighted (modified from Hills, 1984).

northern and eastern rim of the Delaware Basin. In 1948, the concept that allochthonous sediments could be transported into deep water by turbidity currents had not yet been developed. Therefore, geologists relied on shallow water depositional concepts to explain the origin of sandstones and other coarse clastics. Fisher and Sarnthien (1988) proposed that eolian processes were responsible for moving silt to basin margins during sea level lowstands. The transported eolian material then slumped into the basin, generating turbidity currents that flowed into the basin. The fine-grained material would be carried deep into the basin where it was deposited. This hypothesis, although explaining the division of grain size and presence of channels, does not seem likely for several reasons. Most obvious is the lack of any evidence of eolian deposits on the shelf. Another problem is that fine-grained material is not likely to be carried very far from its source in the large amounts needed to explain the volume of sand within the Brushy Canyon (Harms and Brady, 1996). The density current hypothesis that was presented by Harms (1974) and Harms and Williamson (1988) proposes that deposition occurred through large density currents which were initiated by differences in salinity or temperature. This hypothesis explains both the channels and the presence of silt far into the basin. The density current hypothesis is very similar to the turbidity current hypothesis presented by Hull (1957) and Jacka et al. (1968). The primary difference between turbidity currents and density currents is the mechanism for the gravity driven flow. Turbidity currents rely on increased density due to high amounts of sediment present, whereas the density current hypothesis relies on the changes in the salinity and/ or temperature to account for the change in density. Turbidity currents are the generally accepted mechanism for deposition of the Brushy Canyon Formation (Montgomery et al.,

1999). Later in this thesis, detailed sequence stratigraphy is used to better describe the depositional environment.

1.3 PETROGRAPHIC STUDIES AND CLAYS

This research relies on thin section petrography and the presence of clay in the reservoir rock to draw conclusions about the hydrocarbon system of the lower Brushy Canyon. Previous work by Thomerson et al. (1996) used petrography to describe the siltstones and sandstones of the Brushy Canyon Formation. His results closely resemble those recorded in this study. A detailed lab analysis of clays present in the Brushy Canyon can be found in Green et al. (1996), who concluded that both illite and chlorite are present in the siltstone in relatively equal amounts. They also observed that the clay is authigenic in nature and exhibits both pore-lining and pore-bridging textures.

2.0 METHODS AND PROCEDURES

A combination of methods was used to better understand the hydrocarbon system of the lower Brushy Canyon. Contour mapping (using Surfer 7.0) of different properties was performed, and cross-sections were completed utilizing well logs. Well cores from parts of the lower Brushy Canyon were described and petrographic analysis was completed on thin sections taken from the cores. Sequence stratigraphy was used to interpret a possible depositional environment for the formation.

Two small study areas were chosen as the primary geographic areas of comparison. The western study area is an area of sparse hydrocarbon production from the lower Brushy Canyon as indicated from drilling records. It is located southwest of Carlsbad, New Mexico and is roughly the size of two townships (72 square miles). The eastern study area is an area that produces large volumes of hydrocarbons from the lower Brushy Canyon as indicated by drilling records. It is half the size of the western area, one township (36 square miles), and due east of the western study area (Fig. 2.1)

2.1 MAPPING

A database of 96 resistivity and porosity logs was created in order to map the eastern and western study areas. Using log characteristics, the lower Brushy Canyon was separated into four informal lithostratigraphic units A, B, C and D as shown in Broadhead et. al (1998) and defined in the following section. These units make no lithological presumptions regarding depositional environment, but were necessary to better

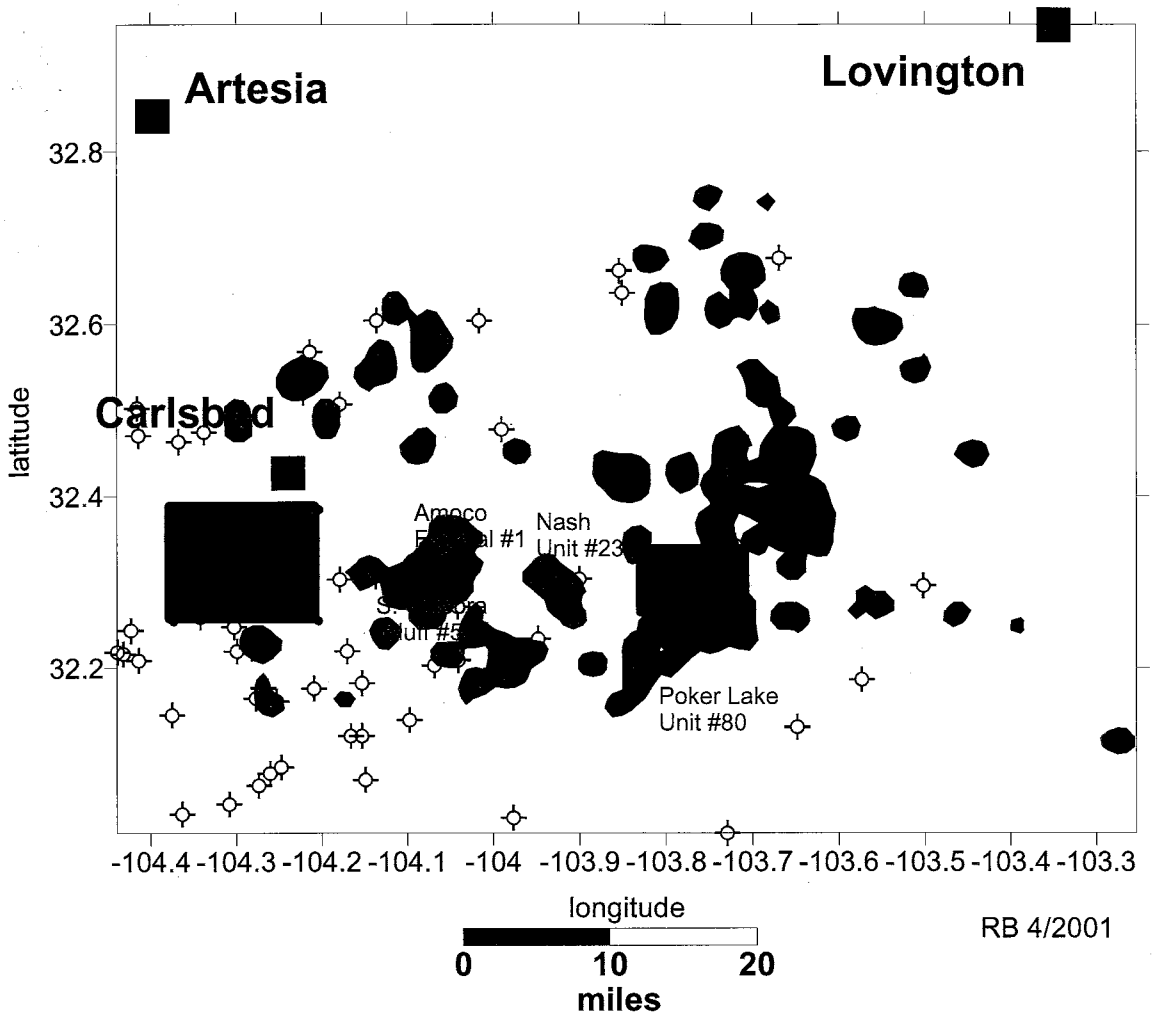

black dot= location of cored wells
green = areas productive from lower Brushy Canyon
purple = unsuccessful lower Brushy Canyon tests
blue = areas of intensive study

Figure 2.1: Location of eastern and western study areas (from Broadhead, 2001).

understand the structure of the formation. All logs were correlated and many were included in one of 16 cross-sections in order to show the continuity of beds across the study area.

Resistivity Logs

Resistivity logs, in conjunction with gamma ray logs, were used to correlate the A, B, C, and D units within the lower Brushy Canyon. The top of the Brushy Canyon was identified as well as the tops of the A, B, C and D units of the lower Brushy Canyon; the top of the Bone Spring Formation was also identified. Resistivity log depths were normalized to sea level in order to best understand the structural relationships among the wells. These depths were used to calculate thicknesses of the units as well as the regional structure.

Porosity Logs

Density porosity logs were correlated to the same depths as the resistivity logs. Using the density porosity curve, each unit was examined to determine the net thickness of sandstones that have greater than 10 percent porosity and greater than15 percent porosity according to the logs. These values were chosen because well logs indicate that production in the lower Brushy Canyon is associated with density porosity values greater than 10 percent, and the highest production rates occur from intervals that have greater than 15 percent density porosity.

Production Mapping

Production for each well was mapped in order to locate productive areas within the Lower Brushy Canyon. Initial production rates of oil, gas and water were examined, as well as cumulative amounts of each. All production data was observed from wells that

produce only from the lower Brushy Canyon. Wells that co-mingle between the lower Brushy Canyon and other formations were not used in the production maps. This was necessary because production rates and cumulative amounts cannot be determined for each co-mingled unit. Areas of production were then contoured in order to locate where the highest initial production rates came from and where the highest cumulative volumes are located.

Clay Content and Average Gamma Ray Mapping

Mapping the average clay content of siltstones as calculated by gamma ray and average gamma ray intensity was completed in order to compare these results to oil and gas occurrence. To perform this task, each stratigraphic unit was mapped separately. The A unit was not mapped because it does not produce hydrocarbons. Clay content of the siltstones was mapped as the thickness of siltstone that contains less than 10 percent clay content and less than 12.5 percent clay content. The mappable variable for gamma ray value is average gamma ray value over each stratigraphic unit.

2.2 WELL LOG CORRELATION

Geophysical well logs were used to correlate subsurface strata and to identify lithologies in conjunction with core descriptions. The lower Brushy Canyon was sub-divided into four stratigraphic units. These units were named from top to bottom A, B, C, and D after Broadhead et al. (1998) (Fig. 2.2).

A Unit

The A unit is the uppermost division of the lower Brushy Canyon. This unit is identified by its high gamma ray and resistivity peaks. It is generally defined by two peaks that are separated by less than 20 feet. In some wells only one peak is present.

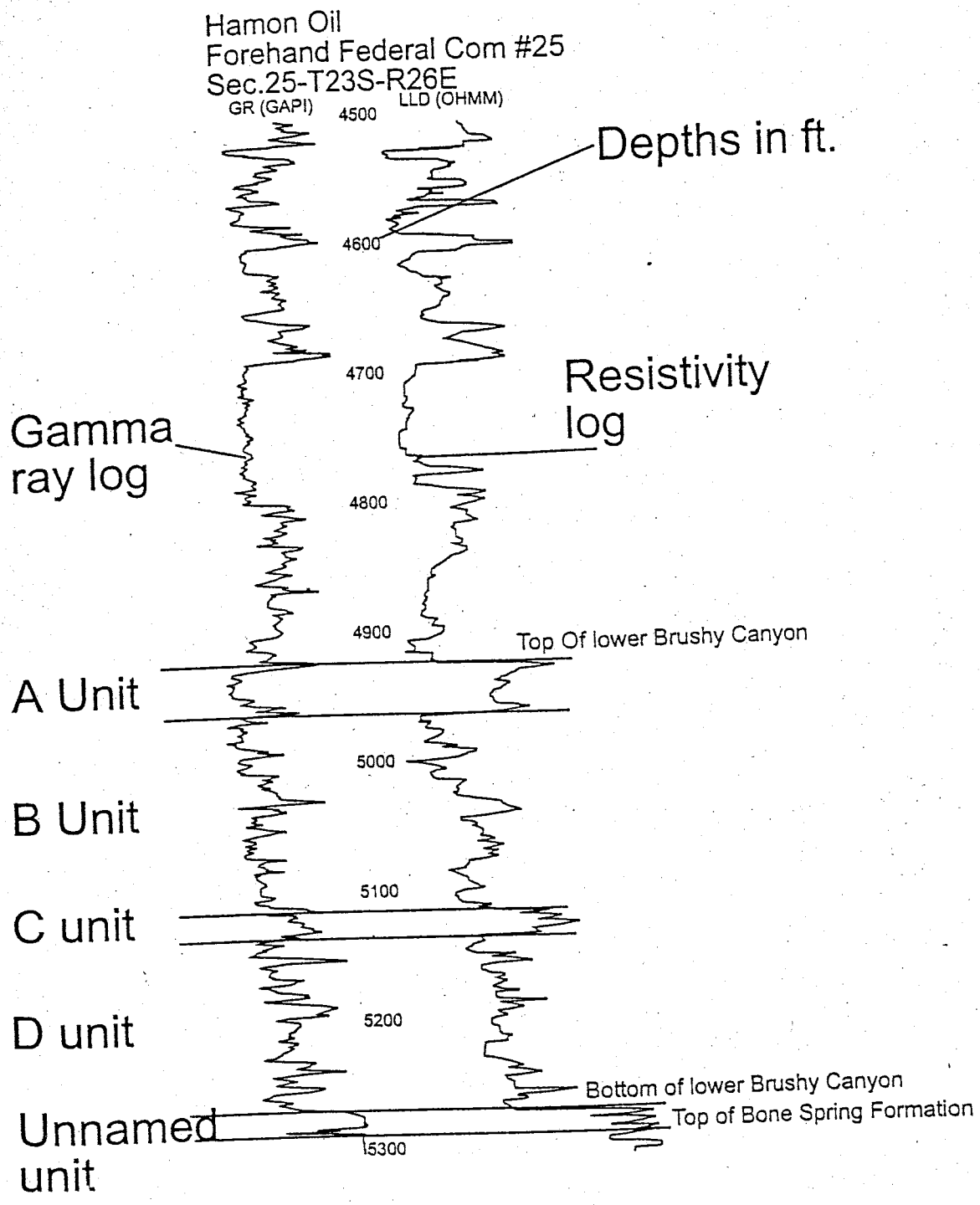

Figure 2.2: Example of a well log with both gamma ray and resistivity curves. All lower Brushy Canyon units are labeled. Well log scales increase to the right.

B Unit

The B unit is directly below the A unit. The top of B unit can be easily recognized by its relatively low gamma ray and resistivity values, when compared to the A unit above. This unit is much thicker than the A unit, between 100 and 150 feet thick. The middle of the B unit is represented by a thin zone of high gamma ray and high resistivity. Directly below this is an even lower gamma-ray and resistivity zone. The bottom of the B unit is marked by the increase of gamma ray and resistivity that marks the top of the C unit.

C Unit

The C unit lies directly below the B unit. This unit is recognizable by its high gamma ray and resistivity values. It is characterized by two to four peaks and bounded both above and below by the B and D units, which are chacterized by low gamma ray and resistivity values.

D Unit

The D unit is the lowest unit in the lower Brushy Canyon, and is characterized by a thick interval of very low gamma ray and resistivity values. About half way through the unit, the gamma ray and the resistivity logs gradually increase. The base of the D unit is identified by the top of an unnamed unit, which is characterized by very high gamma ray and resistivity values. This unnamed unit forms the lowermost part of the Brushy Canyon and may be correlative with the Cutoff Formation.

2.3 WELL LOG DIGITIZATION

In order to more quickly and accurately process well log information it was necessary to manually digitize paper well logs. Well log digitization for this project was done in the Petroleum Recovery Research Center at New Mexico Tech.

The well log digitization process began with first scanning the well log on a fax scanner. Once scanning was complete, well log parameters were set using the Neuralog software. This included identifying depths, determining log scales and identifying what type of log was to be digitized. The most time consuming step was to manually trace the log curve of the scanned image using the screen cursor controlled by the mouse. The computer program attempted to trace the curve automatically; however, there was a frequent need to manually adjust the automated curve trace. The final step was to save the scanned image as several different types of files, including an ASCII file and an image file. These formats create both a digital image of the curve and a numerical data set of curve values at half foot intervals.

2.4 PETROGRAPHY

Petrographic analysis was conducted on 29 thin sections from four cores taken from the lower Brushy Canyon Formation. Thin sections from the Strata Production Corp. Nash Unit 23 well, Fortson Oil Poker Lake Unit 80 well, RB Operating South Culebra Bluff 5 well, and RB Operating Amoco Federal 1 well, were cut from both productive and non-productive sandstones and siltstones. All thin sections were impregnated with blue epoxy in order to best describe and accurately count porosity. The separation between productive and non-productive intervals was based solely on whether the interval was perforated or not. This does not mean that all samples from perforated

intervals actually produce hydrocarbons nor that all samples from non-producing intervals are not capable of being productive. It is quite likely that some non-perforated intervals could be productive had they been perforated, and some sandstone beds within perforated intervals are not productive.

Each thin section was described and point counted (200 points). Components that were counted were quartz, feldspar, detrital carbonate, rock fragments, clay minerals, calcite cement, microporosity, macroporosity, and kerogen. Microporosity was defined as any very faint blue area, generally surrounded by clay minerals or calcite cement. Macroporosity was any dark blue area that could easily be recognized. These properties were chosen because they adequately describe the rock. Thin section descriptions (after Spain, 1992) emphasized the overall framework and matrix of the rock, as well as the manner in which clay minerals and calcite cement are present in the matrix. Descriptions also included the nature of the grain-to-grain contacts and the relative size and distribution of pore space. These descriptions were used to describe the rock physically, and therefore infer its ability to transmit and accumulate hydrocarbons.

2.5 CORE DESCRIPTIONS

Four cores were described in order to better understand and identify the lithologies of the lower Brushy Canyon. Descriptions included lithology, color, description of lamina and any sedimentary structures present (Pettijohn et al., 1964). All cores were taken from the lower Brushy Canyon and all were from producing wells. The four wells that were described are Strata Production Nash Unit 23, Fortson Oil Poker Lake Unit 80, RB Operating Amoco Federal 1, and RB Operating South Culebra Bluff 5 (Fig. 2.1). Complete core descriptions and locations can be found in Appendix I.

3.0 RESULTS

3.1 FACIES OF THE LOWER BRUSHY CANYON

Detailed core descriptions from the four cores revealed three lithofacies present in the lower Brushy Canyon. These facies consist of massive siltstones, thick black shales and interbedded siltstone and shale. The primary facies present in the lower Brushy Canyon is the finely interbedded siltstone and shale. Complete core descriptions are in Appendix I (Figs. 3.1 A, B, C, D, E, F, G).

Interbedded Siltstone and Shale Facies

Units of the interbedded siltstone and shale facies range in thickness from half a meter up to ten meters. These units are composed of interlaminated siltstone and shale. The individual siltstone and shale laminae are often less then a half-centimeter thick but can be up to two centimeters thick. The siltstone laminae within these units are generally gray and contain large percentages of clay matrix (Fig 3.2).

Massive Siltstone Facies

The massive siltstones are tannish to gray, darkening with an increase in shale lamina. These siltstones consist largely of a quartz and feldspar framework in a clay matrix and cemented with calcite. The siltstone units range from centimeters thick to over ten meters. Thin black shale beds are often present at irregular intervals throughout the thicker siltstones. The thinner siltstones are often bounded by thicker shale units and interbedded siltstone and shale units (Fig 3.3).

Black Shale Facies

The black shales occur most frequently in thick units at the base of the lower Brushy Canyon but can be found in smaller accumulations between the siltstones and the

interbedded units. These organic rich black shales occur primarily as the source rocks of the lower Brushy Canyon. Siltstone stringers are sometimes present. These are often very fine thin wavy beds (Fig. 3.4). Justman (2001) noted the presence of fossils including foraminiferans, sponges, gastropods, echinoderms and others. Justman (2001) also noted the high organic content and kerogen type of these black shales.

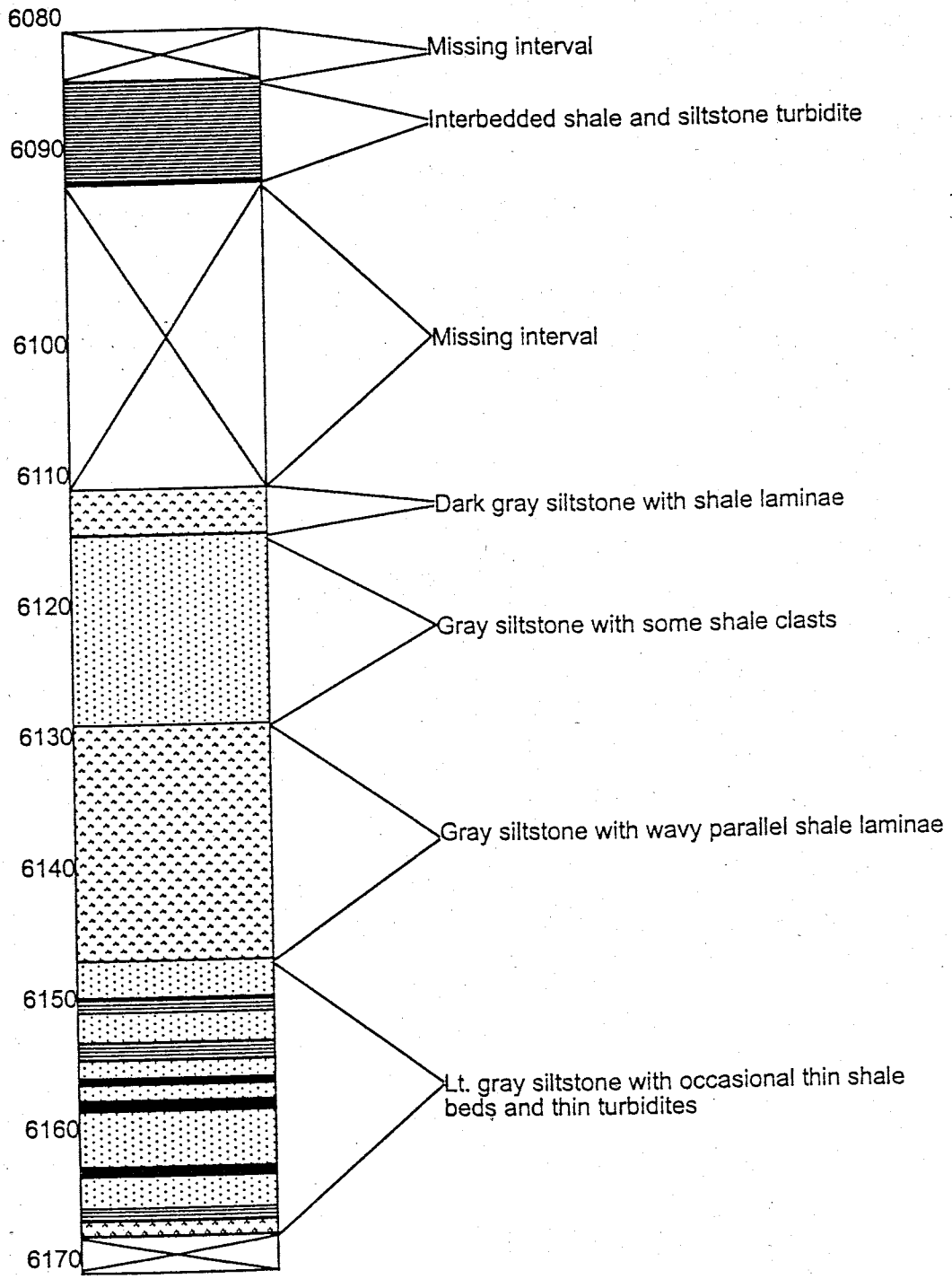

Figure 3.1A: Stratigraphic section of RB Operating, Amoco Federal #1 well S11-T23S-R28E, from core description.

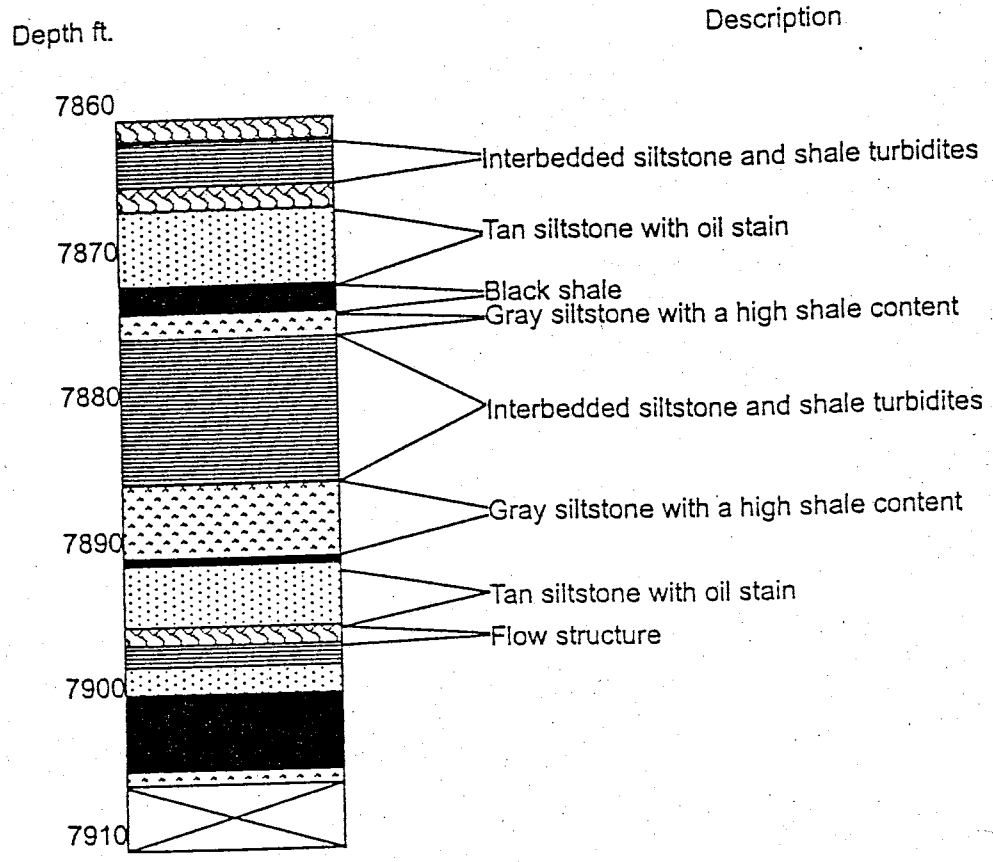

Figure 3.1B: Upper stratigraphic section from Fortson Oil Poker Lake Unit #80 well S19-T24S-R31E, from core description.

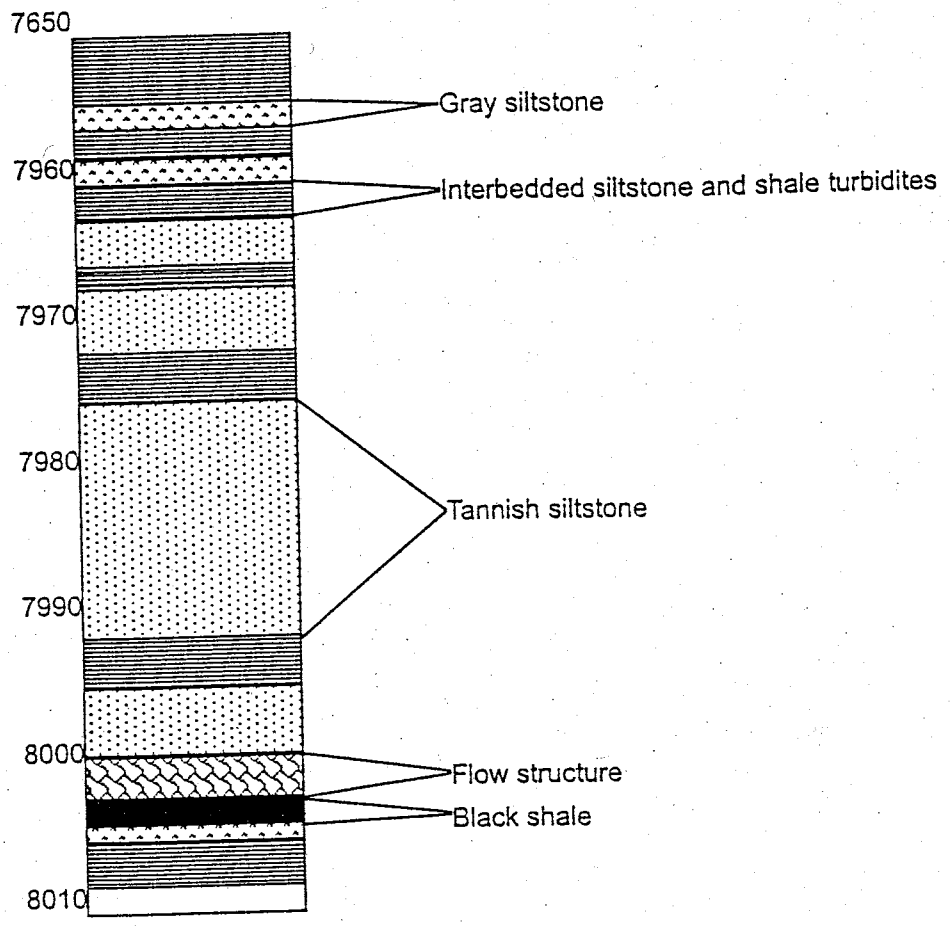

Figure 3.1C: Lower stratigraphic section from Fortson Oil Poker Lake Unit #80 well S19-T24S-R31E, from core description.

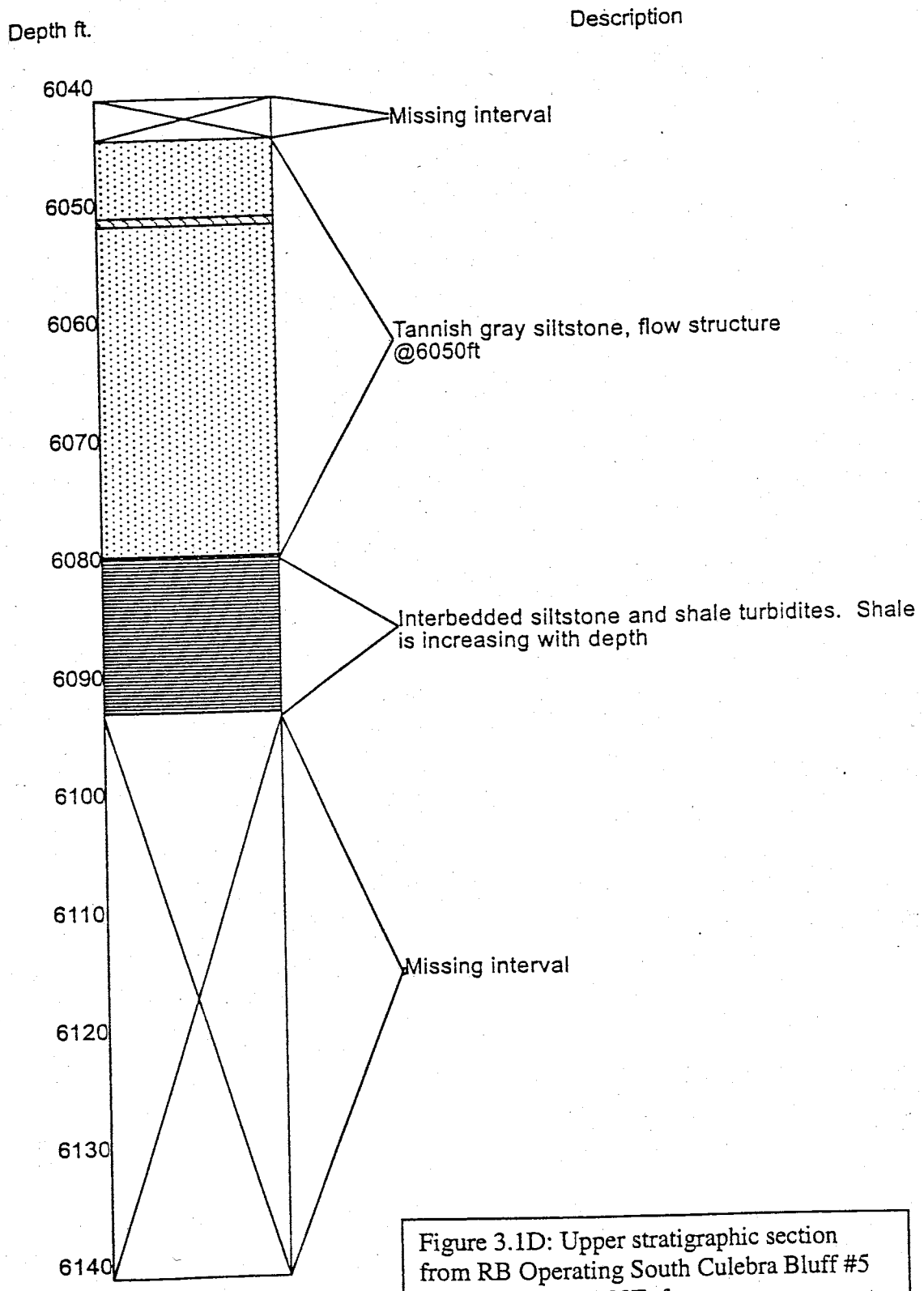

Figure 3.1D: Upper stratigraphic section from RB Operating South Culebra Bluff #5 well S13-T23S-R28E, from core descriptions.

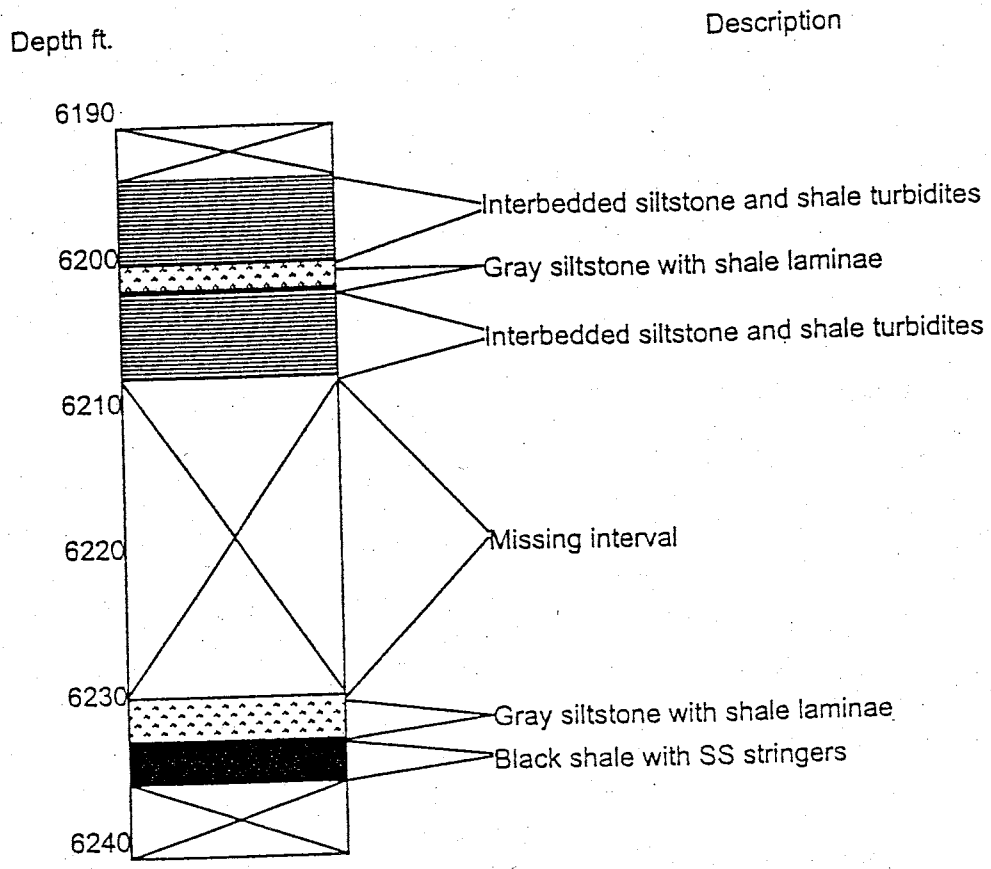

Figure 3.1E: Lower stratigraphic section from RB Operating South Culebra Bluff #5 well S13-T23S-R28E, from core descriptions.

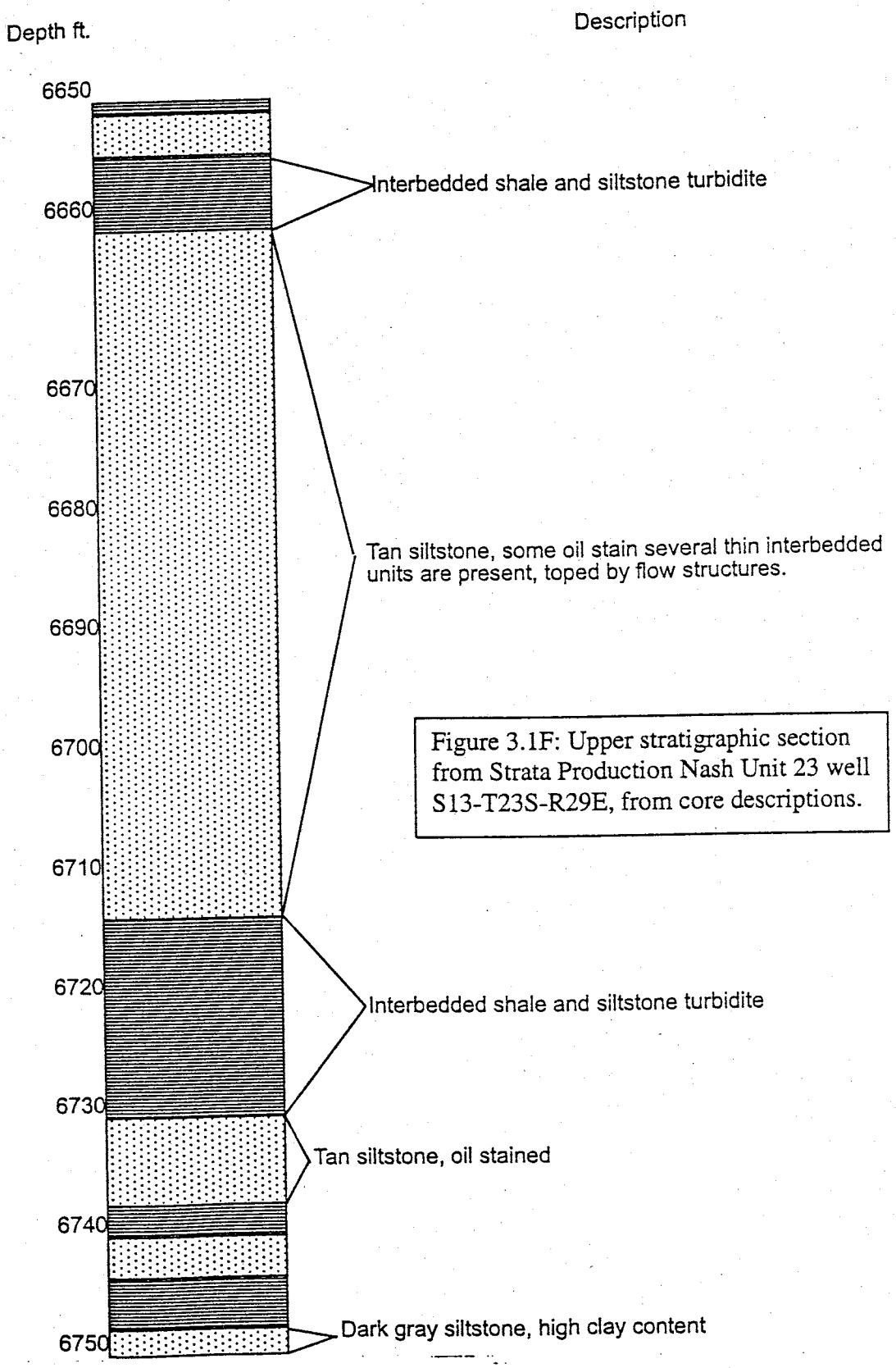

Figure 3.1F: Upper stratigraphic section from Strata Production Nash Unit 23 well S13-T23S-R29E, from core descriptions.

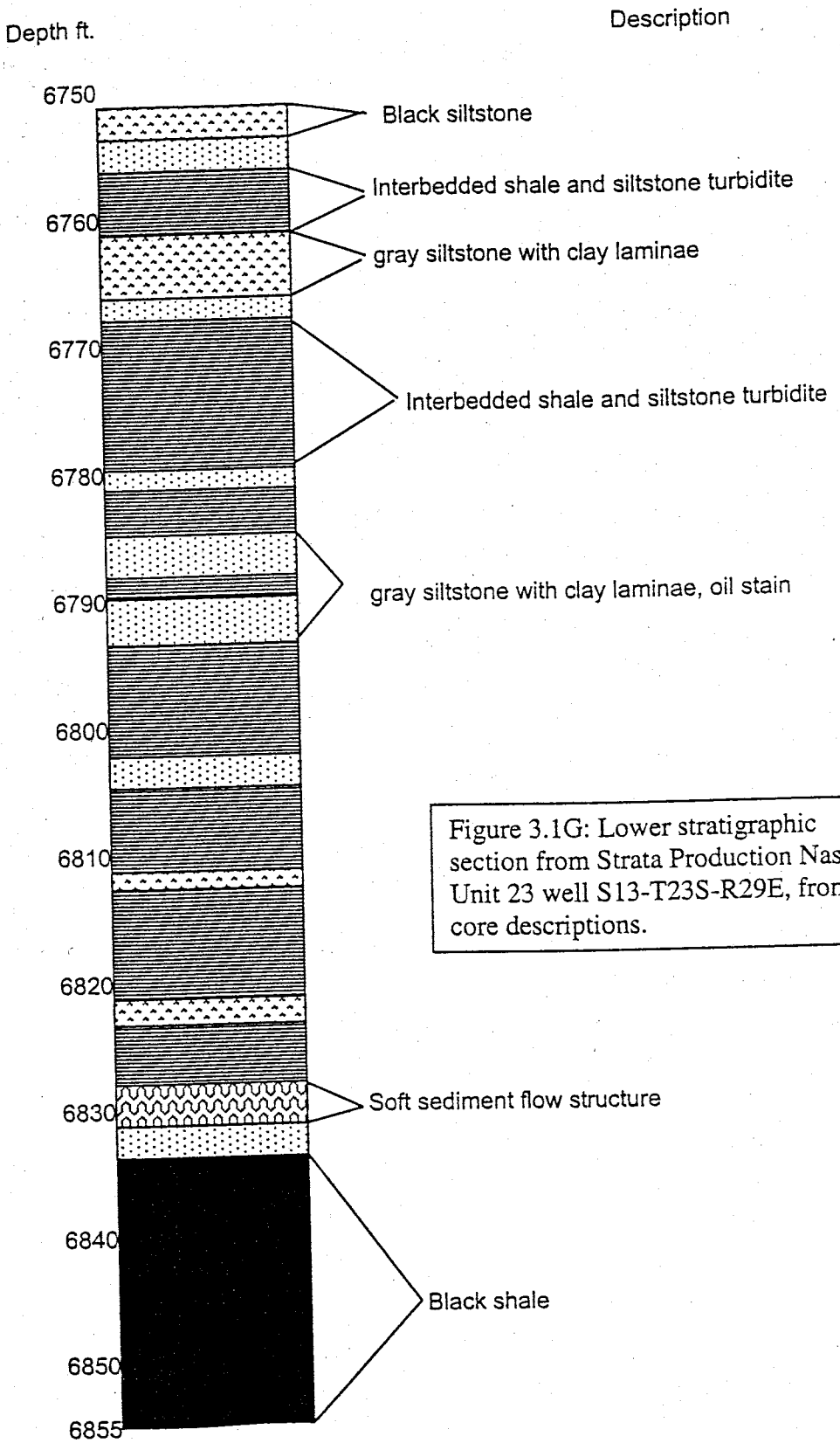

Figure 3.1G: Lower stratigraphic section from Strata Production Nash Unit 23 well S13-T23S-R29E, from core descriptions.

Figure 3.2: Photo of Poker Lake Unit #80 Core, interbedded siltstone and shale interval. (Core sections are two feet long, 7.5 feet of core in picture.)

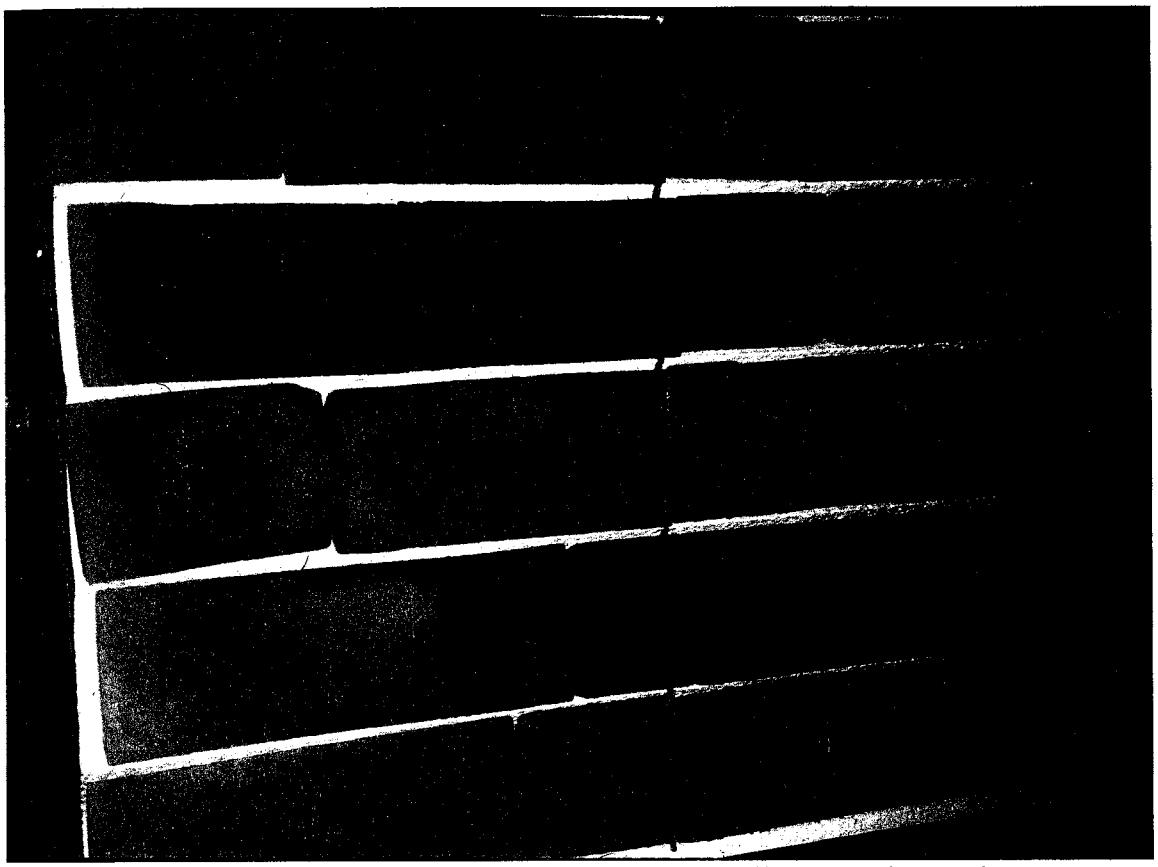

Figure 3.3: Photo of Poker Lake Unit #80 core. Massive siltstone units, tan in color. Around some of the sections it is noticeable where drill mud has entered the rim of the core. (Core sections are two feet thick, ten feet of core in picture.)

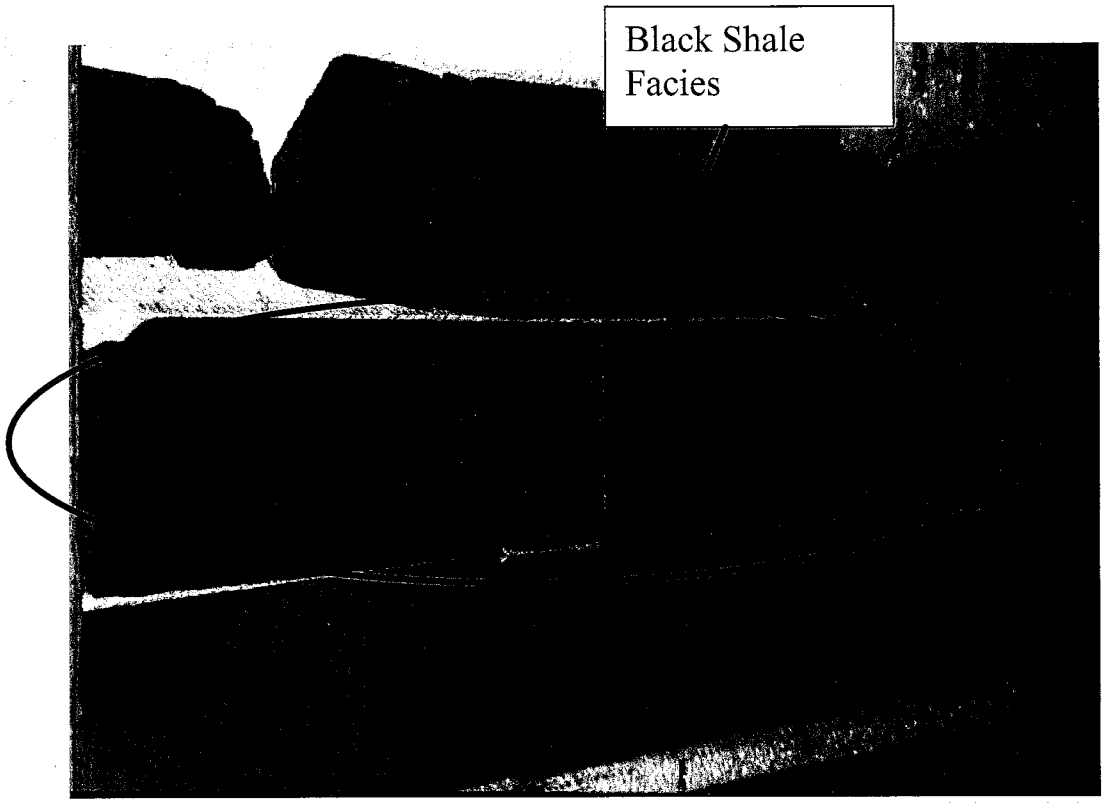

Figure 3.4 Photo of Poker Lake Unit #80 core. Thick black shale unit bounded above and below by gray siltstone. (Core sections are two feet long, six feet of core in picture.)

Sedimentary Structures

Very few sedimentary structures other than laminae are present within the cored sections. The most recognizable structures present in all of the cores are soft sediment flow structures (Pettijohn and Potter,1964). Flow structures often contain siltstone in a shale matrix and appear to be mixed. Generally, at the base of these flow structures, rip-up clasts of black shale are present in the siltstone (Fig. 3.5). Some thin zones of bioturbation have been noted by Justman (2001).

3.2 PETROGRAPHY AND WELL INFORMATION

Petrographic descriptions and point counts revealed a great deal about the composition of the siltstones. Point count results are used in comparison with well log properties. Point count data and thin section descriptions are located in Appendix II.

Nash Unit 23

The Strata Production Nash Unit 23 well is located in S13-T23S-R29E in Eddy County, New Mexico. This well was drilled to a total depth of 7100 ft in the Bone Spring Formation, and was completed on October 25th 1995. The productive intervals of this well are from 6654 to 6703 ft and from 6755 to 6801 ft. Both intervals are perforated in the lower Brushy Canyon B and D units. Core which was taken from 6650 to 6854 ft, consisted mainly of thinly interbedded shale and siltstone facies, with occasional thick siltstone units where most of the production comes from.

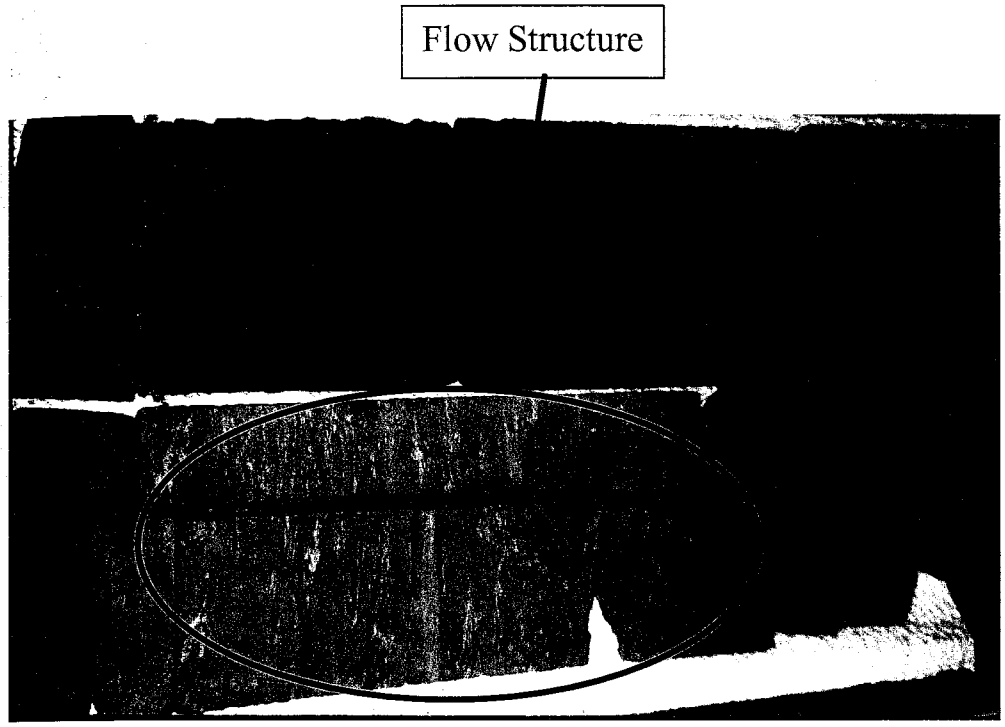

Figure 3.5: Photo of Poker Lake Unit #80. Flow structure.
(Core sections are two feet long, four feet of core in total picture.)

Productive Siltstones

Samples that were labeled as productive only came from perforated well intervals. Thin section samples are of very fine-grained sandstones and siltstones with sub-rounded to sub-angular quartz and feldspar framework grains. Matrix in these rocks is primarily clay minerals although calcite is also present as cement. The productive siltstones have a high porosity (16-25.5%) and pores are well interconnected. Grain-to-grain contacts are long and point contacts (Pettijohn et al.,1973) (Fig. 3.6).

Non-Productive Siltstones

The non-productive siltstones were taken from non-perforated intervals. Generally the average thickness of these non-productive units (<2m) is less than the average thickness of the productive intervals (>10m). These thin sections represent very fine-grained sandstone and siltstones with an angular quartz and feldspar framework. Clay minerals and calcite cement greatly reduce pore size and interconnectedness by wrapping around grains and filling in pore space. Grain-to-grain contacts are long (Fig 3.7).

Poker Lake Unit 80

The Fortson Oil Poker Lake Unit No.80 well is located in S19-T24S-R31E, in Eddy County New Mexico. This well was drilled to a total depth of 8200 ft into the Bone Spring limestone, and was completed on November 18th, 1993. Production in this well occurs from the intervals 7864 to 7986 ft, 8033 to 8036 ft and 8042 to 8044 ft, all located in the lower Brushy Canyon B, C, and D units respectively. Two cores were taken from this well. Core No. 1 is from 7860 to 7904 ft, and core No. 2 is from 7950 to 8005 ft. Both

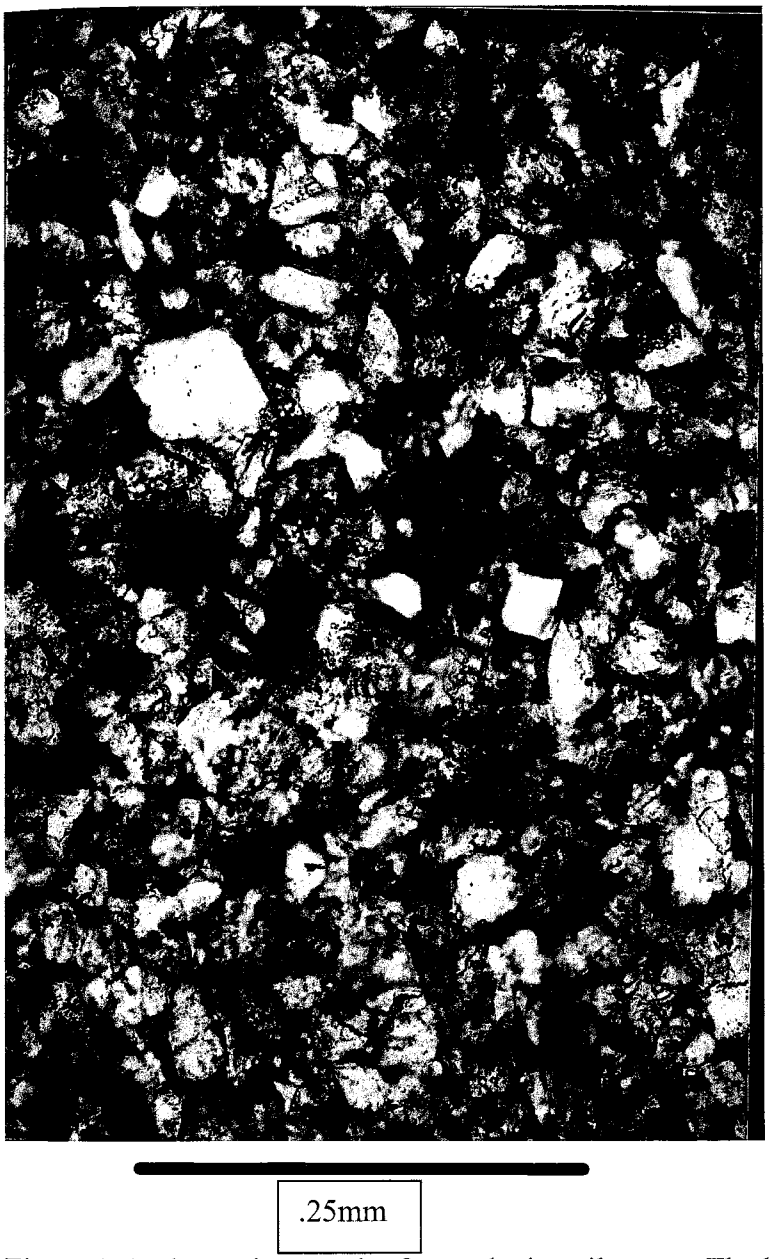

Figure 3.6: Photomicrograph of a producing siltstone. The blue area is epoxy, infilling porosity.

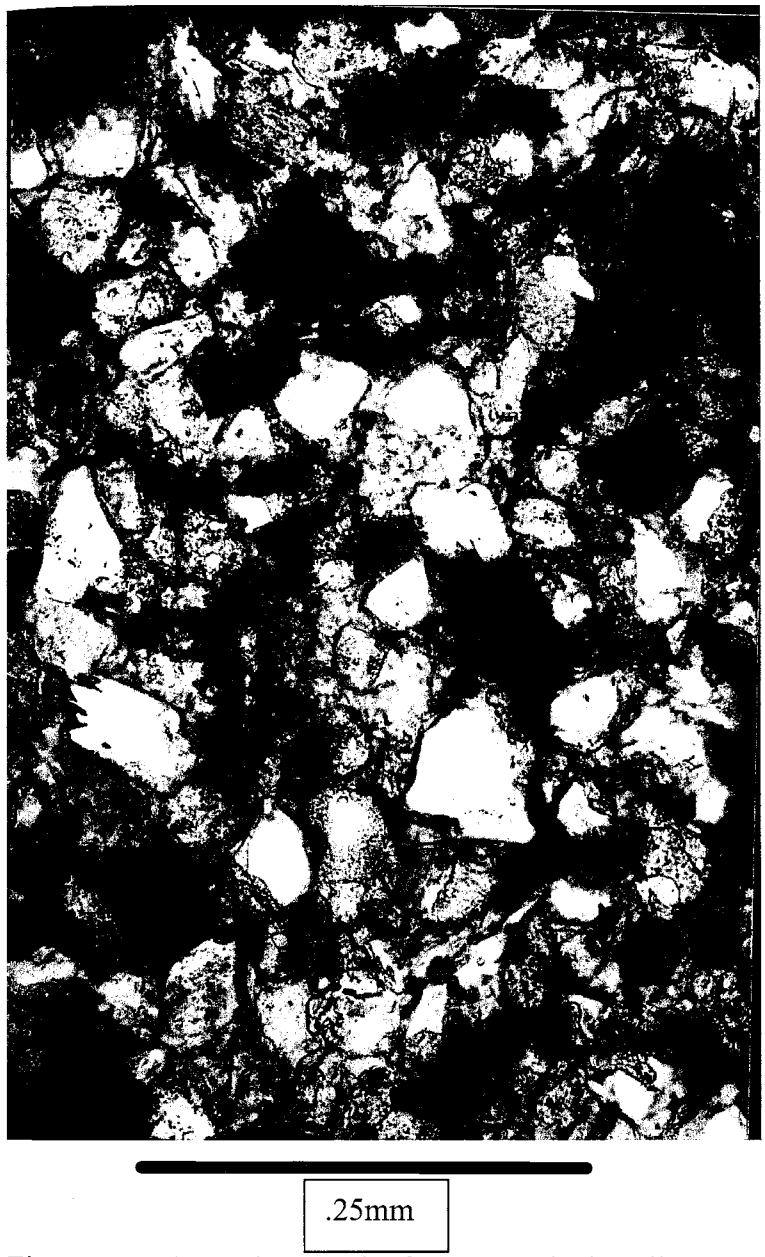

Figure 3.7: Photomicrograph of a non-producing siltstone. Blue area is epoxy, infilling porosity.

cores are within the lower Brushy Canyon. Core No.1 is primarily thinly interbedded siltstone and shale deposits of siltstone and shale. Core No.2 consists of thick siltstone units with occasional thin interbedded shale and siltstone deposits.

Productive Siltstones

The productive siltstones from these cores are composed of a quartz and feldspar framework. Clay minerals and calcite cement surround framework grains and pore space. The porosity in these siltstones is high (19-29%) and pores are fairly well interconnected. The grain-to-grain contacts are long and point contacts.

Non-Productive Siltstones

The non-productive siltstones of these cores were difficult to locate because core was taken mostly from producing zones. Core from the non-productive zones consists of the interbedded siltstone and shale facies. From the samples that were taken from the non-productive zones, the siltstones consist of a very fine-grained quartz and feldspar framework. Framework grains are angular to sub-angular. The clay matrix and calcite cement are more abundant than in the productive rocks (up to 47%) (Appendix II). The clay minerals and calcite cement surround framework grains and fill in pore space. The pores are poorly interconnected and very small (<.05 mm).

South Culebra Bluff 5

The RB Operating South Culebra Bluff No.5 well is located in S13-T23S-R28E in Eddy County, New Mexico. This well was drilled to a total depth of 13,171 ft in the Morrow Formation (Pennsylvanian), and completed on December 18^{th,} 1990. It is productive from the lower Brushy Canyon from 6217 to 6228 ft. Three cores were taken from this well. The first core, from 6043-6092 ft, is the longest of the three. It consists

primarily of the massive siltstone facies, underlain by a unit of the interbedded shale and siltstone facies. The other two cores are from depths of 6193 to 6207 ft and 6229 to 6235 ft. Both of these consist mainly of interbedded shale and siltstone with small shaley siltstone units. Only three thin sections were taken from these cores due to the lack of siltstone beds, and the small amount of core available.

Productive Siltstones

Two siltstone samples were taken from productive intervals in this well. Both siltstones are composed of a quartz and feldspar framework, with clay matrix and calcite cement present in some of the pore space. These thin sections have a low percentage of clay matrix and calcite cement (15-16%). The clay matrix and calcite cement generally fill in pore space and surround grains. Porosity in these productive intervals is very high (more than 29%). The pores are well interconnected in both samples (Appendix II).

Non-Productive Siltstones

Only one thin section was taken from a non-productive siltstone. This siltstone is dominated by clay matrix and calcite cement (39%). Porosity is very low (3%) and pores are very poorly interconnected.

Amoco Federal 1

The RB Operating Amoco Federal 1 well is located in S11-T23S-R28E in Eddy County New Mexico. This well was drilled to a total depth of 11,900 ft, in the Atoka Formation (Pennsylvanian). This well is productive from 6124 to 6208 ft in the lower Brushy Canyon Formation. Two cores were taken from this well. The upper core is from 6083 to 6092 ft. and consists of only interbedded shale and siltstone. The second core is from 6110 to 6167 ft. This core consists mainly of shaley siltstone, and occasionally thin

interbedded shale and siltstone. Only four samples were taken from this unit due to the lack of siltstone.

Productive Siltstones

The productive siltstones from this well are composed of a quartz and feldspar framework with little clay matrix and calcite cement. The porosity in these thin sections is very high (up to 31%) and very well interconnected.

Non-Productive Siltstones

The non-producing siltstones are composed of a quartz and feldspar framework dominated by clay matrix and calcite cement that surrounds grains and fills in pore space. Porosity in these samples is very low (9%) and poorly interconnected (Appendix II).

3.3 MAPPING

Mapping of each individual unit of the lower Brushy Canyon was done in order to determine if there is any correlation between hydrocarbon production and any of several mapable properties that were identified. These maps included structure, isopach, porosity, net sand thickness and production. Map descriptions are separated by location within the study area.

Western Area

The western study area is characterized by sparse production from the lower Brushy Canyon Formation. The regional structure in the area dips to the east –southeast, which can be seen on all structure maps (Fig. 3.8 & Appendix III). The isopach map of the lower Brushy Canyon shows a relative thickening to the east and west and thinning to the center of the study area (Fig. 3.9 & Appendix III). However, each unit in the lower Brushy Canyon shows a slightly different geometry. The A unit dips to the east-southeast but shows a thickening to the northeast of over 35 feet. The B unit also dips to the east-southeast but thickens to the south about 50 feet. The C unit dips to the east-southeast, however the unit thickens westward to more than 50 feet. The D unit dips to the east-southeast and thickens to the north and to the west over 100 feet (Appendix III).

Porosity mapping in the western area proved of little value because there was little production from the lower Brushy Canyon. However, in all units there is a noticeable difference in the thickness of sands with greater than 10 percent porosity (Fig. 3.10 & Appendix III) versus the thickness of sands with greater than 15 percent porosity, which is much lower (Fig. 3.11 & Appendix III).

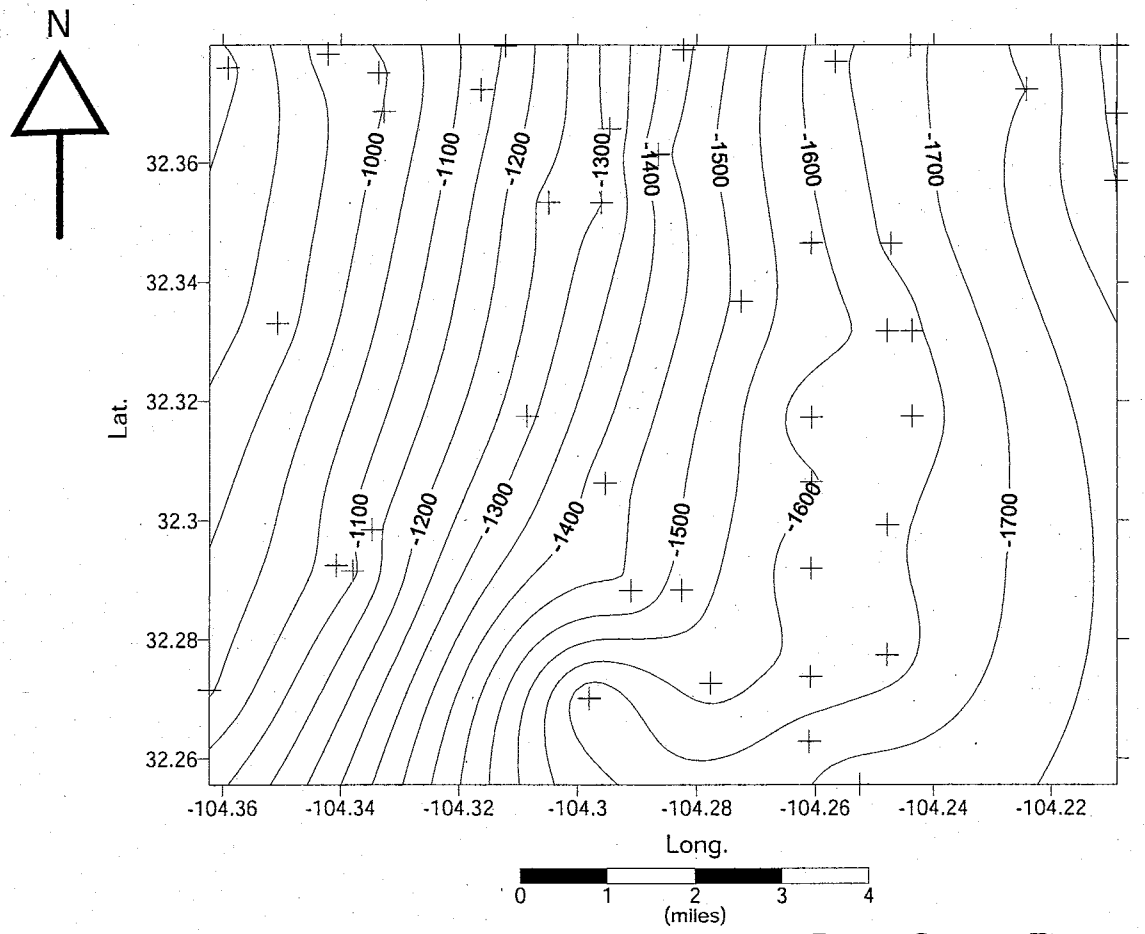

Figure 3.8: Western study area, structure of the top of the lower Brushy Canyon. The top of the lower Brushy Canyon is dipping to the east-southeast. Contour interval is 50 ft. Datum is sea level. (+ = well location)

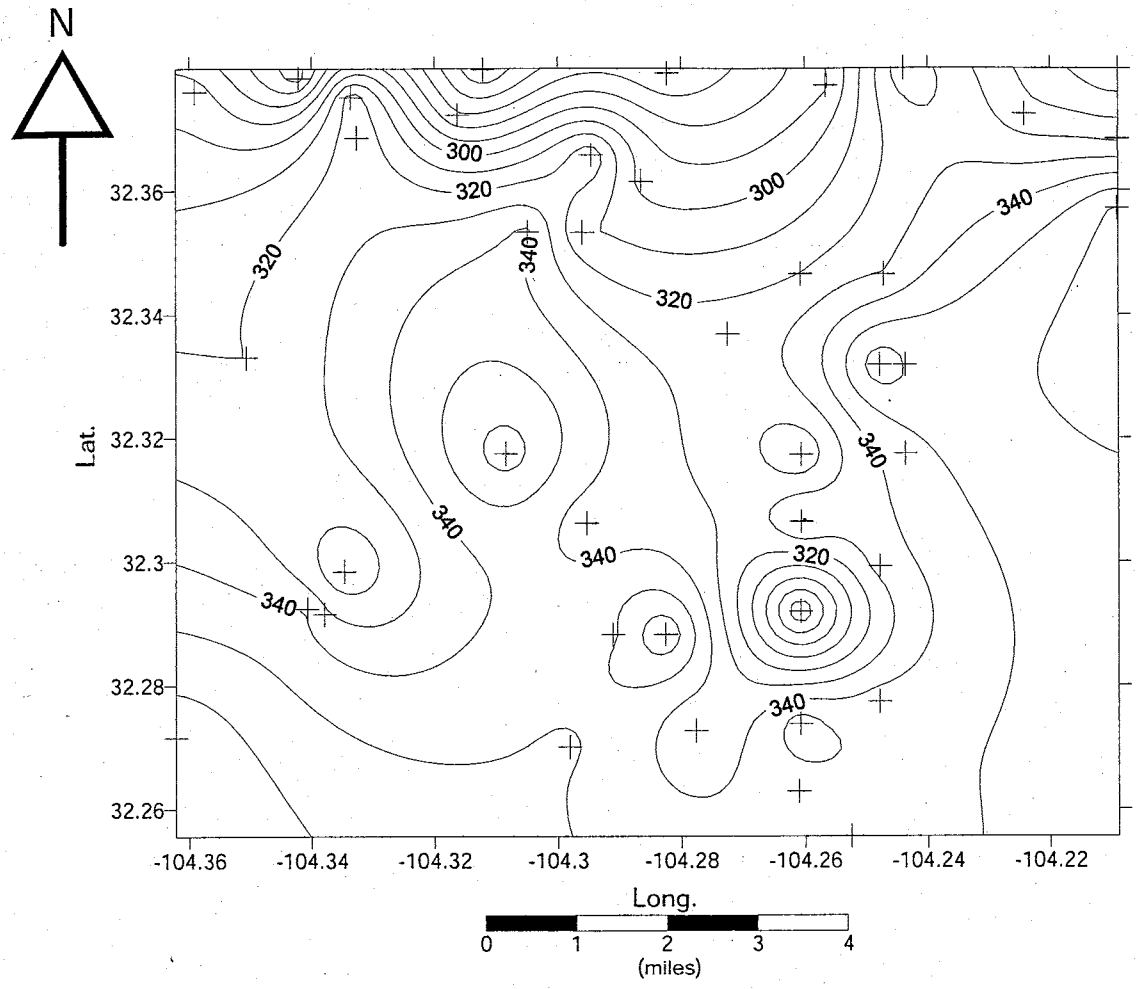

Figure 3.9: Western study area, isopach map of the lower Brushy Canyon. Contour interval is 10 feet. (+ = well location)

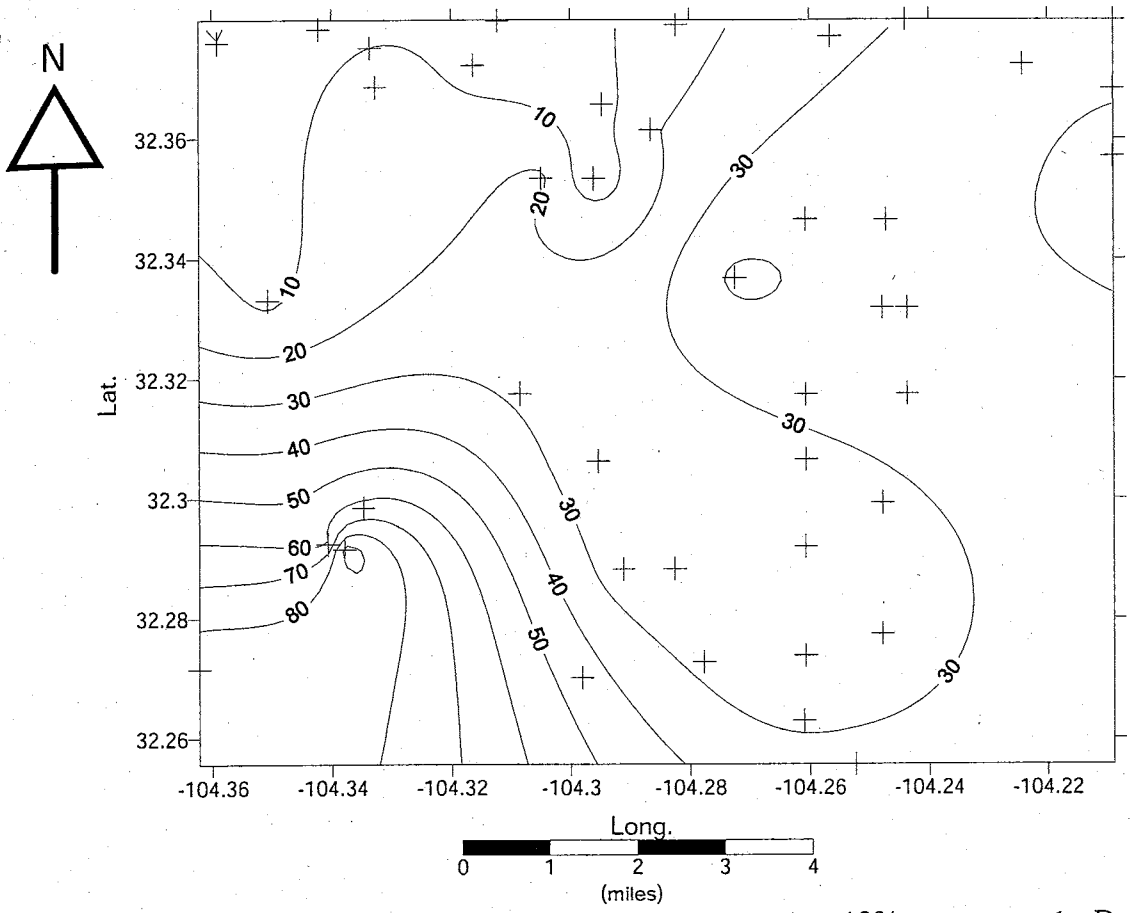

Figure 3.10: Western study area, thickness of sand with more than 10% porosity in the D unit of the lower Brushy Canyon. Contour interval is 10 feet. (+ = well location)

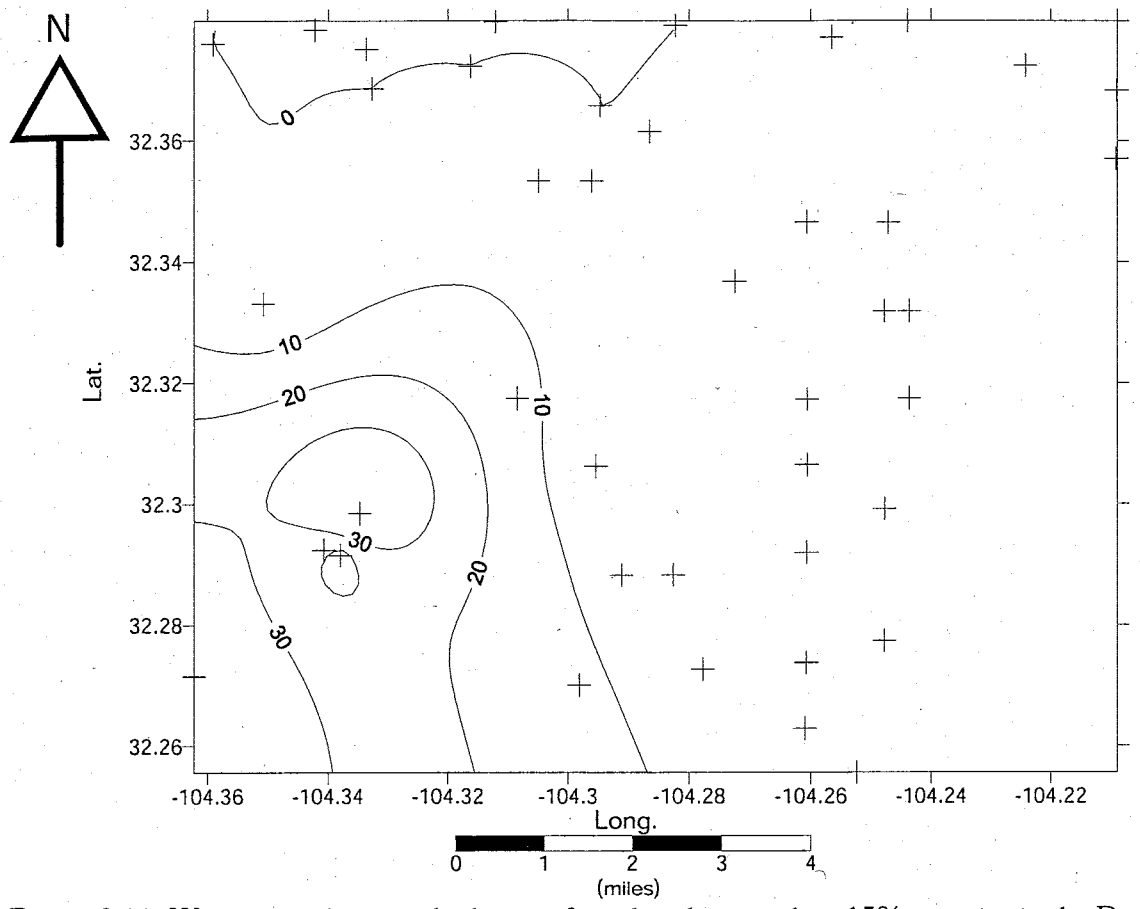

Figure 3.11: Western study area: thickness of sand with more than 15% porosity in the D unit of the lower Brushy Canyon. Contour interval is 10 feet. (+ = well location)

Production from this area is limited to just three wells, none of which produce large volumes of hydrocarbons (Fig. 3.12 & Appendix III).

A variety of maps were compared in order to relate hydrocarbon production to other mapped variables such as porosity, structure, and net sand thickness. Due to the limited nature of the production within this area it was not possible to relate production to any other variables, such as porosity and clay content.

Eastern Area

The lower Brushy Canyon produces relatively large volume of hydrocarbons from the eastern area when compared to the western area (>6.5million Barrels Oil (BO), >21,780,000 Million Cubic Feet of Gas (MCFG), and >8.1million Barrels Water (BW). The regional structure in this area dips to the east (Fig. 3.13 & appendix III). The isopach maps of the lower Brushy Canyon show a relatively even surface with only about 30 feet of variation (Fig. 3.14 & Appendix III). However, each unit is very different in its thickness. The A unit dips to the east and thickens to the east-southeast. The B unit dips to the east, but thickens to the northwest. The C unit is relatively flat with only about 14 feet of structural relief. The D unit, which dips to the east thickens to the northeast and southwest, but only has about 30 feet of relief.

Porosity mapping in the eastern unit was valuable because it indicated large areas of high porosity sand (>15%) (Figs. 3.15, 3.16 & Appendix III). Zones of thick sands were identified and mapped (Fig. 3.17 & Appendix III).

Production mapping of the eastern area indicated two north-south running trends of production (Fig. 3.18 & Appendix III). The western trend (Ingle Wells) is slightly larger and produces greater quantities of hydrocarbons.

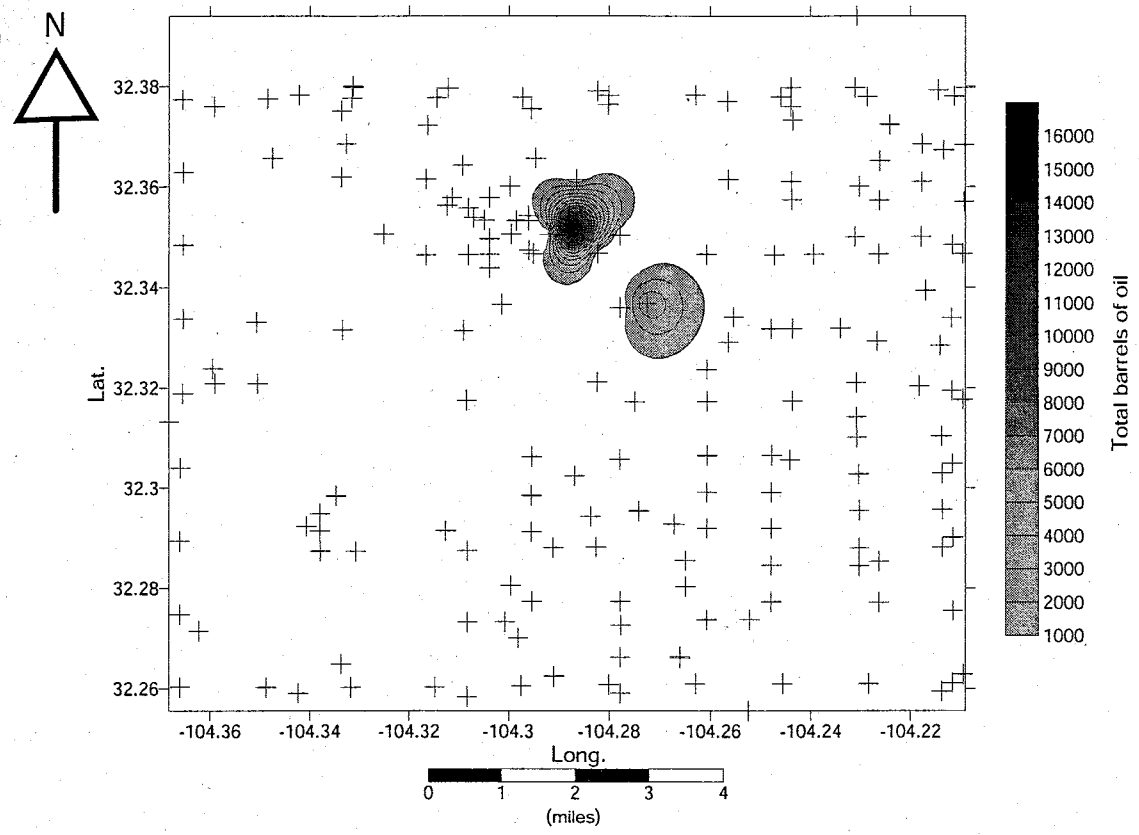

Figure 3.12: Western study area, cumulative oil production. Only three wells produce from the lower Brushy Canyon in this study area. (+ = well locations)

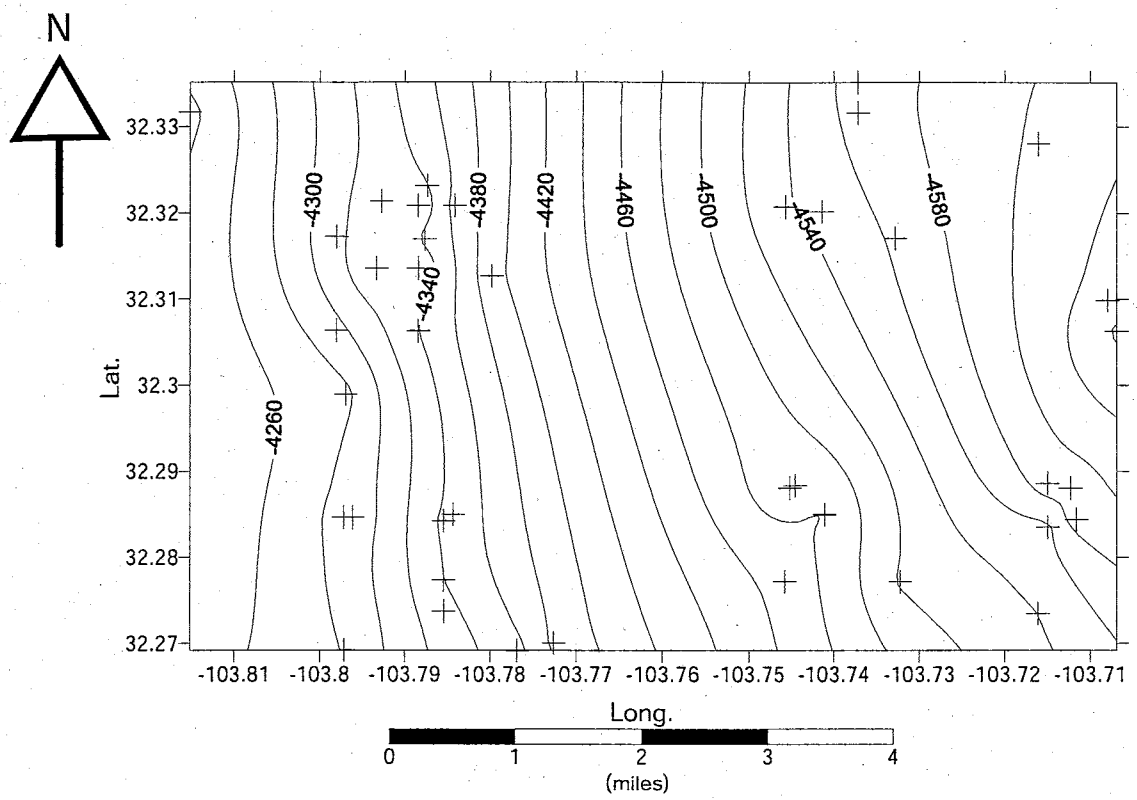

Figure 3.13: Eastern study area, structure of the top of the lower Brushy Canyon. The top of the lower Brushy Canyon dips to the east. Contour interval is 20 feet. Datum is sea level. (+ = well location)

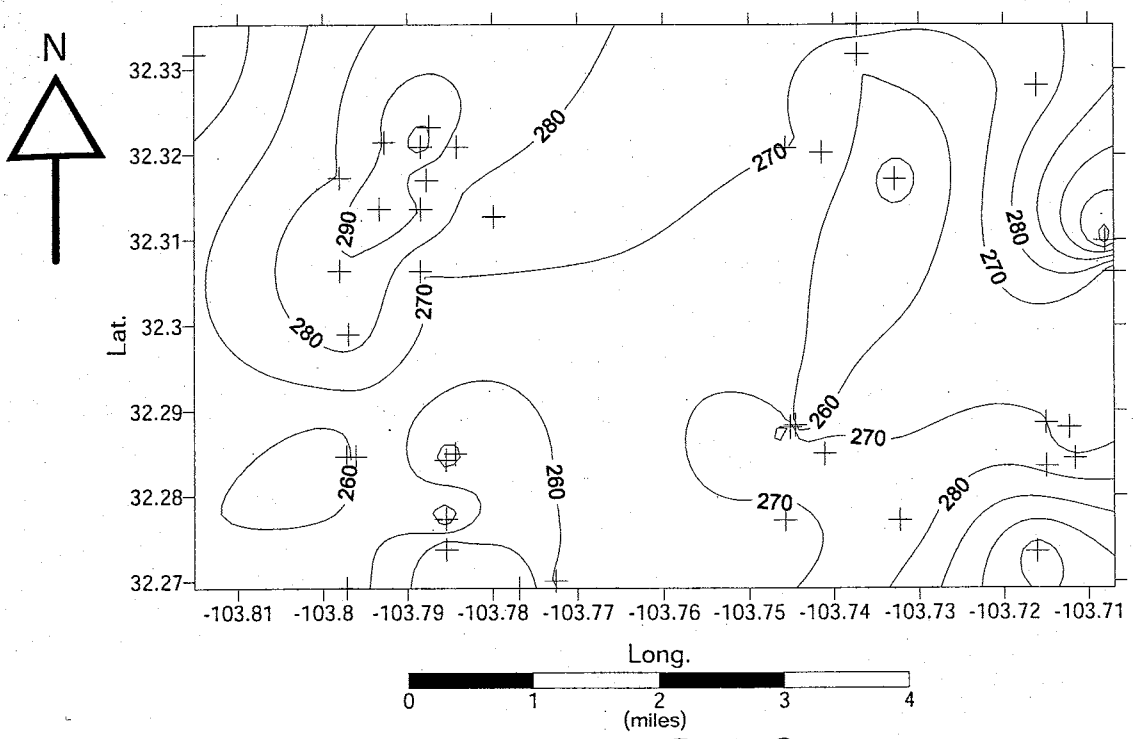

Figure 3.14: Eastern study area, isopach of the lower Brushy Canyon. Contour interval is 10 feet. (+ = well location)

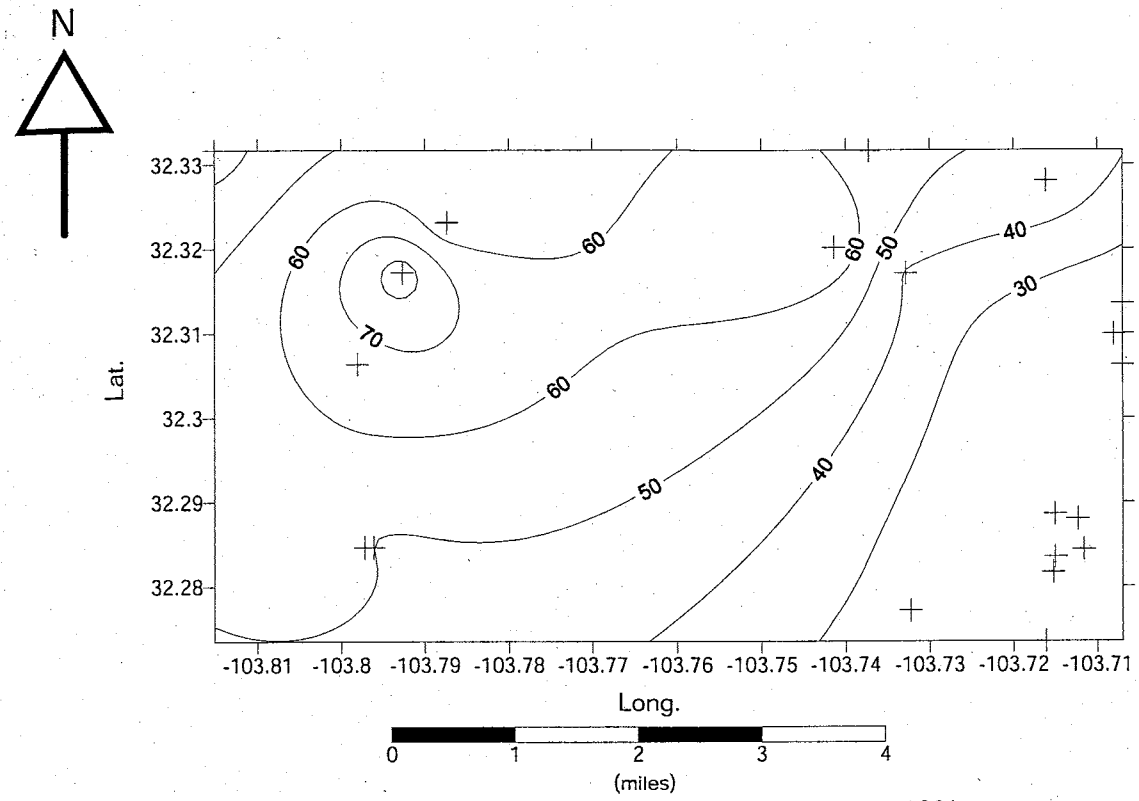

Figure 3.15: Eastern study area, net sand thickness of D unit with over 10% porosity. Contour interval is 10 feet. (+ = well location)

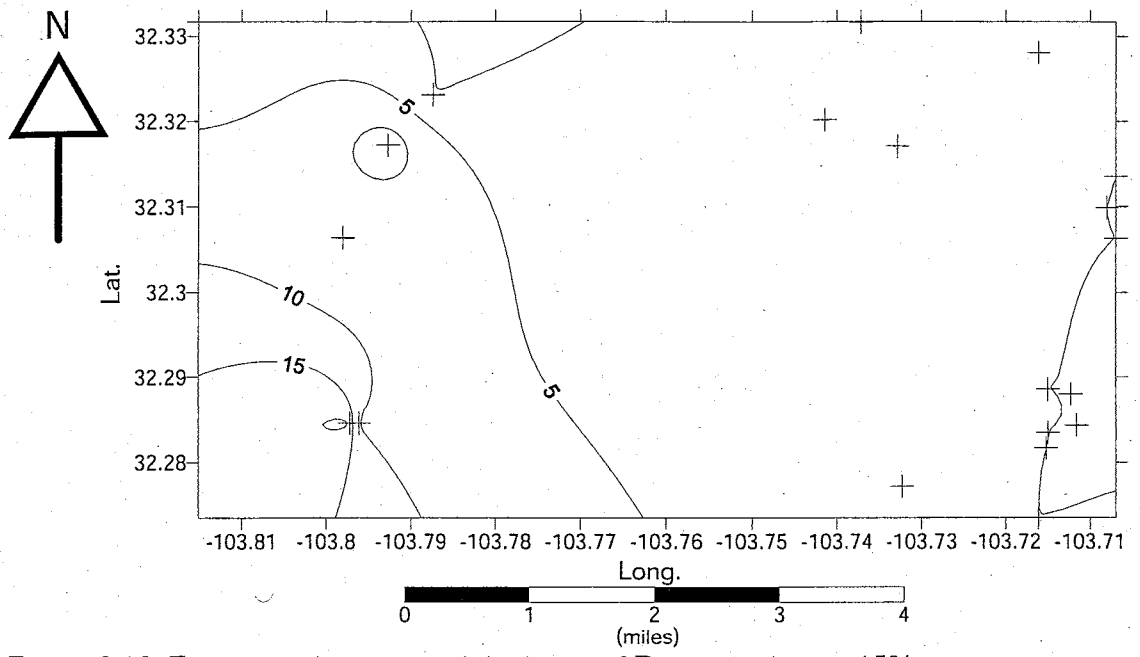

Figure 3.16: Eastern study area, sand thickness of D unit, with over 15% porosity. Contour interval is 5 feet. (+ = well location)

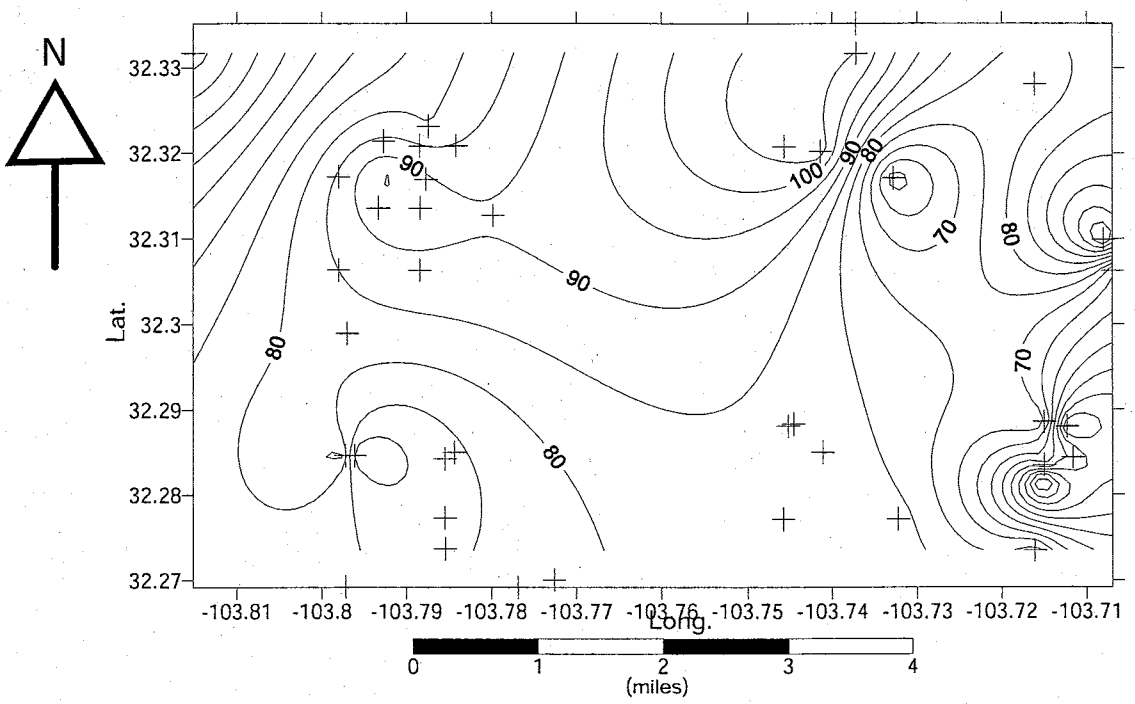

Figure 3.17: Eastern study area, net sand thickness of the D unit. Contour interval is 5 feet. (+ = well location)

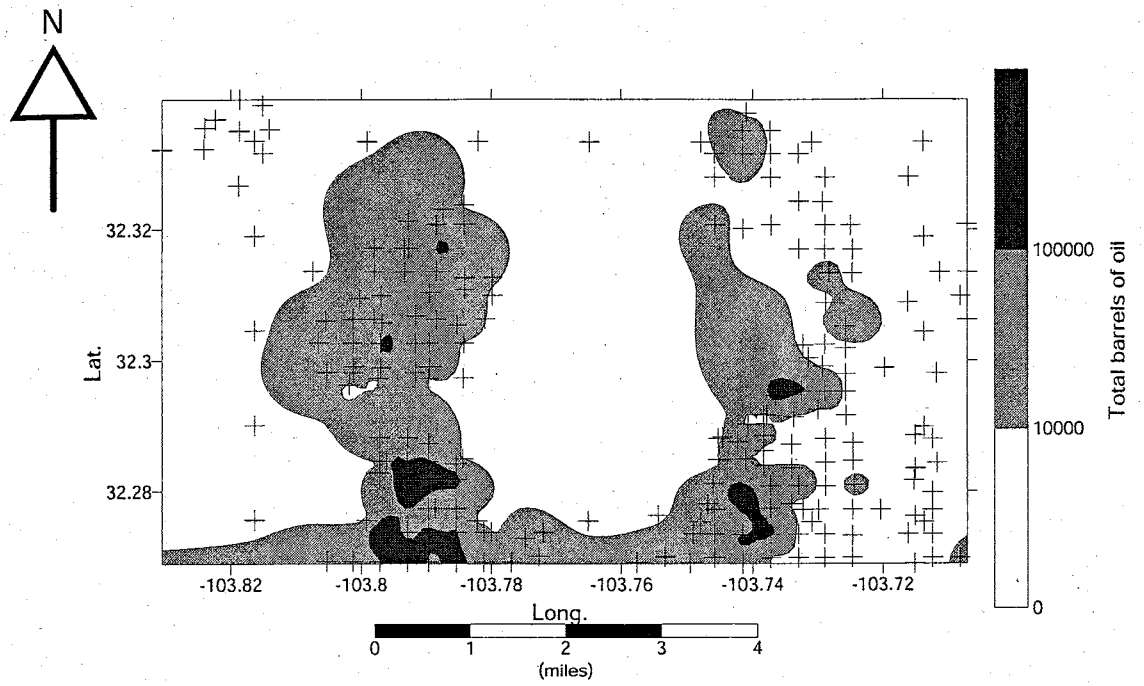

Figure 3.18: Eastern study area, cumulative oil production. Darkest areas indicate highest cumulative production volumes. (+ = well locations)

Water production in this region is much lower, when compared to the eastern trend (Livingston Ridge; Fig. 3.19). However, the Livingston Ridge trend is smaller and produces lower volumes of hydrocarbons.

3.4 WELL LOG CORRELATION

Well log correlation was used to create several cross sections from both the western and eastern areas as well as a cross section that connects the two study areas. These cross sections demonstrate that the lower Brushy Canyon is present throughout the entire study area. They also show that while small changes in thickness do occur, the unit's thickness remains essentially constant. Stratigraphically, the cross sections indicate slight differences between the two areas, mainly the pinching out of certain gamma and resistivity peaks and the stratigraphic position of certain beds, particularly within the B unit where the middle gamma peak appears higher in the column in the eastern area and stratigraphically lower in the western area. (Figs. 3.20, 3.21, 3.22, 3.23, 3.24, 3.25).

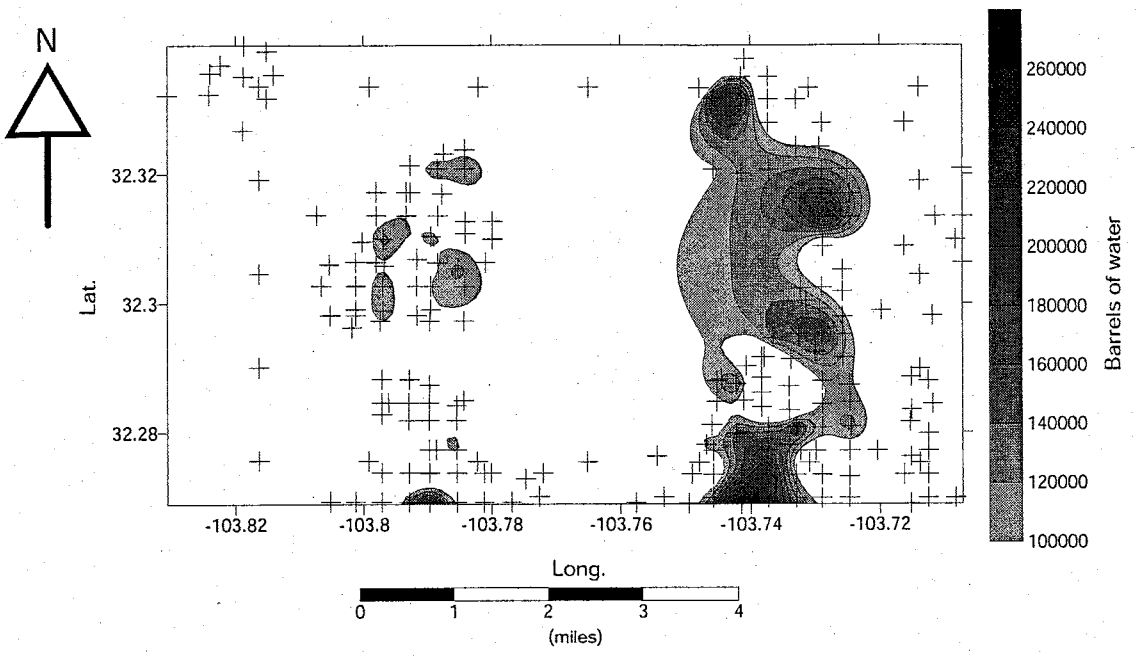

Figure 3.19: Eastern study area, cumulative water production. Darker areas indicate higher volumes of water. (+ = well location)

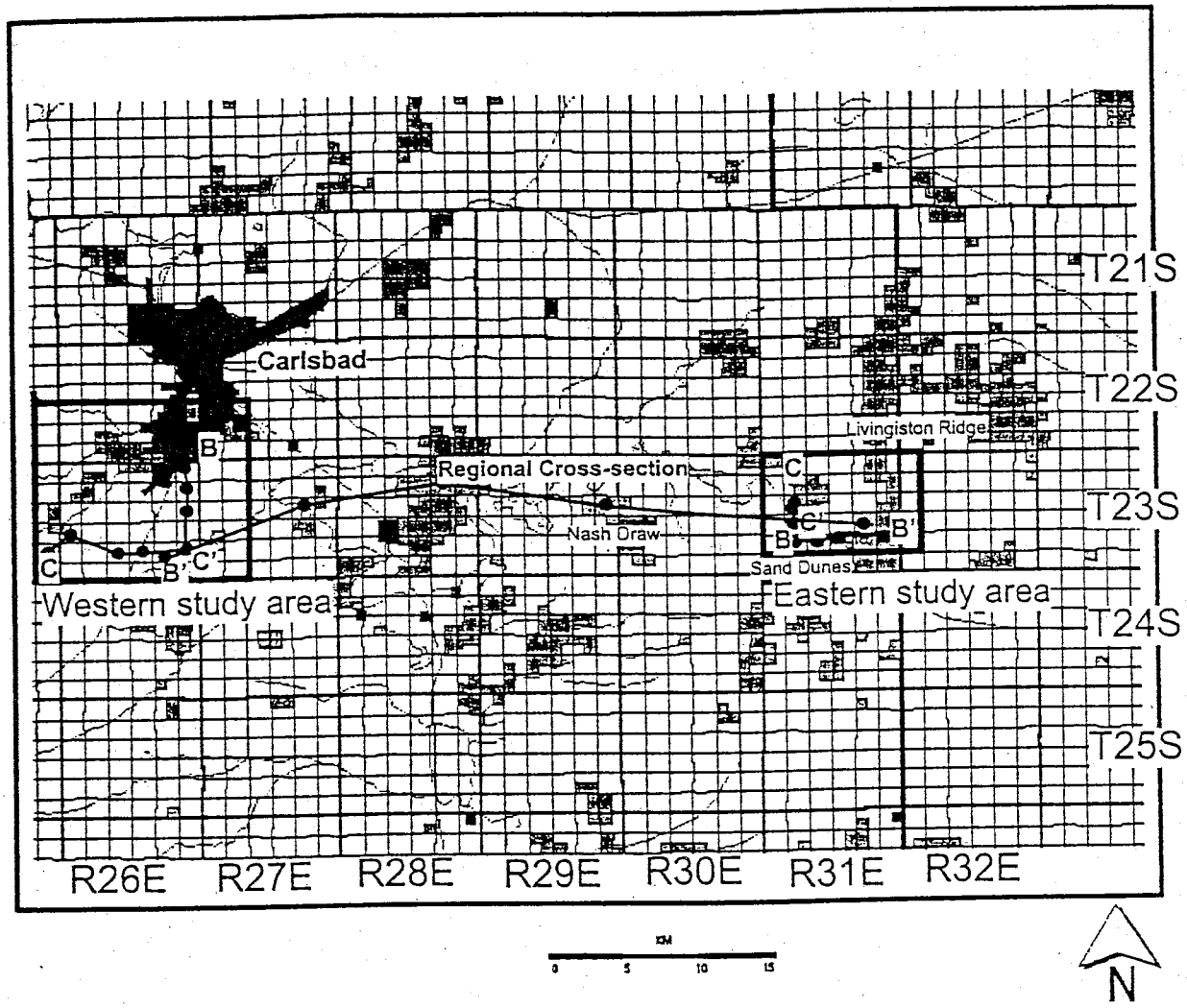

Figure 3.20: Cross section locations (basemap from Read, et al.,2000).

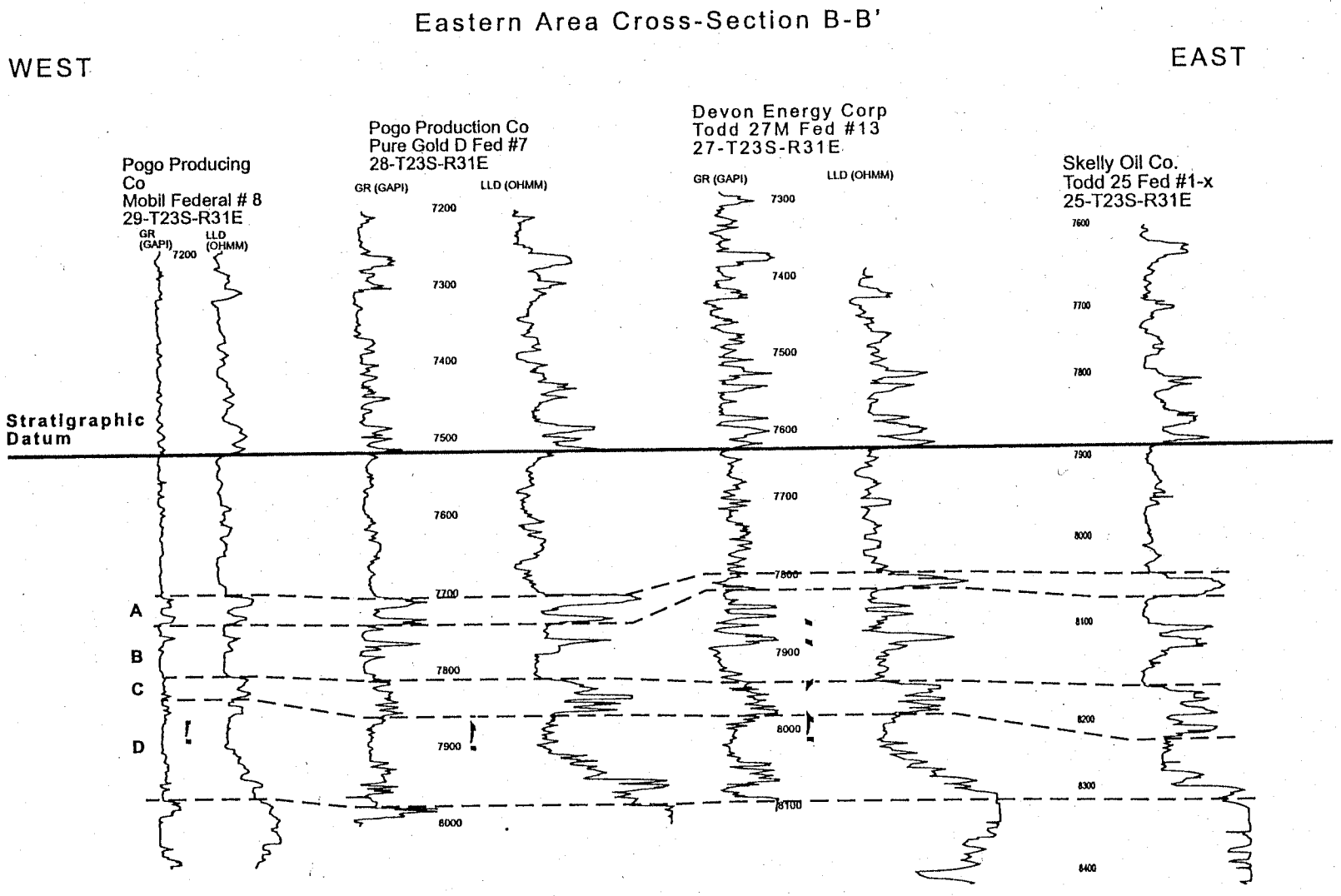

Figure 3.21: An eastern area, west to east cross section of the lower Brushy Canyon with all four units.

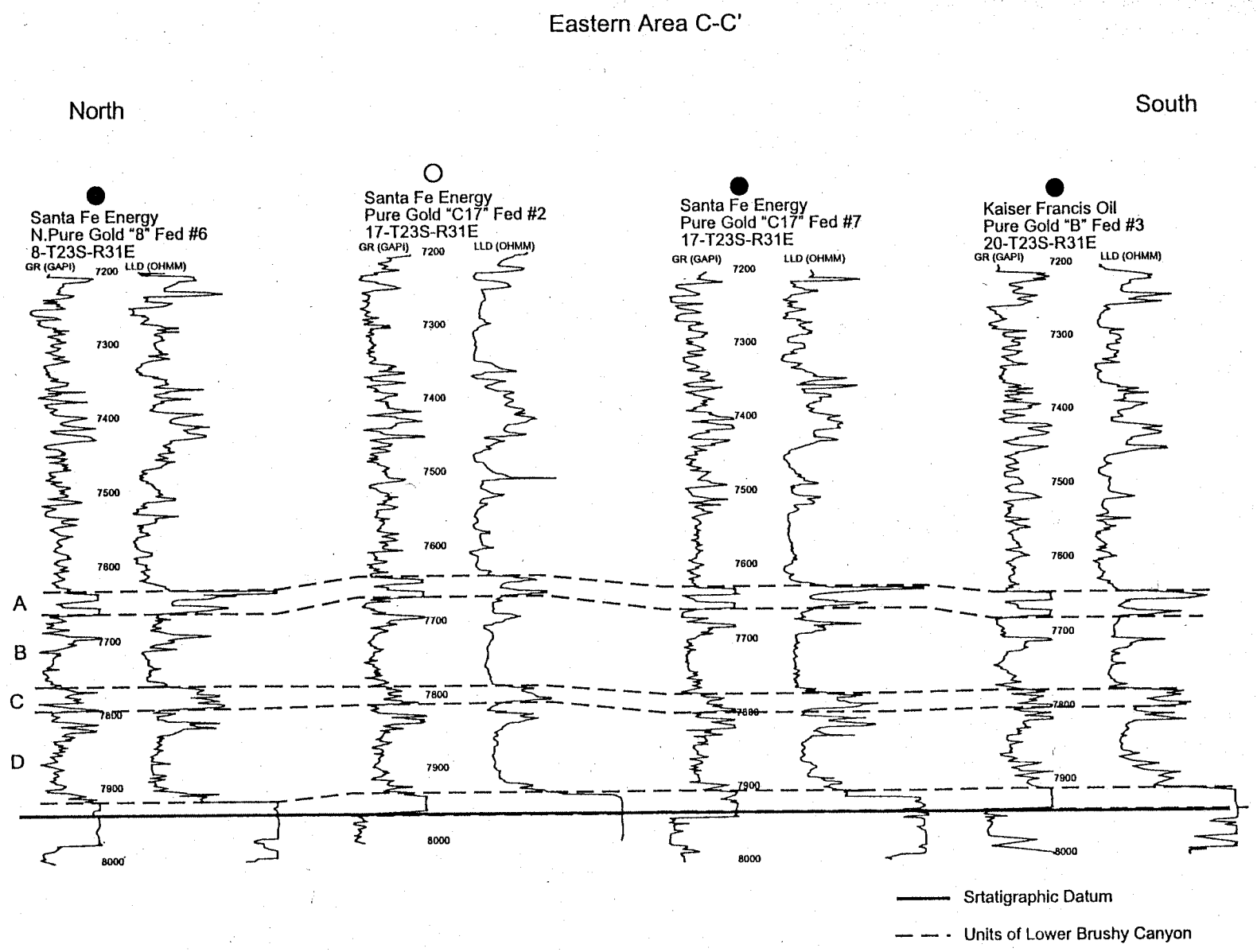

Figure 3.22: A north- south cross section of the eastern study area. All four units of the lower Brushy Canyon are marked. Here the datum is the top of the Bone Spring Formation.

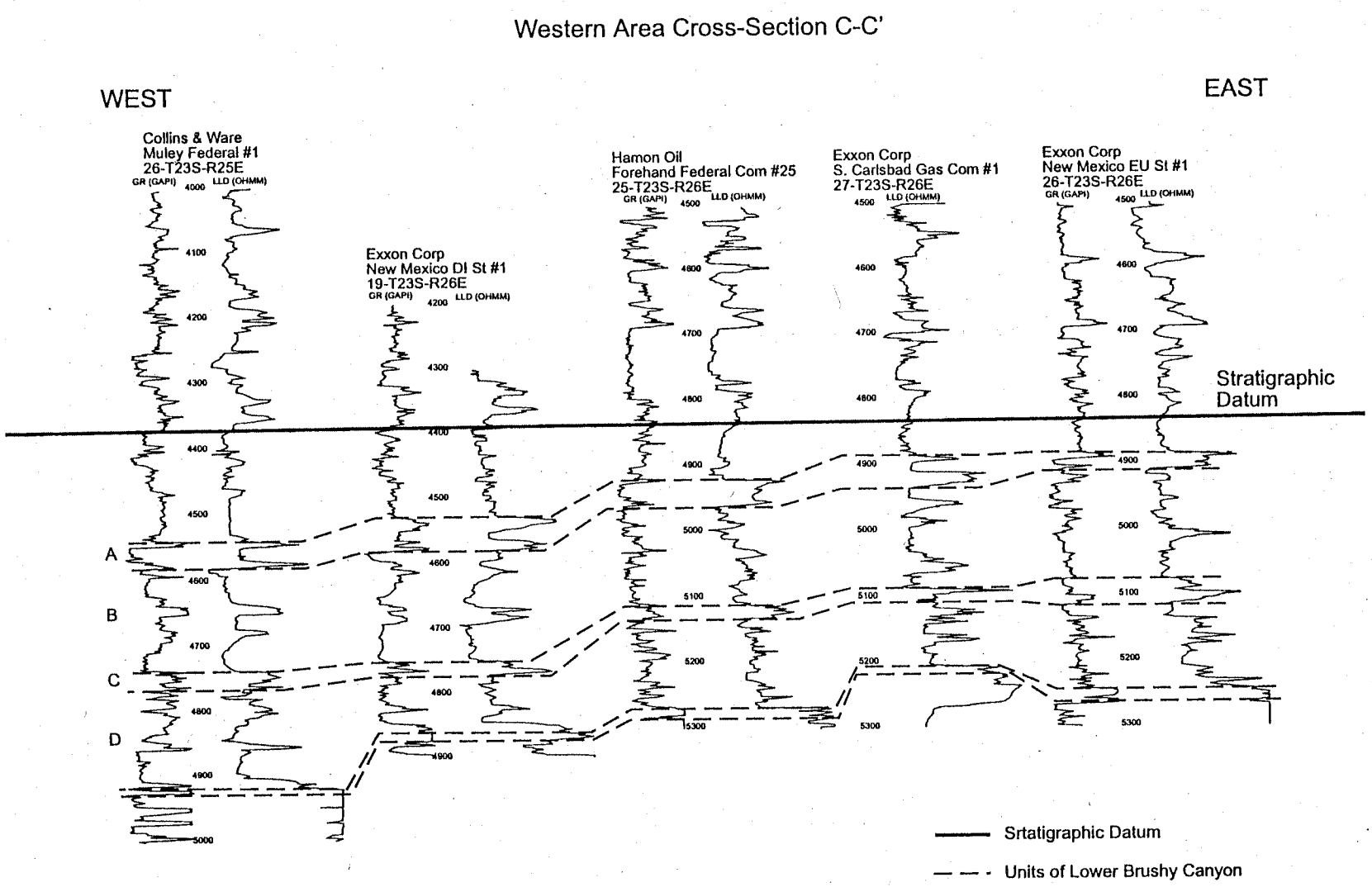

Figure 3.23: A cross section of the western study area. This is an west to east view of the lower Brushy Canyon.

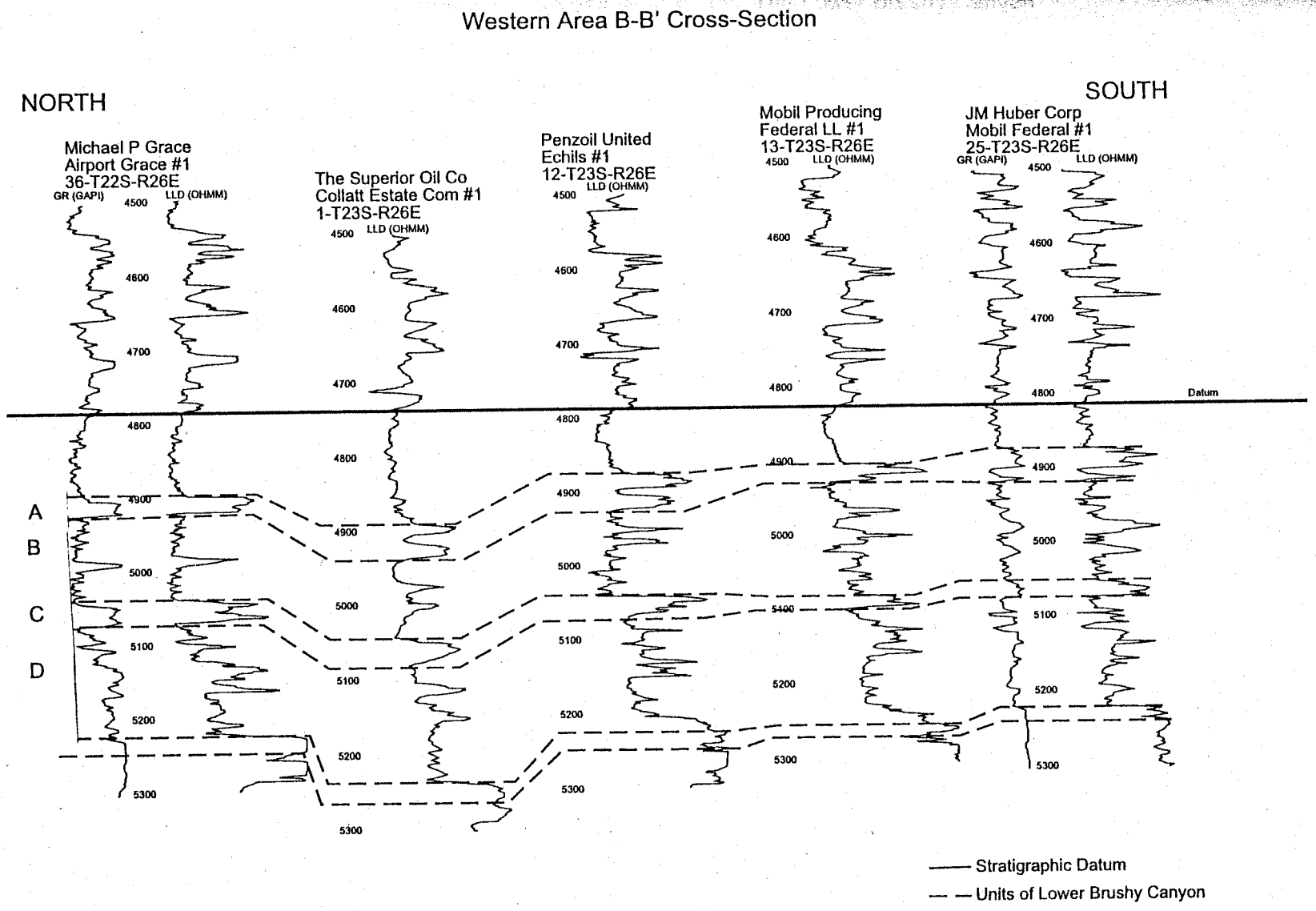

Figure 3.24: A north-south cross section of the lower Brushy Canyon, in the western study area.

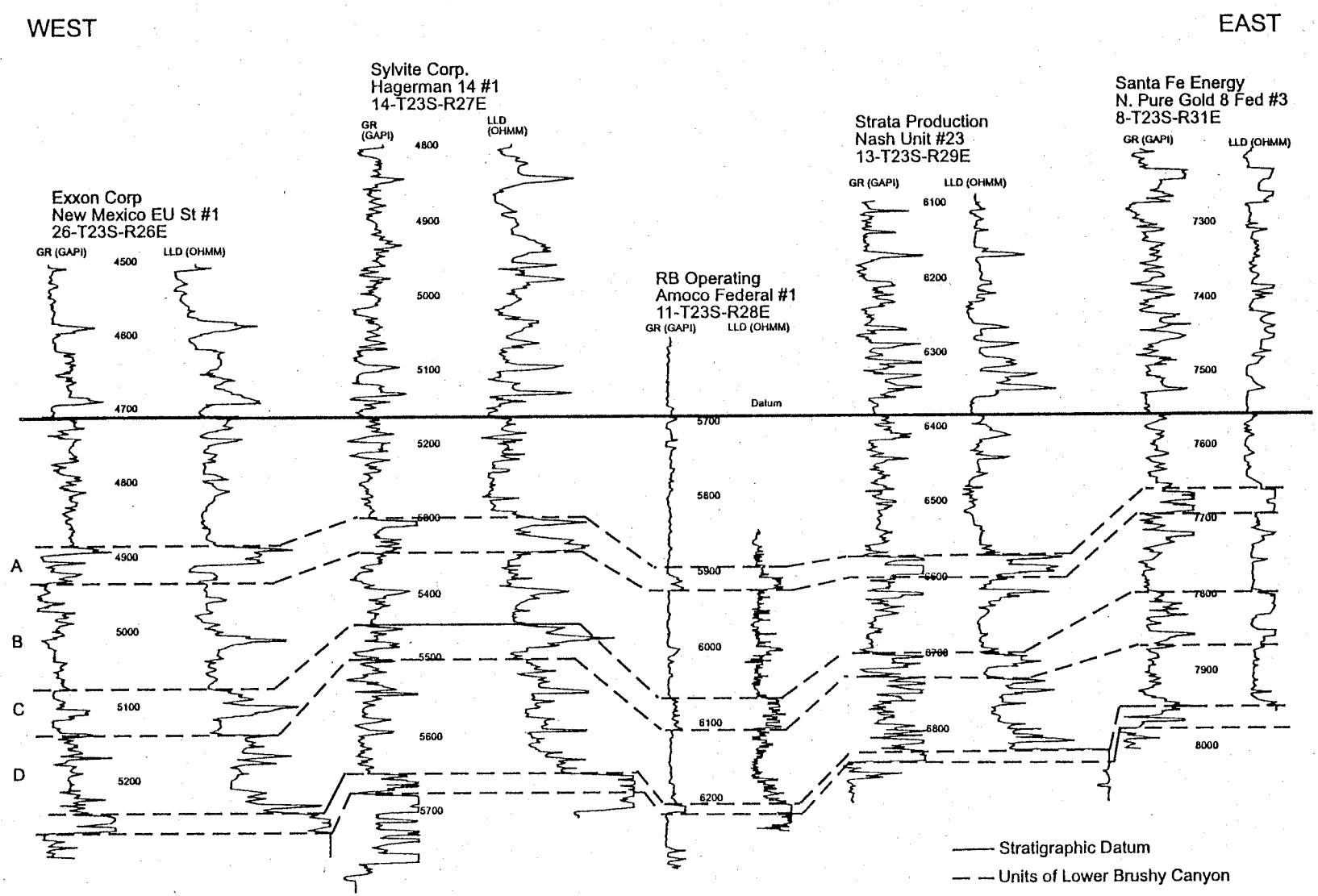

Figure 3.25: Regional west-east cross section of the lower Brushy Canyon. This cross section runs between the two study areas.

3.5 POROSITY REDUCTION IN THE LOWER BRUSHY CANYON

Several components that may be responsible for the reduction of porosity include kerogen, framework grains, clay matrix and calcite cement. Point count results of these components were plotted against porosity in order to determine which components were major factors in reducing porosity. When kerogen and framework grains were plotted against porosity no correlation could be seen. However, when clay matrix and calcite cement were combined, they showed a very strong correlation when plotted against porosity (Table 3.1).

Table 3.1: Correlation coefficients of kerogen, framework grains, clay matrix and calcite cement versus porosity. This table indicates that neither, kerogen or framework grains play a very important role in the reduction of porosity. Clay matrix and calcite cement combined have a strong R^2 value indicating that they play a major role in the reduction of porosity.

	Kerogen versus Porosity	Framework Grains versus Porosity	Clay Matrix versus Porosity	Calcite Cement versus Porosity	Clay Matrix + Calcite Cement versus Porosity
Correlation Coefficient (R^2)	.1037	.0246	.3946	.6646	.7454

As shown in table (3.1), the presence of clay matrix and calcite cement play a major role in the reduction of porosity. In the lower Brushy Canyon, this relationship is easily identified. Porosity decreases as the percentage of clay matrix and calcite cement increases. By studying individual wells, it is apparent that clay matrix and calcite cement reduce the porosity (Figs. 3.26, 3.27).

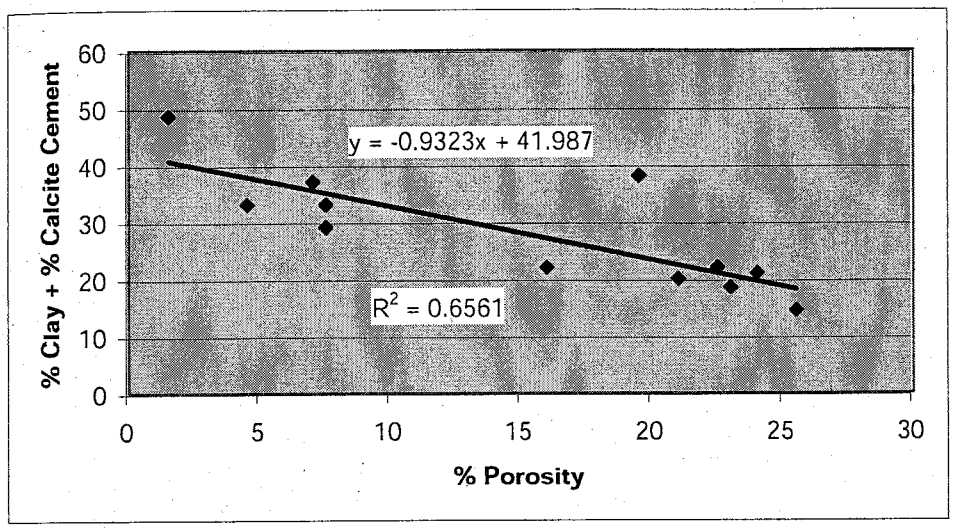

Figure 3.26: Graph of %porosity versus %clay + %calcite cement, Nash Draw Unit 23. As the clay and calcite increase, the porosity on the X-axis decreases. This data is taken from thin section point counts from the Nash Draw Unit 23 well.

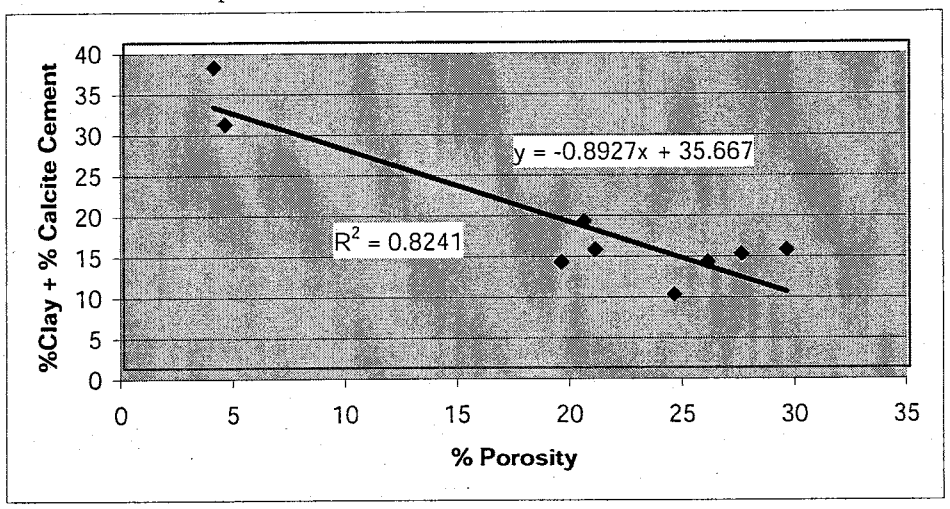

Figure 3.27: Graph of %porosity versus %clay + %calcite cement, Poker Lake Unit 80. This graph of point count data from the Poker Lake Unit 80 well also show how porosity decreases as clay and calcite increase.

From these two graphs (Figs. 3.26 & 3.27) it is apparent that the presence of clay matrix and calcite cement within the lower Brushy Canyon siltstones greatly reduces porosity. The slope of the line doesn't appear to be constant from one well to the next. However, when all four wells are plotted, it becomes apparent that clay matrix and calcite cement have a very direct effect in the reduction of porosity within the lower Brushy Canyon (Fig. 3.28). Data from the Amoco Federal 1 well and the South Culebra Bluff 5

well are not displayed separately due to the lack of data points. Point count data from these wells are included below where all the well data are combined.

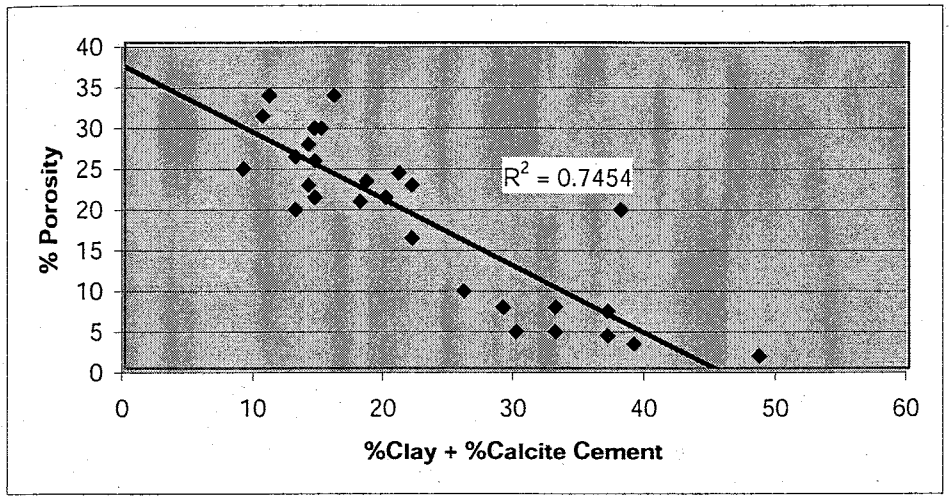

Figure 3.28: Graph of %porosity versus %clay + %calcite cement, all data. This graph combines point count data from all four wells. Note how porosity decreases as the percent clay and calcite increase.

Importance of Clay Matrix and Calcite Cement

In showing how clay matrix and calcite cement are responsible for the reduction of porosity it is also important to show how each component individually reduces porosity. The following set of graphs show the importance of each component separately, and the role each plays in the reduction of porosity.

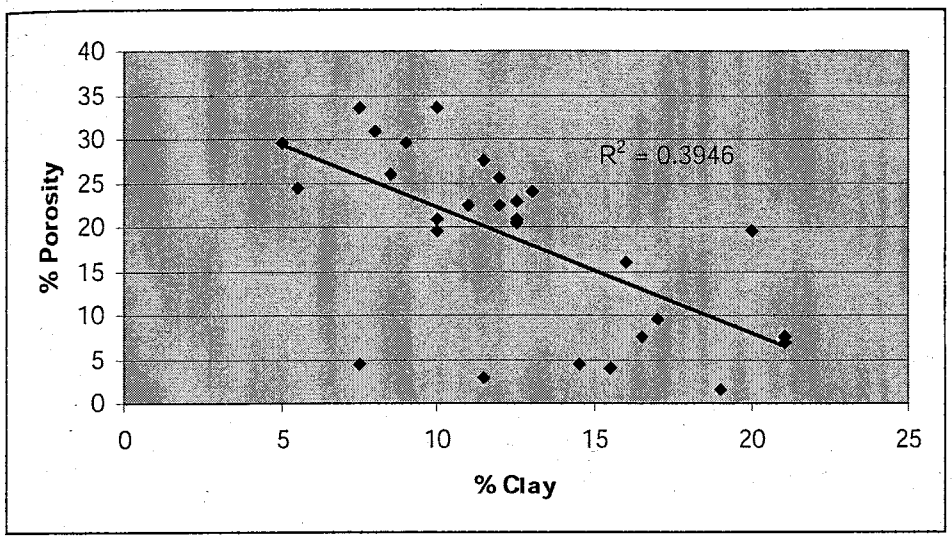

Figure 3.29: Graph of %porosity versus %clay. Shows little relationship between clay and porosity.

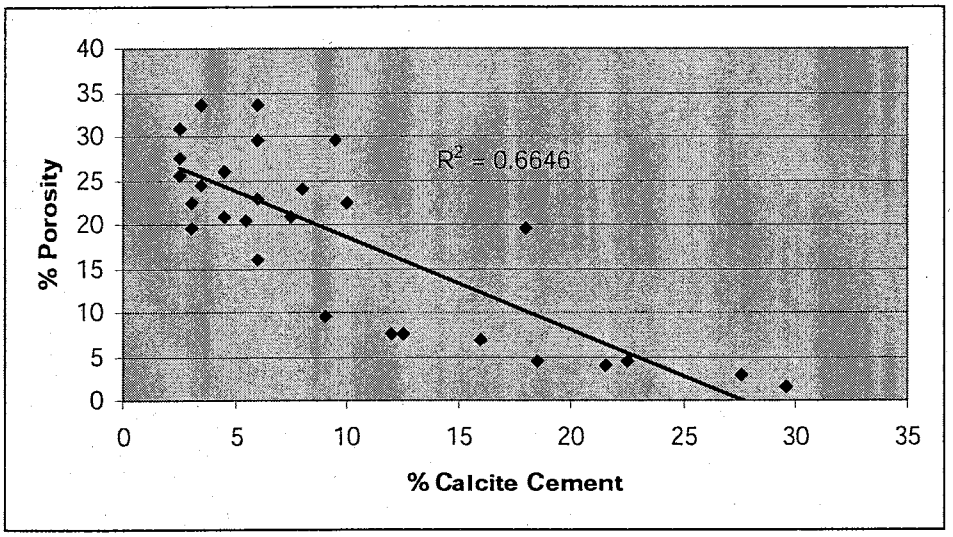

Figure 3.30: Graph of %porosity versus %calcite cement. Shows a strong relationship between calcite cement and porosity.

These figures (3.29 &3.30) indicate that calcite cement plays a more important role in the reduction of porosity than clay matrix. However, if points with high gamma ray values are separated from points with low gamma ray values the relationship between clay matrix and porosity becomes stronger as does the relationship of calcite cement and

porosity (Figs. 3.31, 3.32).

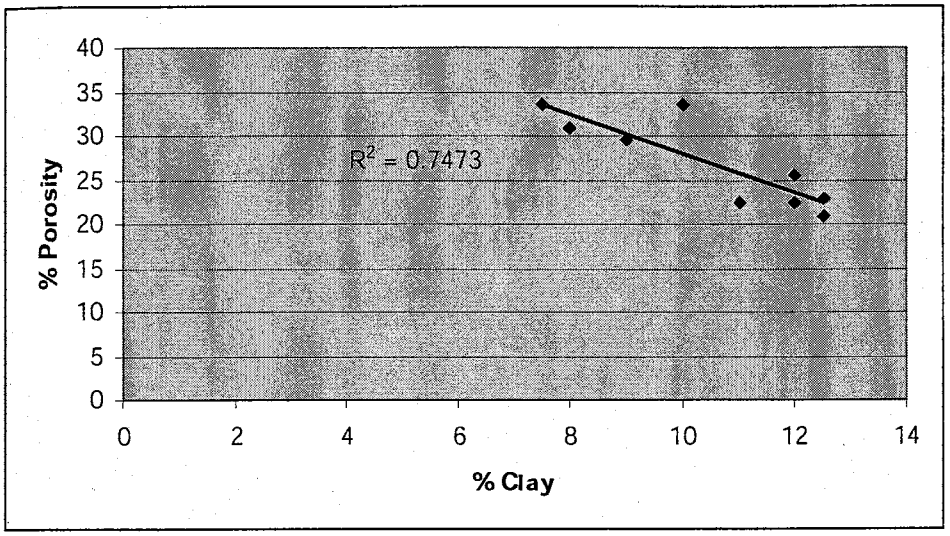

Figure 3.31: Graph of %porosity versus %clay, in siltstones with less than 50 Gamma Ray Units (GAPI). This graph indicates a very strong relationship between porosity and clay in low gamma siltstones.

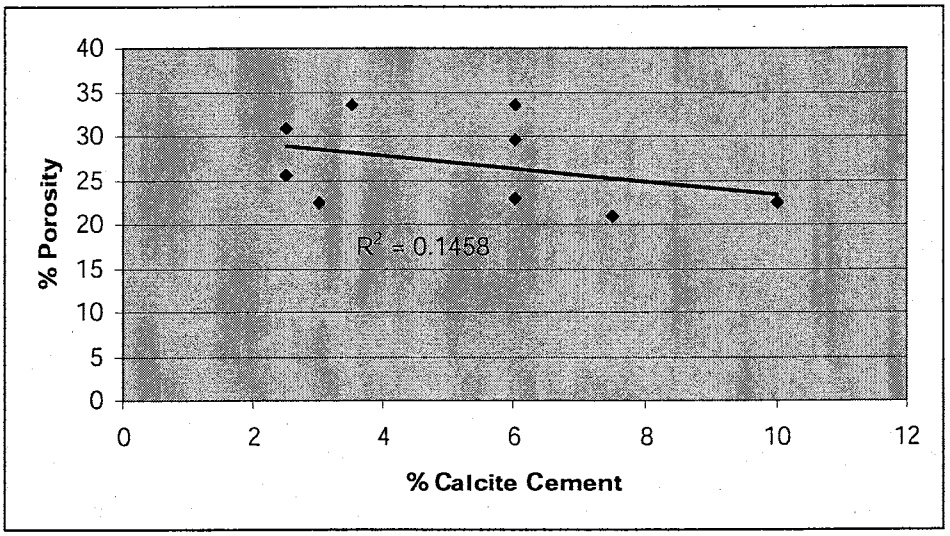

Figure 3.32: Graph of %porosity versus %calcite cement, in siltstones with less than 50 GAPI. Shows that for low gamma ray siltstones there is almost no correlation between porosity and calcite cement.

The previous graphs (3.31 & 3.32) indicate that for low gamma ray siltstones (less than 50 GAPI) clay matrix is a more important factor in porosity reduction than calcite cement. For siltstones with higher gamma ray (greater than 50 GAPI) calcite cement is responsible for porosity reduction (Figs. 3.33, 3.34).

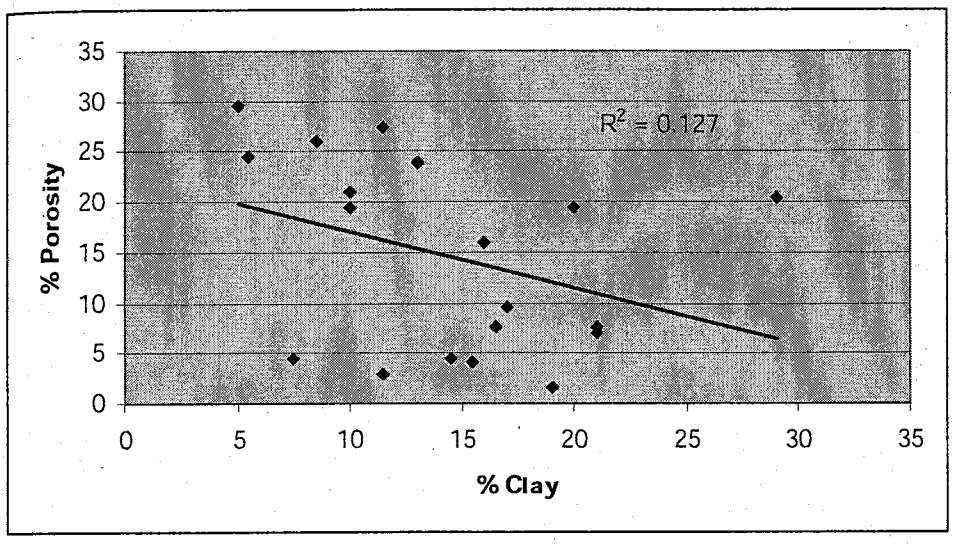

Figure 3.33: Graph of %porosity versus %clay for gamma ray values over 50 GAPI. This indicates no relationship between porosity and clay for siltstones with high gamma ray.

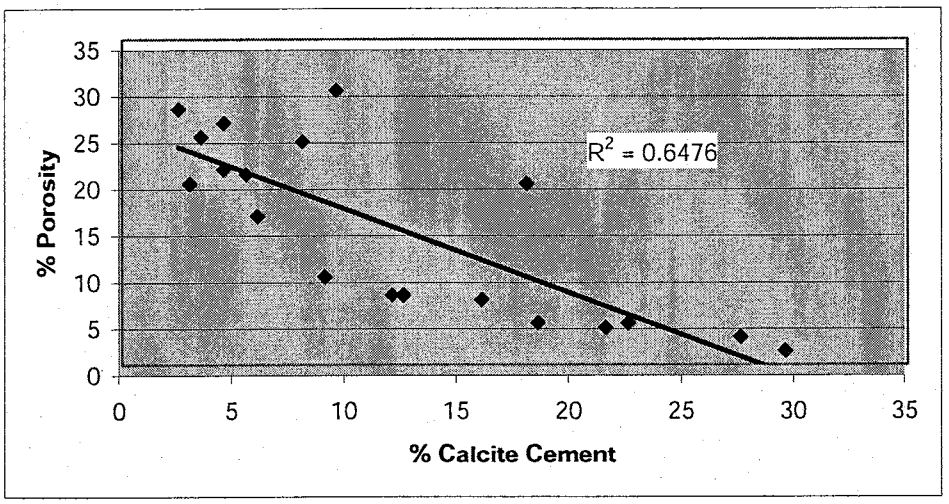

Figure 3.34: Graph of %porosity versus %calcite cement for gamma ray values over 50 GAPI. This graph shows a strong relationship between calcite cement and porosity for high gamma ray siltstones.

From figure 3.30 it would appear that calcite cement appears to be a dominant control on porosity in all siltstones. This only occurs because a majority of the samples are over 50 GAPI. We can also conclude that when calculating clay content from the gamma ray curve, our values are only accurate for points with less than 50 GAPI.

3.6 RELATIONSHIP BETWEEN WELL LOGS AND ROCK PROPERTIES

Well logs measure several different types of properties, including rock properties and fluid properties. In this section the relationship between the gamma ray curve and both clay content and porosity will be discussed.

Gamma Ray Curve Versus Clay Content

The gamma ray log measures the intensity of radioactivity emitted from a rock. In clastic rocks like those of the lower Brushy Canyon, radioactive elements tend to be concentrated in clay minerals. Therefore, the gamma ray curve should indicate the amount of clay matrix present within the rock. In order to confirm this, the percent clay content from point counts was plotted against the gamma ray intensity (GAPI) (Fig. 3.35). Distinguishing each sample by grain size as either a siltstone or sandstone showed no strong relationship between the clay content and the gamma ray curve.

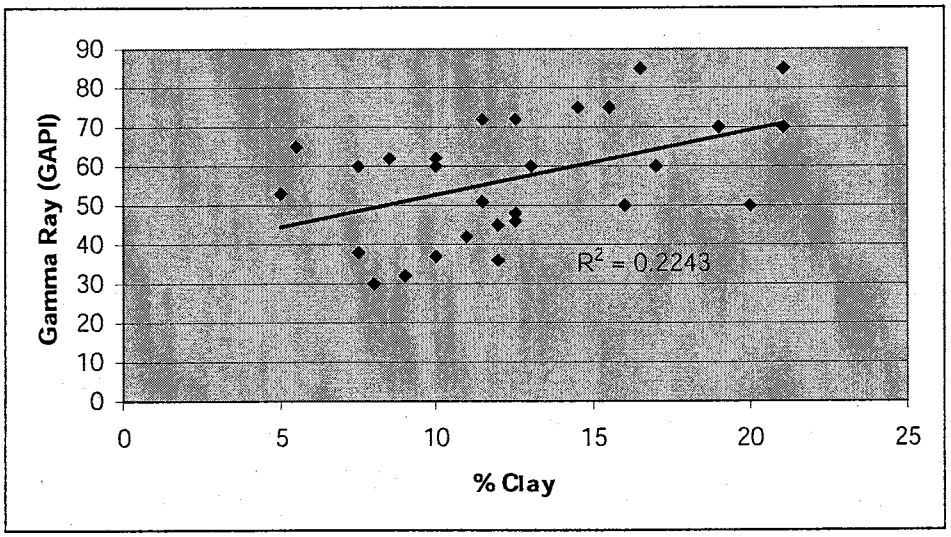

Figure 3.35: Gamma ray versus %clay, all data. This graphs shows the lack of a relationship between clay content and the gamma ray curve.

This graph (Fig. 3.35) shows that no obvious relationship can be drawn between the gamma ray curve and clay content. However, when graphing the same data and

excluding points above 50 GAPI, which don't affect porosity (Fig. 3.33), it appears that gamma ray values below 50 GAPI have a much stronger correlation to clay content (Fig. 3.36). Siltstones with gamma ray values above 50 GAPI show almost no statistical correlation to clay content (Fig. 3.37).

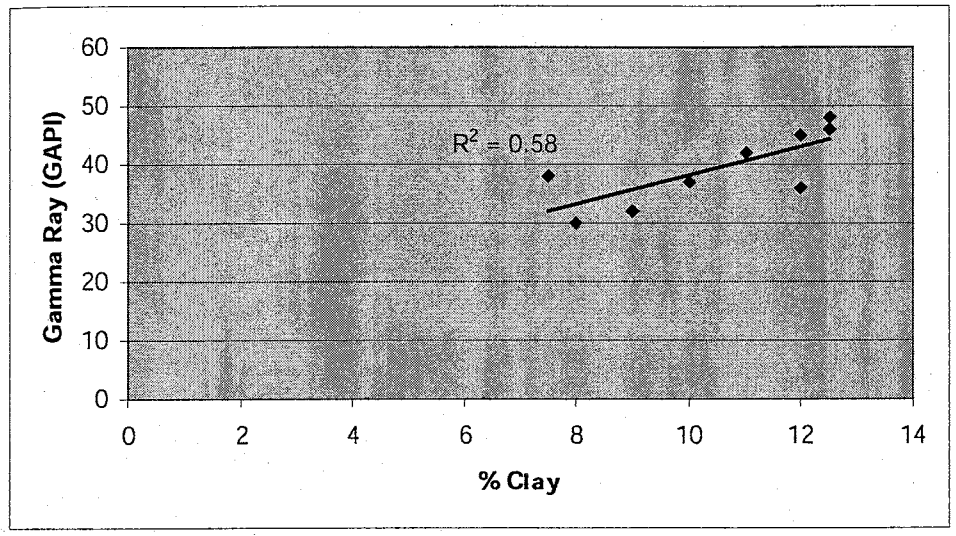

Figure 3.36: Gamma ray versus %clay, gamma ray values less than 50 GAPI. This shows that as clay content increases the gamma ray intensity also increases.

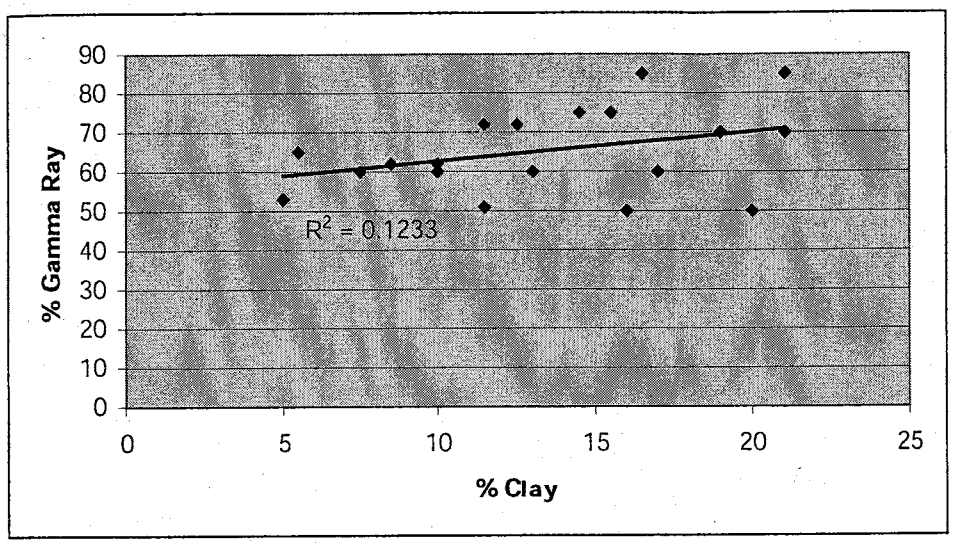

Figure 3.37: Gamma ray versus %clay, gamma ray values greater than 50 GAPI. Here the relationship between clay and gamma ray is not apparent.

Gamma Ray Curve Versus Calcite Cement

Calcite cement is also largely responsible for the reduction of porosity in the reservoir rock as discussed previously. Using well logs to estimate calcite cement does not seem possible with the suite of logs that are available. Sonic logs could possibly be used to calculate the amount of calcite cement present in sandstone, however these logs are not readily available for the wells of this data set. Sonic logs may work because they would identify changes in the density of the rock, which in many cases is related to the degree of cementation of the rock. As can be seen from figure (3.38) there is no noticeable relationship between the gamma ray curve and calcite cement.

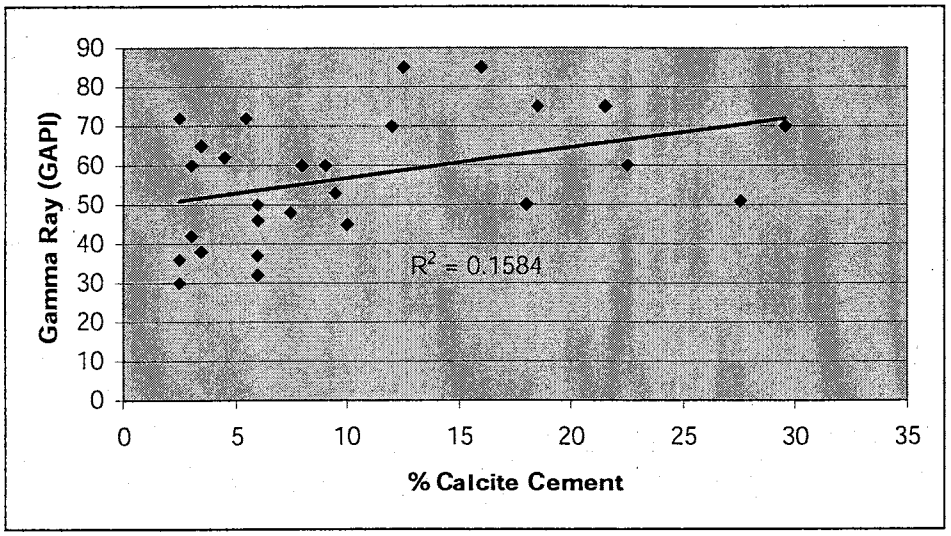

Figure 3.38: Gamma ray versus %calcite cement, all data. There is no noticeable correlation between calcite cement and the gamma ray curve.

The following graph shows that there is no relationship between clay content and calcite cement (Fig. 3.39).

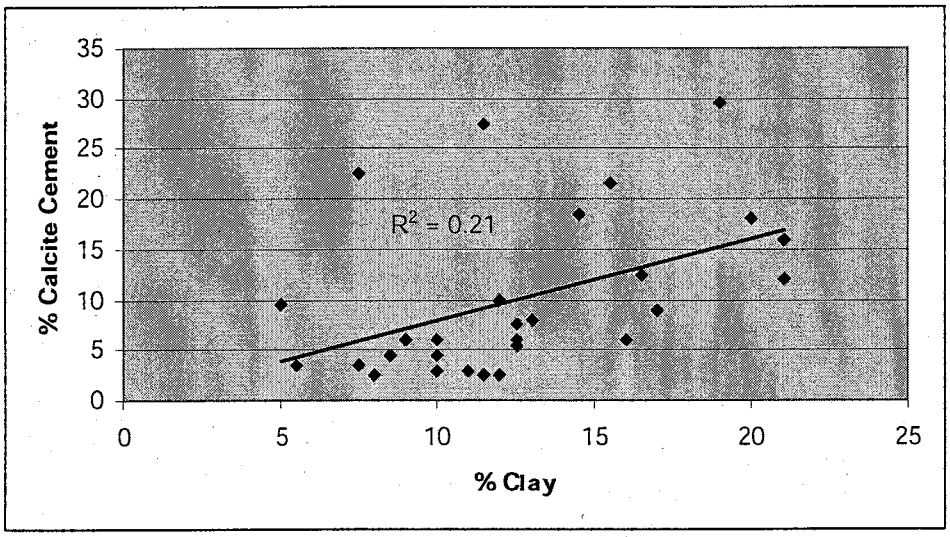

Figure 3.39: Graph of %calcite cement versus %clay, all data. There is no distinct relationship between calcite cement and clay that can be interpreted from this graph.

Gamma Ray Curve Verses Porosity

As discussed earlier in the petrography section, it is apparent that clay matrix and calcite cement reduce porosity. Therefore it should be possible to estimate porosity utilizing the gamma ray curve (Fig. 3.40).

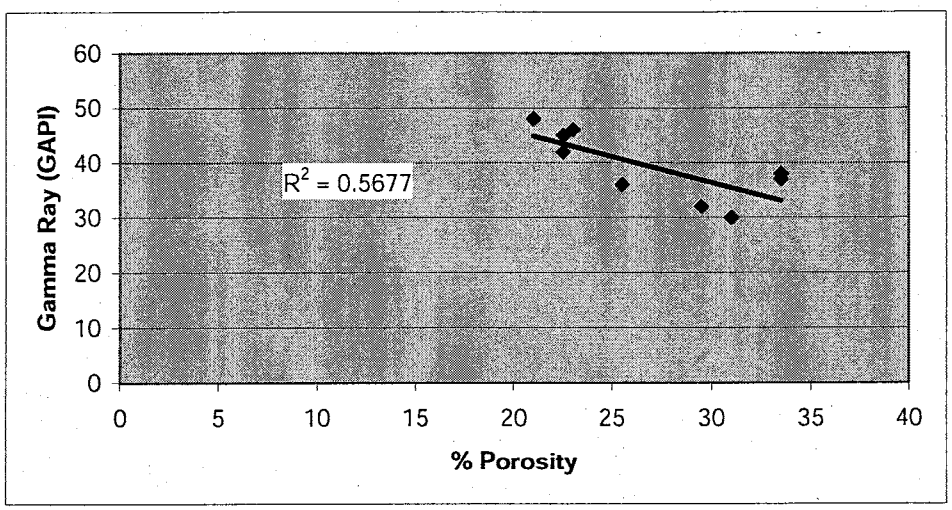

Figure 3.40: Graph of gamma ray versus %porosity, for gamma ray values less than 50 (GAPI).

Figure 3.40 shows that as porosity increases on the X-axis, the gamma ray curve decreases on the Y-axis. This relationship is expected due to the relationship between gamma ray and clay content and between porosity and clay content. It is clear that using the gamma ray log to estimate actual rock properties is viable in the lower Brushy Canyon, particularly for rocks with gamma ray values less than 50 GAPI units.

3.7 CREATING ARTIFICAL CLAY PERCENT LOGS

Artificial clay percent logs were created in order to map areas of low clay content and therefore attempt to locate areas within the lower Brushy Canyon where hydrocarbons would be likely to accumulate.

Utilizing the relationship between the gamma ray curve and percent clay matrix that was determined by point counts, an artificial well log of clay content in siltstones was created at one-half foot intervals using the formula:

Percent Clay = (Gamma Ray Value- 6.5122)/3.7491

This formula was determined by graphing thin section data points, but excluding those with gamma ray values greater than 50 GAPI. These data points were excluded because it was apparent that clay matrix is not the primary control on porosity reduction for siltstones with greater than 50 GAPI. For siltstones with greater than 50 GAPI calcite cement is more influential in reducing porosity. As previously discussed calcite cement cannot be estimated from the gamma ray log. This did not affect the results because data were only acquired from low clay content units, and gamma ray values over 50 GAPI don't indicate a low clay content. Following the calculation of percent clay matrix, the net thickness of sandstone with less than 10 percent and less than 12.5 percent estimated clay content were calculated for each stratigraphic unit. Average gamma ray values for each unit in each well were also calculated for later analysis.

4.0 DISCUSSION

4.1 DEPOSITIONAL HISTORY

The depositional history of the lower Brushy Canyon is complex. Harms and Brady (1996) pointed out that understanding the depositional environment is important in how hydrocarbon exploration is approached throughout the basin. It is necessary to understand how sediment is deposited, because the depositional environment controls the distribution, orientation, and quality of the reservoir. This is particularly important in the lower Brushy Canyon as the depositional environment determines many factors such as clay content, porosity, and trapping mechanisms.

Sequence Stratigraphy

The entire Brushy Canyon Formation is a lowstand sequence set, composed of third order, deep-water sandstones and siltstones (Fig. 4.1) (Beaubouef et al., 1999). A lowstand sequence set is deposited during a time of low relative sea level. These sequences often contain slope fans, basin floor fans, and a lowstand wedge (Miall, 1997). The lower Brushy Canyon is part of the basin floor fan of this system. The formation was deposited during exposure and bypass of the adjacent carbonate shelf (Beaubouef et al., 1999). This system was highly channelized as can be seen in the B and D units in each cross-section (Figs. 4.2 & 4.3). The small scale of the study area restricts the ability to trace the channels.

The lower Brushy Canyon can be divided into four separate depositional sequence sets. A sequence set is a group of genetically related strata (Mitchum et al., 1977). Each sequence set starts from directly above a condensed shale unit, indicated on the well logs by a high gamma ray reading. A condensed interval is a depositional bed that represents

a period of maximum flooding. The condensed intervals are deposited slowly over a long period of time; therefore, they tend to be organic rich shales. The high organic content of these shales explains the extremely high gamma ray reading.

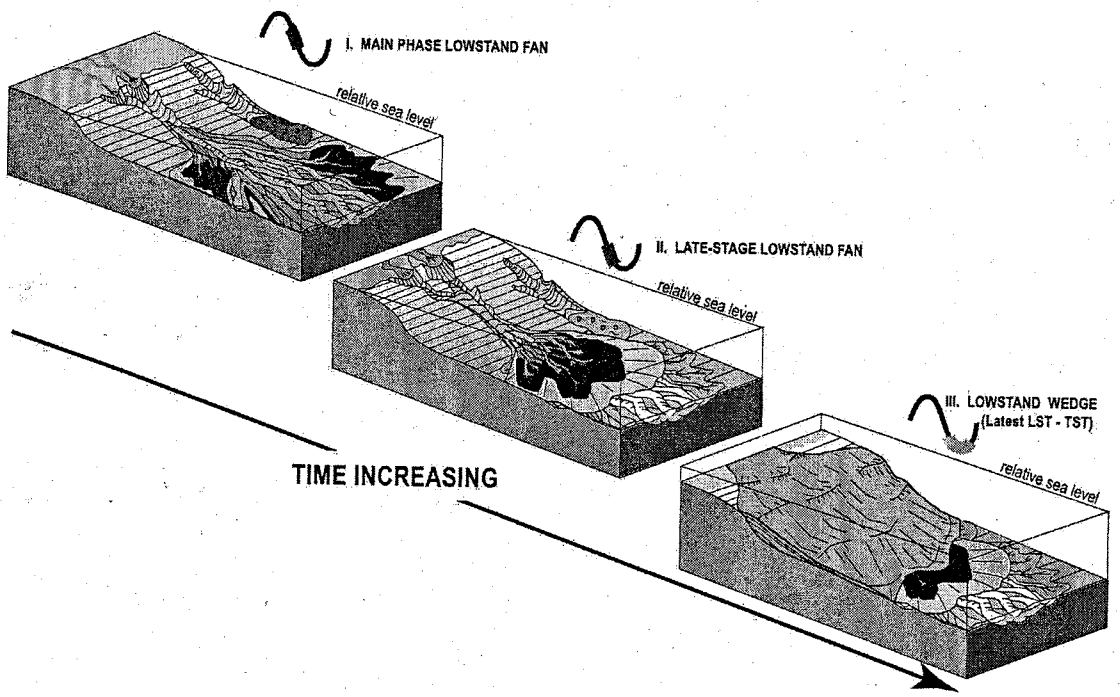

Figure 4.1: Interpreted depositional environment of the Brushy Canyon Formation. Shows deposition of the lowstand fan as sea level falls (from Beaubouef et al. 1999).

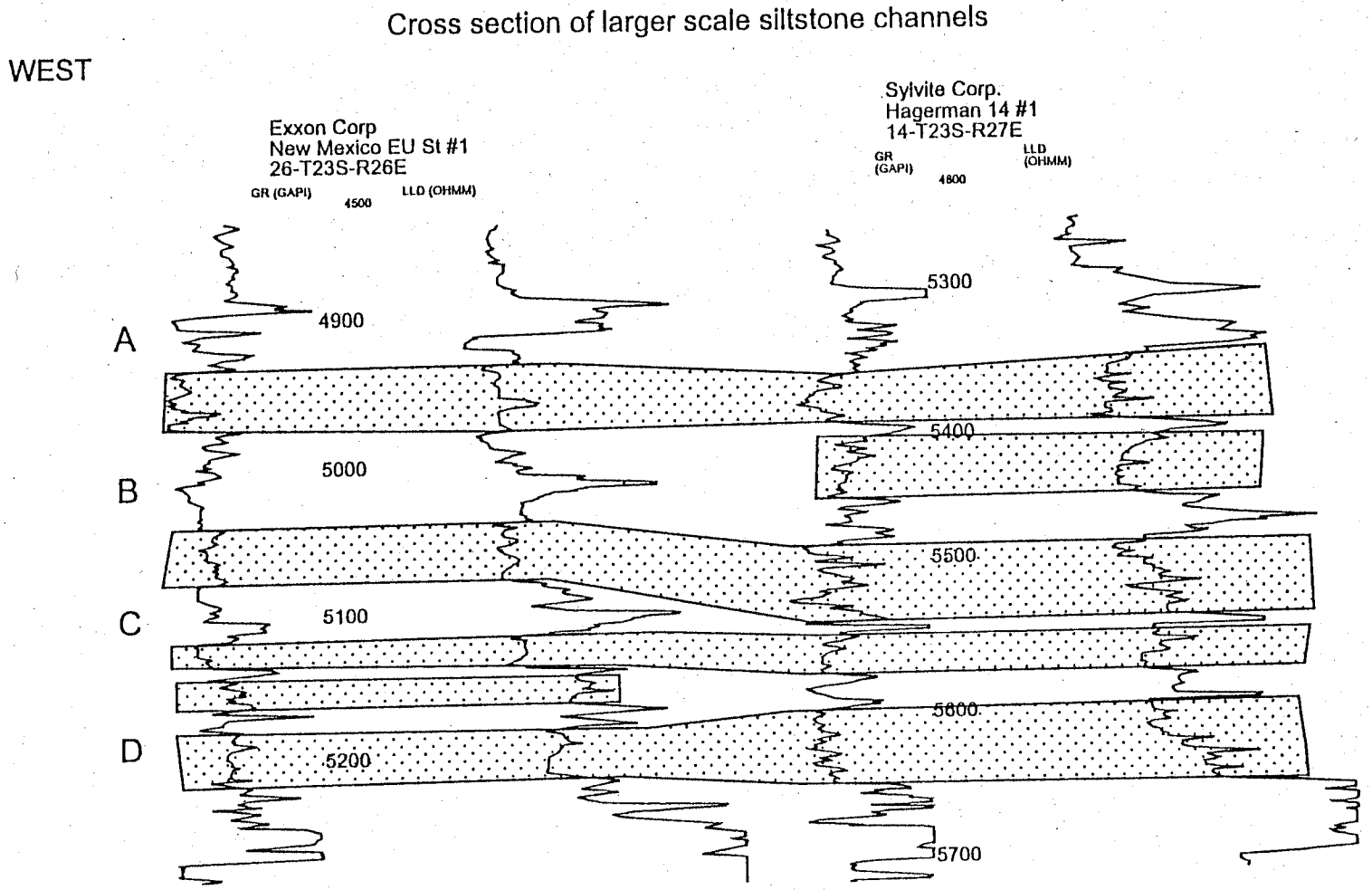

Figure 4.2: Central portion of the regional cross section (Fig. 3.25) where the thicker channel sands are highlighted.

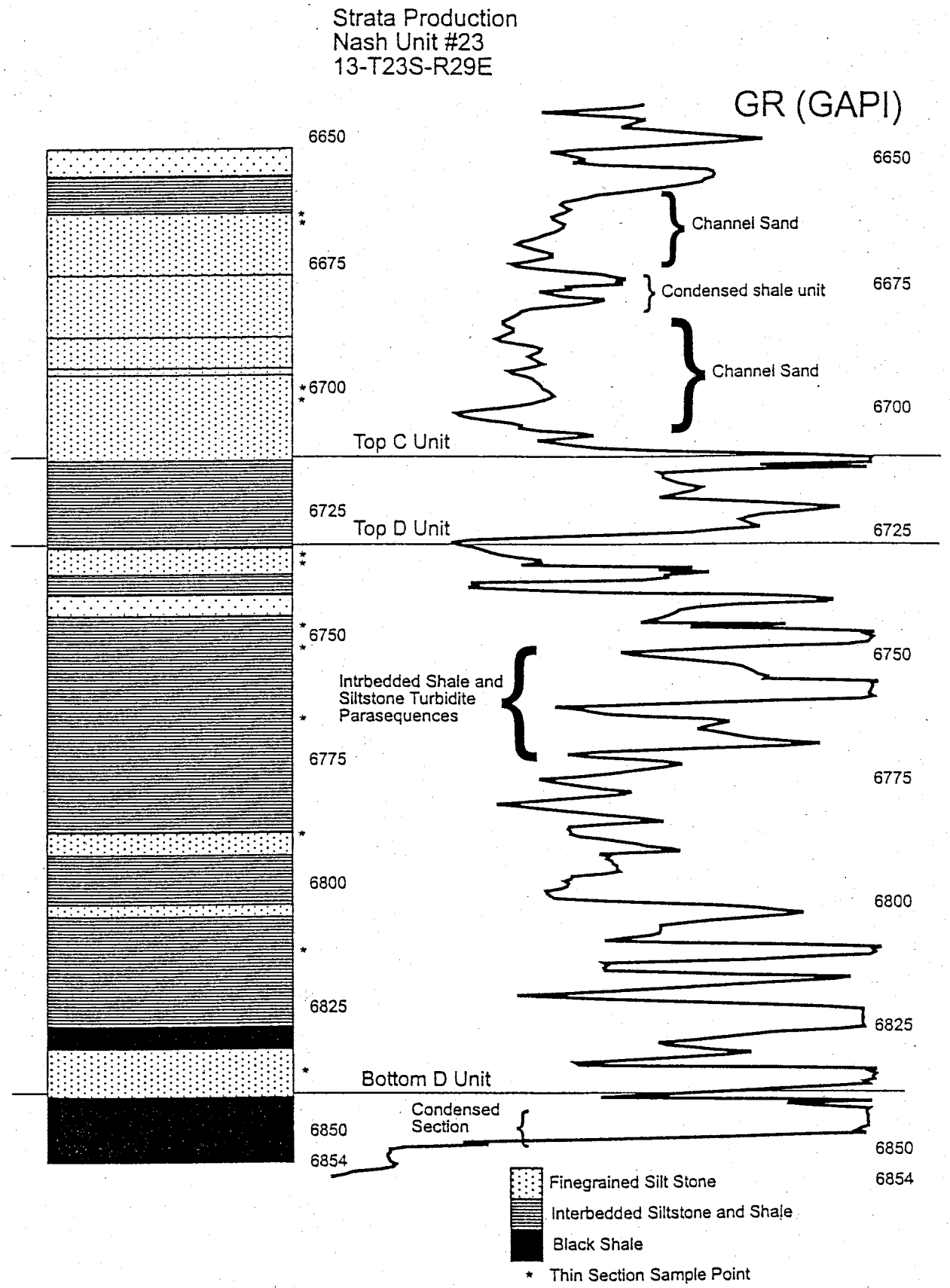

Figure 4.3: Cored section of Nash Draw Unit #23. This figure indicates the condensed section, channel sands, interbedded turbidite deposits, and shows their respective well log signature.

Above these condensed shale units are massive siltstone facies indicated by a low gamma ray reading. A black shale facies defines the top of each set. The turbidite deposits throughout these sets represent periods of relative low sea level and correspond to periods of channelization, indicative of lowstand sequence sets (Miall, 1997). The interbedded turbidite deposits are equivalent to the finely interbedded black shale and siltstone facies that were discussed previously. Each set begins with a relative lowstand of sea level and an increase in sediment supply to the basin during which both the interbedded turbidites and the channel siltstones were deposited. The end of each set is defined by a period of slow deposition and a deepwater environment, where the condensed shales were deposited (Fig. 4.4).

The unnamed shale unit at the base of the lower Brushy Canyon has been described by Beaubouef et al. (1999) as a condensed interval. This bed can be traced throughout the basin, and was most likely deposited as a single unit at a constant time during a highstand in a deep-water environment (Fig. 4.5). This bed marks the base of Set I. Set I comprises the entire D unit, which consists mainly of thinly interbedded turbidite deposits and thin siltstone channels. This section is representative of a lowstand distal fan complex with shallow broad channels, indicative of a low relative sea level. The broad channels indicate a low angle distal channel system. The interbedded siltstone and shale facies that are present throughout the set are turbidity current deposits. The cyclicity of these deposits probably represent failure of the slope, due to a storm or tectonic event. The C unit overlies the D unit and is characterized by thin turbidite deposits consisting of the interbedded siltstone and shale. It represents a distal fan in which sea level remained relatively constant and deposition was slow. This can be

determined by the lack of any channels throughout the C unit. The top of the C unit forms the base of set II. The lower channel siltstone of the B unit, which displays thick (>15m) siltstone channels, represents a slight rise in sea level and a proximal to medial canalized fan facies. The shale unit that separates the two B unit channels forms the upper part of set II. Set III is deposited above set II and is composed mainly of interbedded turbidite deposits and thick channel siltstones. Above the siltstones a shale unit is deposited in the lower A unit. The top of this shale marks the base of Set IV. Set IV is a very thin siltstone bed overlain by a thick shale unit, marking the uppermost bed in the lower Brushy Canyon.

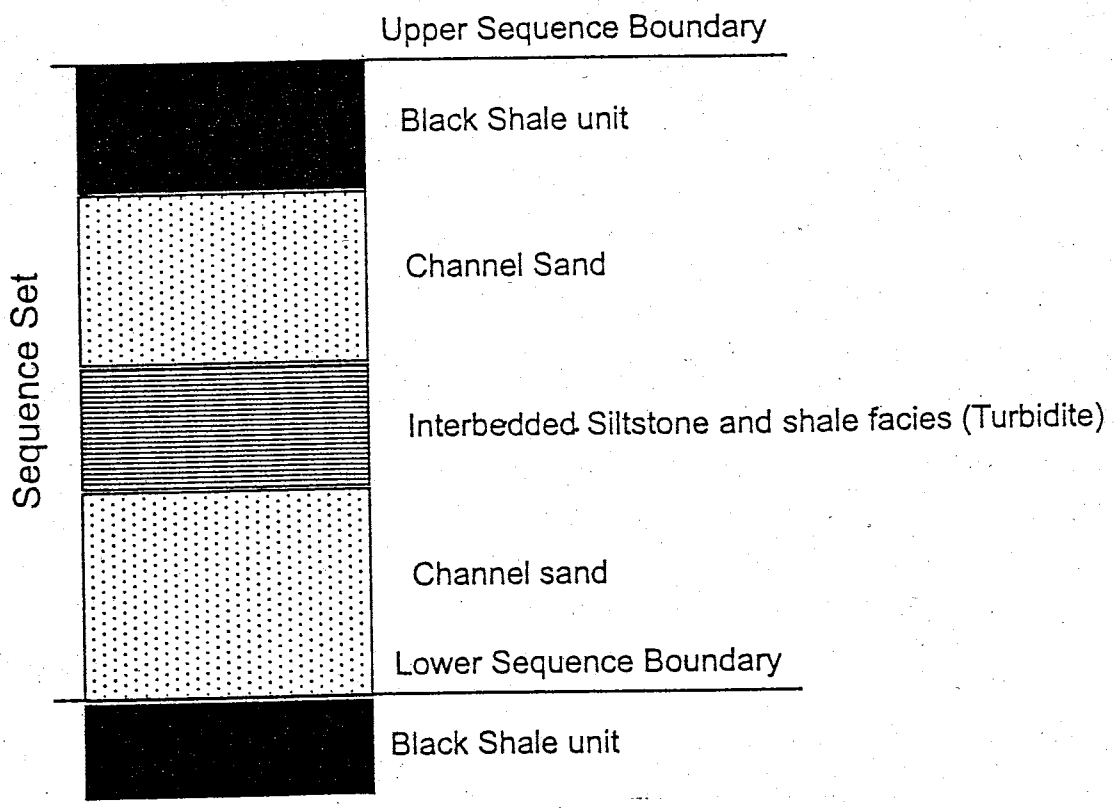

Figure 4.4: Schematic diagram of a sequence set. All three lithologies are present including the black shale, massive channel sandstone, and the interbedded siltstone and shale facies.

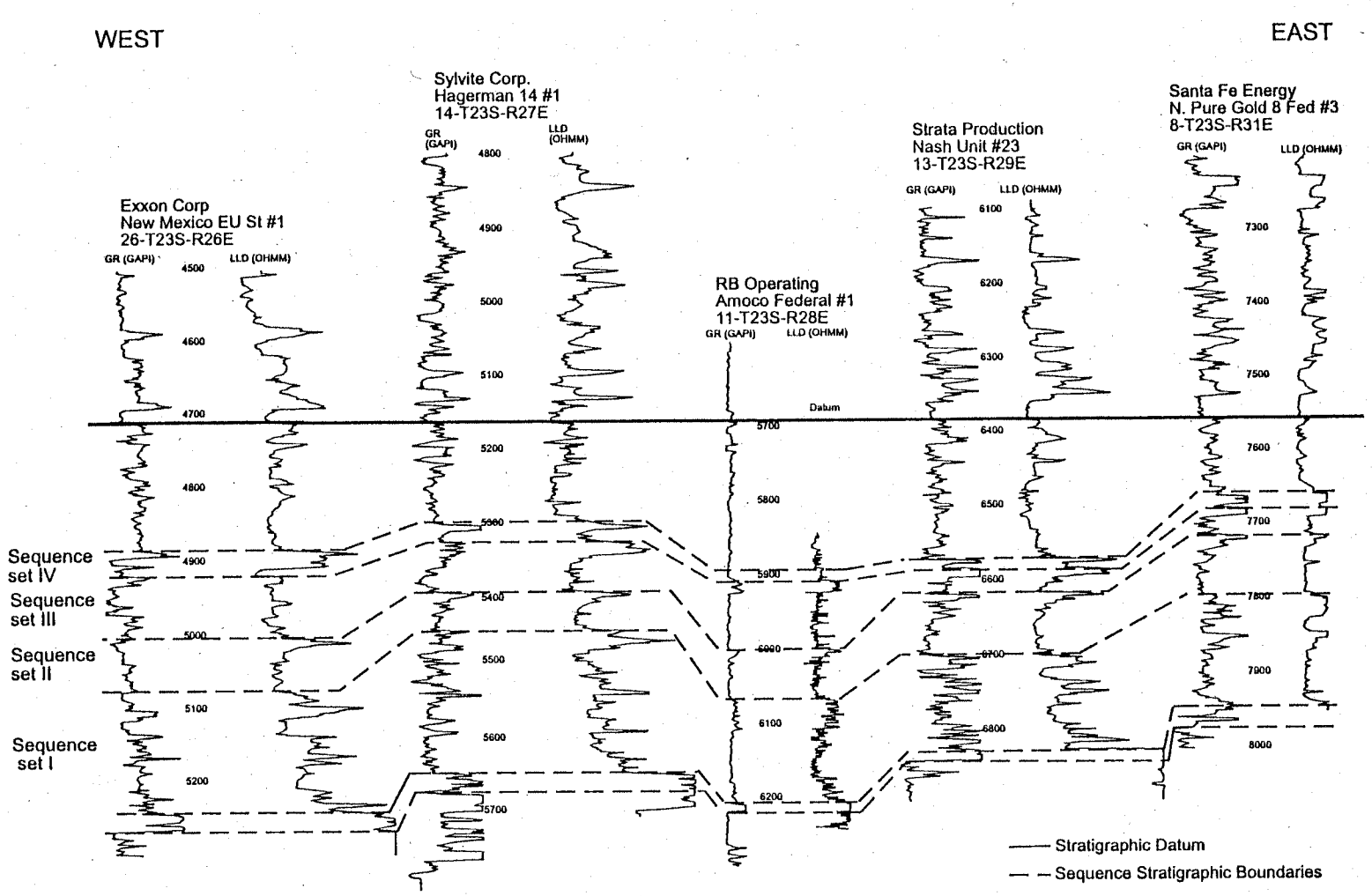

Figure 4.5: Regional cross section of the lower Brushy Canyon that connects the eastern and western study areas. This cross section displays the four sequence sets.

4.2 CONTROLS ON HYDROCARBON ACCUMULATION IN THE LOWER BRUSHY CANYON

The primary intent of this research is to identify the main variables that control the accumulation of hydrocarbons in the lower Brushy Canyon. In the lower Brushy Canyon, as with most hydrocarbon systems, it is not correct to conclude that only one factor is responsible for controlling the entire hydrocarbon system. Many different factors control where hydrocarbons accumulate including porosity, clay matrix, and calcite cement.

Porosity

Porosity obviously plays a major role in the accumulation and storage of hydrocarbons. Aside from controlling the amount of fluid a rock can hold, the interconnectedness of the pores also controls permeability. The volume of fluid in a rock means nothing if that fluid is incapable of being produced (North, 1985). Within the lower Brushy Canyon several different factors control the amount and size of pore space. Clay minerals and calcite cement tend to be deposited and precipitated in pore space and around framework grains. This is what reduces the porosity of the rocks in the lower Brushy Canyon

The morphology of the clay matrix and calcite cement affects porosity in two ways. First, these materials fill in portions of the pore space, greatly limiting the pores ability to transmit fluids. Second, these materials seal pore throats thereby reducing the pores ability to transmit fluids (Fig. 4.6). There is a direct relationship between the amount of porosity and the amount of clay matrix and calcite cement within the rocks of the lower Brushy Canyon. These materials not only reduce porosity but also increase pore entry pressures. This restricts the ability of hydrocarbons to displace pore waters

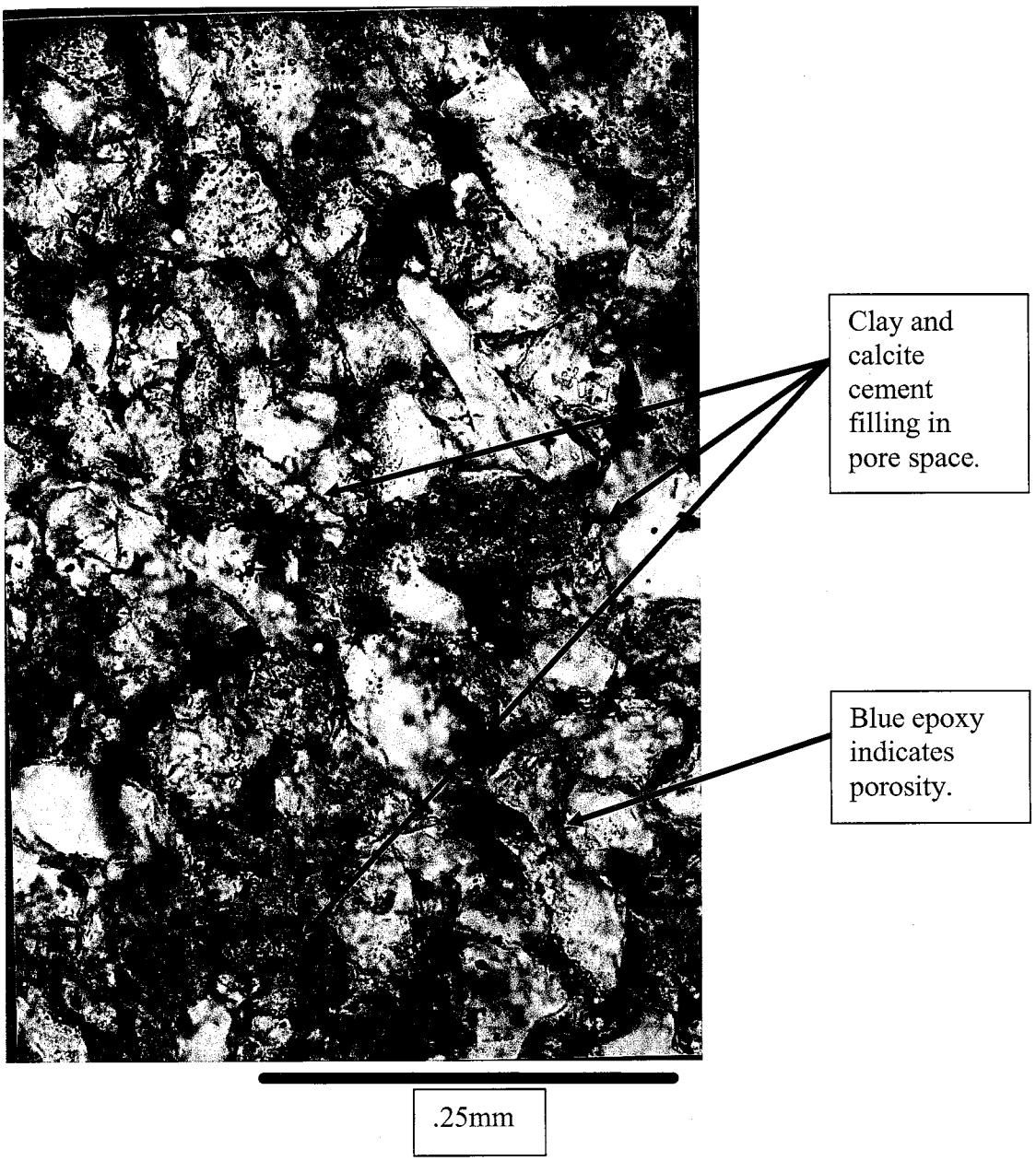

Figure 4.6: Photomicrograph of a producing siltstone where clay and calcite cement can be seen filling in pore space.

and migrate into the rock (North, 1985). Thus, hydrocarbons are often not present in the rocks with lower porosity.

Other controls on porosity include the amount of kerogen present. Kerogen, while not usually present in large amounts, acts as a matrix, reducing porosity. The kerogen generally occurs as large masses that surround, and encompass grains (Fig. 4.7). Grain size and rounding also have a small part in the morphology of the pores within these rocks. These factors are relatively minor compared to the clay matrix and calcite cement.

Clay Distribution

Clay distribution throughout the basin is a major factor in locating and producing hydrocarbons. Because low clay content is associated with increased production rates, it is desirable to prospect in areas with thick sandstones that have low clay content. In the lower Brushy Canyon it is very difficult to correlate individual sandstones for long distances. This is particularly true for channel sandstones, which are likely to have lower clay content than other sandstones within the lower Brushy Canyon. The sandstones of the distal fan facies tend to be thin and clayey as indicated by core. This is most likely due to the loss of energy that the turbidities undergo as the angle of deposition decreases toward the basin floor. Each channel represents a single small event such as a storm or failure of the slope during lowstand fluctuations in sea level. Once sea level rose, these channels underwent slow, low energy burial by clay material as indicated by the organic rich shales.

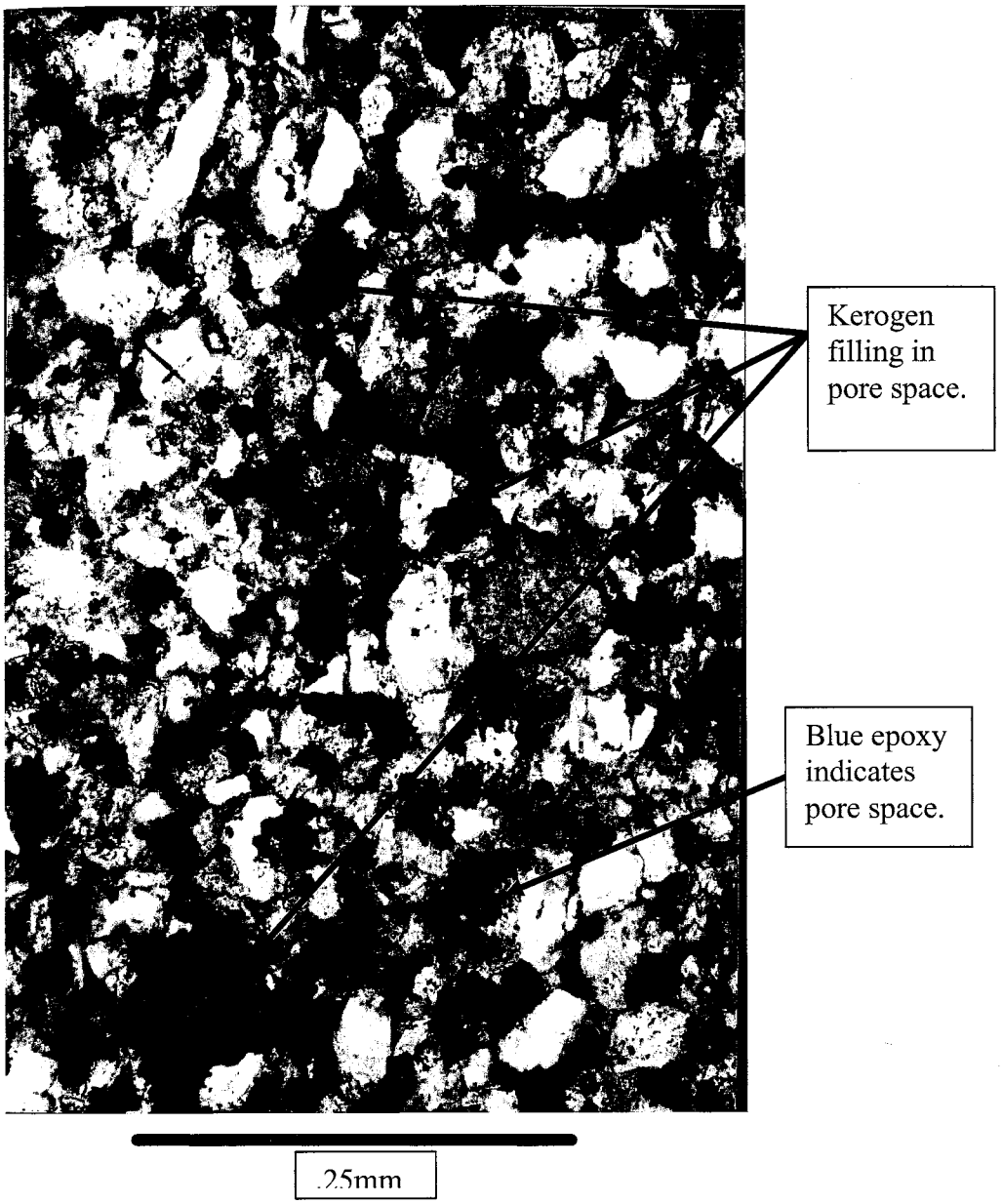

Figure 4.7: Photomicrograph of kerogen filling in pore space.

Origin of Clay Matrix

The clay matrix is present as a result of either authigenic growth or detrital infilling. Green et al. (1996) indicate that the chlorite and illite which are present in the sandstone are authigenic. They report the presence of pore-lining and pore-bridging textures. However, if the clay material is authigenic, the clay minerals would exhibit crystalline habits. Chlorite should show some form such as plates, rosettes, or honeycombs. Authigenic illite commonly forms lath-like sheets that can be relatively long. These forms are not present in thin sections examined in this project. Thin sections indicated that clay material was conforming to framework grains and showed no form (Wilson and Pittman, 1977). In this study petrographic analysis indicates that the clay matrix is both lining and bridging pores, but does not appear to be precipitated. The majority of clay material appears to be characteristic of a detrital origin.

Origin of Calcite Cement

The calcite cement that is present in the lower Brushy Canyon has a micrite crystal size. Thin sections show micrite sized irregular crystal forms present in the cement. The actual shape of the crystal forms is hard to determine because the crystal size is so small. Calcite cement is present in clumps indicating that grains precipitated around a central core. This indicates that the cement was deposited in-situ.

Importance of Clay Matrix and Calcite Cement in Porosity Reduction

As indicated previously, clay matrix and calcite cement together play important roles in the reduction of porosity. Individually each material is also very important in the reduction of porosity. As shown previously (Fig 3.31) the clay matrix is responsible for

reducing porosity in siltstone with less than 50 GAPI while calcite cement plays a more important role in reducing porosity in siltstone with over 50 GAPI (Fig3.34). This relationship does not mean that low GAPI rocks don't have calcite cement and high GAPI rocks don't have clay matrix. This indicates that clay matrix reduces porosity in both low and high GAPI siltstones, but is more important in low GAPI siltstone (<50 GAPI). In high GAPI siltstone (>50GAPI) clay is abundant in the rock, as indicated by the high radioactivity. In these rocks calcite cement is responsible for reducing the porosity that the clay matrix does not occupy.

Location of Source Rocks

The Lower Brushy Canyon is, in part, a self-sourcing system. As indicated by Justman (2001), the interbedded arrangement of the source rock and reservoir rock allows the formation to act as its own seal. Limits on hydrocarbon production related to the lack of source rock are not evident, however certain trends can be identified. Higher production is associated with greater net thickness of source rock. In most cases, production is updip of major accumulations of source rock. However, these trends do not explain the lack of production to the west where thermally mature source rock is present (Fig. 4.8). The most likely explanation is the escape of hydrocarbons through faulting in this region. It is apparent that source rock availability, while important, is not a primary control on production in the Lower Brushy Canyon (Justman, 2001).

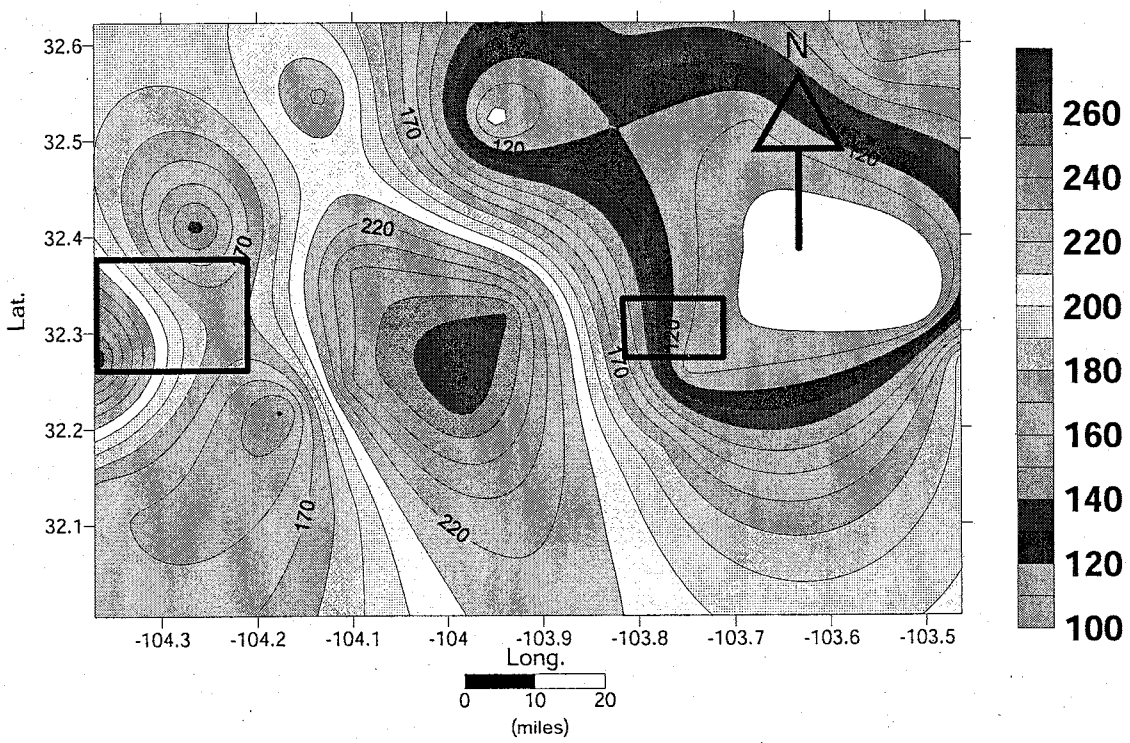

Figure 4.8: Map of generative potential (from Justman 2001) overlain by eastern and western study areas.

4.3 LOCATION OF HYDROCARBONS

After determining the factors that control hydrocarbon accumulation in the lower Brushy Canyon, it is necessary to map the areas likely to contain hydrocarbons to determine if these conclusions are accurate and if this research could be used as a tool in hydrocarbon exploration. Several criteria must be met in order to locate areas favorable to exploration. First, the area must have relatively thick siltstone channels or several thinner channels in close vertical succession. Second, these siltstone units must have low clay content in order for hydrocarbons to accumulate. To accurately map areas likely to accumulate hydrocarbons the best method is to study maps of variables that relate to hydrocarbon accumulation and determine which areas have the highest potential for hydrocarbon accumulation. Isopach maps of high porosity sands were compared with

clay content maps and sand isopach maps. Production maps of each unit were also examined.

The relationships between the different maps can best be seen in the eastern study area where hydrocarbon production is good. Here maps of initial production rates are compared to maps of high porosity, sand thickness, and clay content. Only the B unit and the D unit are shown because these stratigraphic units yield the bulk of the production (Fig. 4.9). This same type of mapping in the western study area indicates that much of the western study area is not likely to accumulate hydrocarbons because there is not a large area of low clay high porosity sands. This is what was expected given the western study area only produces small amounts of hydrocarbons (Fig. 4.10). However, these maps do indicate that certain unexplored regions of the western study area are likely to accumulate hydrocarbons.

This appears to be an effective method for determining where hydrocarbons may accumulate because it accounts for several different factors including clay content, porosity, and unit thickness, all which are very important in the accumulation of hydrocarbons.

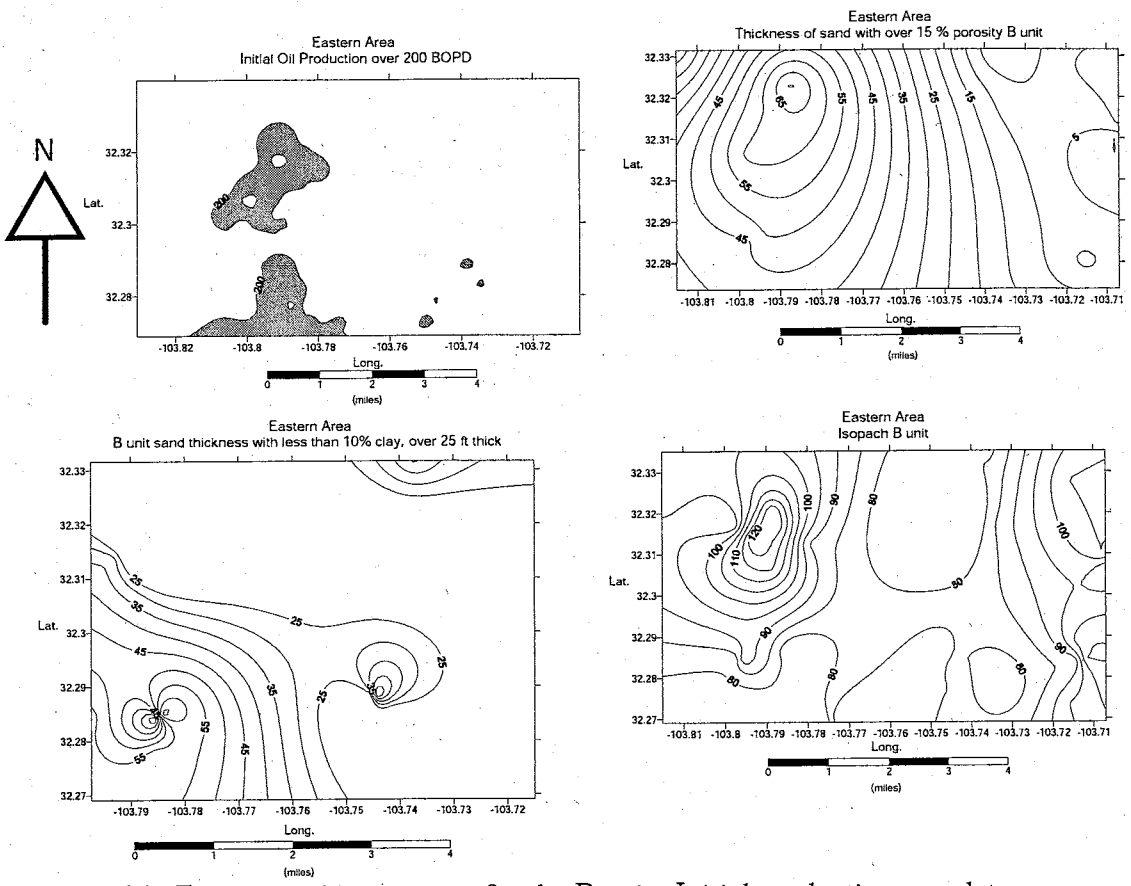

Figure 4.9A: Eastern study area maps for the B unit. Initial production correlates very well with both high porosity sands and low clay content sands.

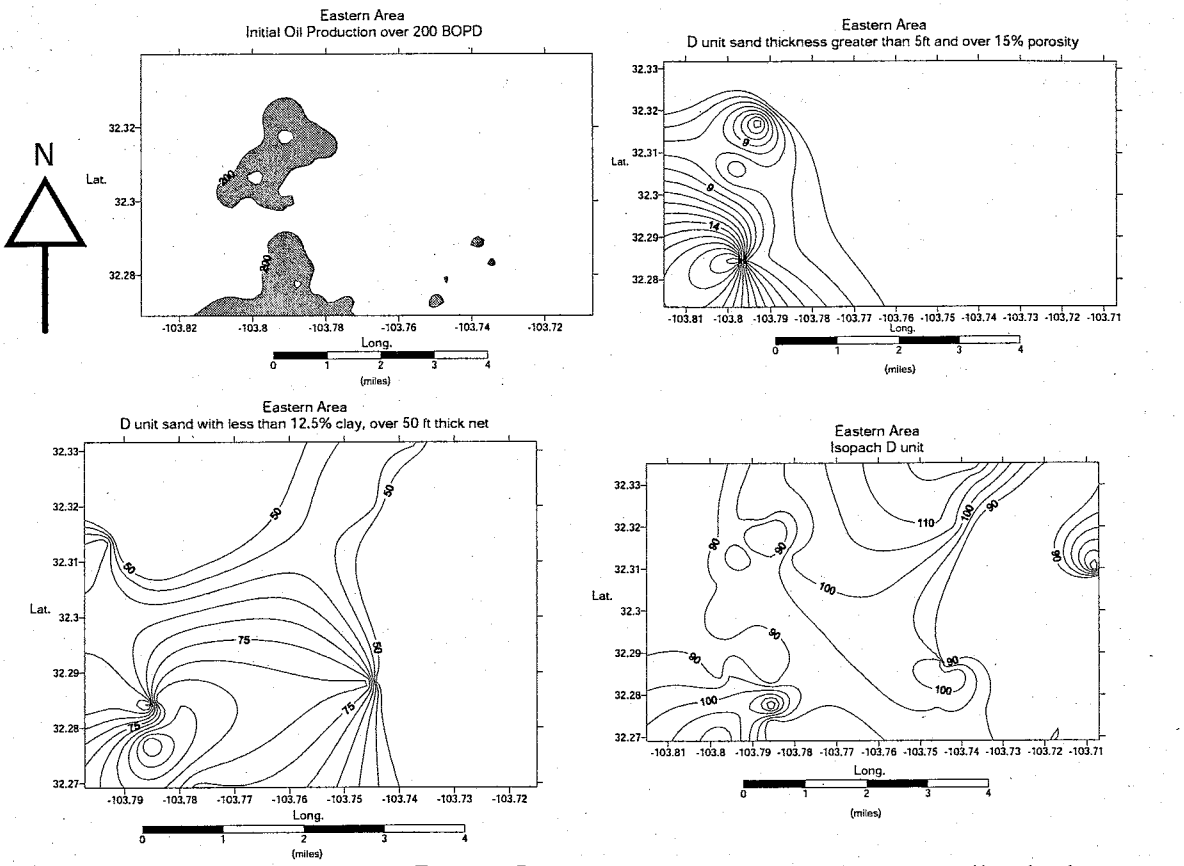

Figure 4.9B: Eastern study area, D unit. Initial production correlates very well to both porosity and clay content.

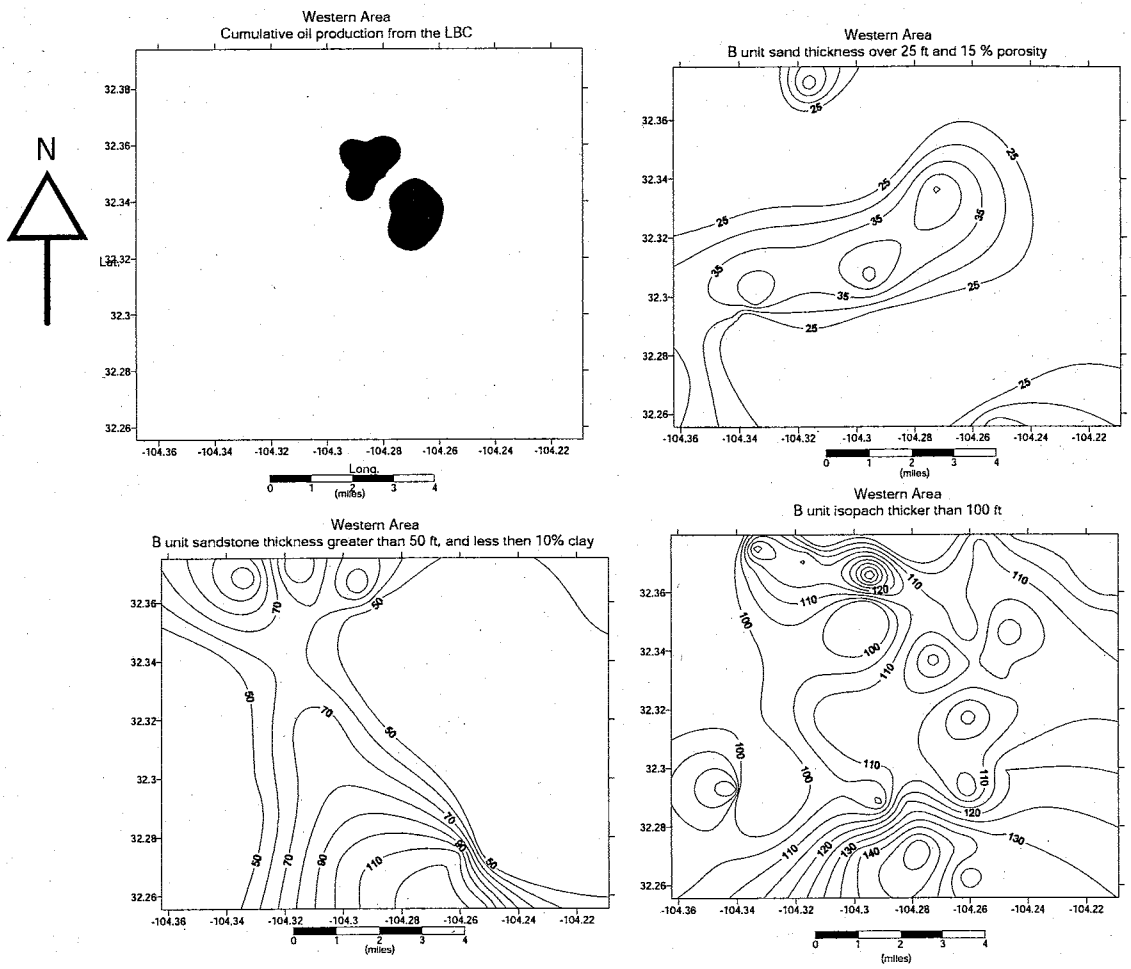

Figure 4.10A: Western study area B unit. The small amount of production from this area slightly relates to the high porosity sands but not at all to clay content. These maps indicate that some possible accumulation of hydrocarbons may be present.

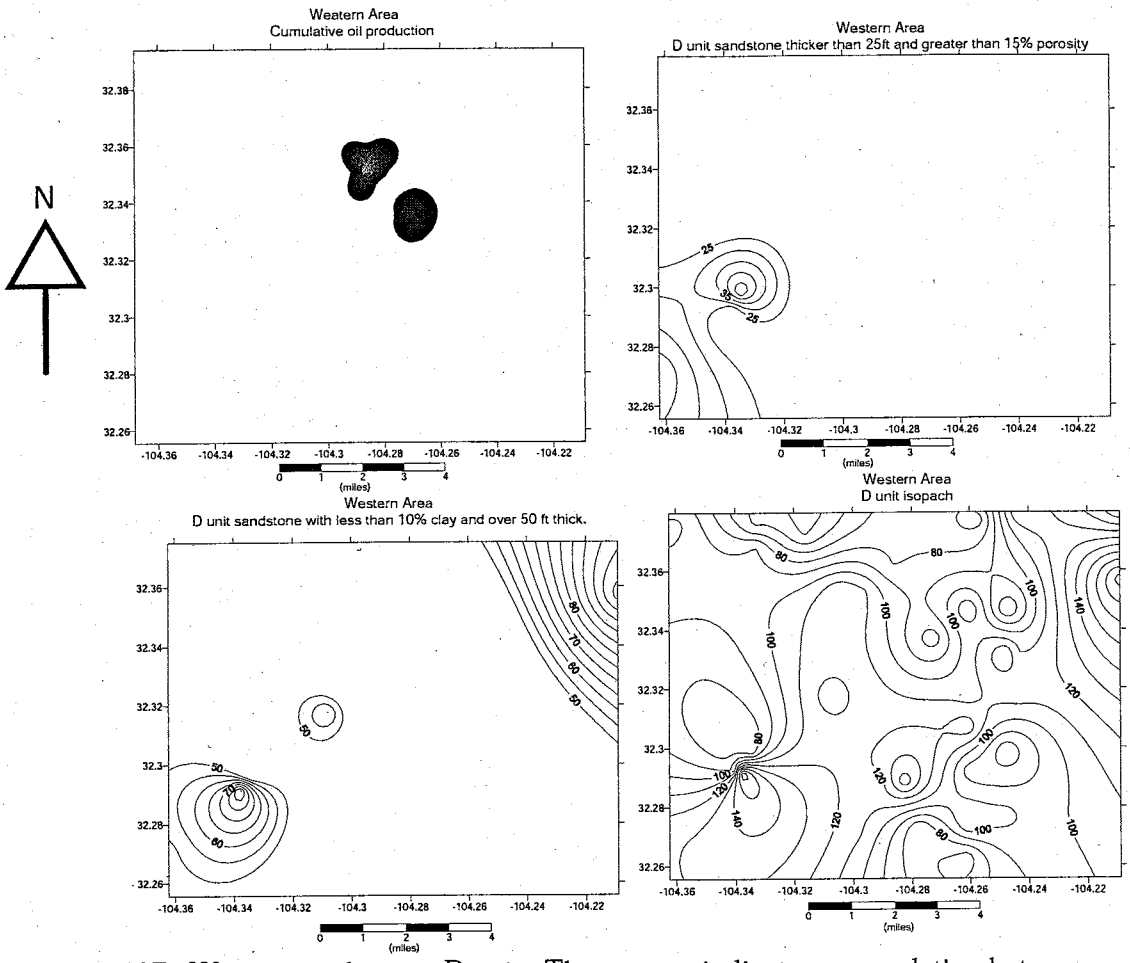

Figure 4.10B: Western study area, D unit. These maps indicate no correlation between production and either clay or porosity. They also indicate that hydrocarbons are not likely to accumulate in the D unit of the western study area.

4.4 IMPLICATIONS

This research has several implications. Through the detailed core descriptions, thin section point counts and descriptions, and sequence stratigraphic analysis, this thesis has produced a better understanding of the lithologies and depositional history of the lower Brushy Canyon, which may prove very valuable in hydrocarbon exploration. By identifying quantifying and mapping variables that control hydrocarbon accumulation, it is possible to reduce risk in hydrocarbon exploration. By using well logs to estimate controls on hydrocarbon accumulation, this research can also lower exploration costs in the lower Brushy Canyon. This will happen because well logs are a relatively cheap and abundant form of subsurface data. If the results of this research can be applied to other basins with similar depositional systems, exploration costs in those basins can potentially be reduced as well.

5.0 CONCLUSIONS

The primary goal of this research was to identify variables that control the accumulation of hydrocarbons in the lower Brushy Canyon. After completing petrographic analysis of 29 thin sections it became obvious that the presence of clay matrix and calcite cement reduces porosity. It was also shown that clay matrix is the primary porosity reducer in low gamma ray siltstones (less than 50 GAPI), and calcite cement is more important in reducing porosity in high gamma ray siltstones (greater than 50 GAPI). This occurred through reduction of the volume of pore space and pore diameters. This reduction of porosity limits the volume of hydrocarbons the rock can hold, but more importantly it increases the pore entry pressures. This means that hydrocarbons are less likely to displace water from the reservoir and may not be able to exit the source rock and accumulate.

Well log analysis along with thin section point counts revealed that clay content of the siltstones could be determined from rocks with gamma ray intensities of less than 50 GAPI units. This allowed the mapping of clay content throughout the study area in comparison to hydrocarbon production. These maps indicate that production is best in sandstones with low clay content and high porosity.

The distribution of these clays was difficult to determine in the small study areas. Stratigraphically, the lower Brushy Canyon is described as a basin floor fan with several sequence sets that are related to the rise and fall of sea level. Associated with this basin floor fan are channels where most of the hydrocarbon production comes from. These channels tend to be siltstones with low clay content. At the margins of these channels clay content is increased and hydrocarbons can't accumulate.

6.0 REFERENCES

Beaubouef, R. T., C. Rossen, F. Zelt, M. Sullivan, D. Mohrig, and D. Jennette, 1999, Deep-water sandstones, Brushy Canyon Formation, West Texas: Field guide for AAPG Hedberg field research conference: AAPG continuing education course note series no. 40, p. 50.

Broadhead, R.F., 2001, Risk reduction with a fuzzy expert exploration tool: Unpublished semiannual report of project activities, New Mexico Bureau of Geology and Mineral Resources, Socorro, New Mexico 87801, 8p.

Broadhead, R.F. and H.A. Justman, 2000, Regional controls on oil accumulations, lower Brushy Canyon Formation, southwest New Mexico, *in* W.D. DeMiss, M.K. Nelis, and R.C.Trentham, eds., The Permian Basin: proving ground for tomorrow's technologies: West Texas Geological Society, Publication 00-109, p. 9-18.

Broadhead, R. F., and F. Luo, 1996, Oil and gas resources in the Delaware Mountain Group at the WIPP site, Eddy County New Mexico, *in* W. D. DeMiss and A. G. Cole, eds., The Brushy Canyon play in outcrop and subsurface: concepts and examples: Permian Basin Section SEPM, Publication 96-38, p. 119-130.

Broadhead, R.F., F. Luo, and S.W. Speer, 1998, Oil and Gas Resources at the Waste Isolation Pilot Plant (WIPP) Site, Eddy County New Mexico: New Mexico Bureau of Mines and Mineral Resources Circular 206, p. 1-72.

Downing, A. and J. Mazzulo, 2000, Slope fan deposits of the 2nd Bone Spring sand, Young North Field, Lea County, New Mexico (abstract), *in* W.D. DeMiss, M.K. Nelis, and R.C. Trentham, eds., The Permian Basin: proving ground for tomorrow's technologies: West Texas Geological Society, Publication 00-109, p. 73.

Fisher, A.G. and M. Sarnthein, 1988, Airborne silts and dune derived sands in the Permian of the Delaware Basin: Journal of Sedimentary Petrology, v.58, no. 4, p. 637-643.

Green, K.M., S.M. Frailey, and G.B. Asquith, 1996, Laboratory analysis of the clays within the Brushy Canyon Formation and their reservoir and petrophysical implications: Red Tank Field, Lea County, New Mexico, *in* W. D. DeMiss and A. G. Cole, eds., The Brushy Canyon in outcrop and subsurface: concepts and examples: Permian Basin Section SEPM, Publication 96-38, p. 165-171.

Harms, J.C., 1974, Brushy Canyon Formation, Texas: A deep-water density current deposit: Geological Society of America Bulletin, v. 85, p. 1763-1784.

Harms, J.C. and M.J. Brady, 1996, Deposition of the Brushy Canyon Formation: 30 years of conflicting hypotheses, *in* W. D. DeMiss and A. G. Cole, eds., The Brushy Canyon in

outcrop and subsurface: concepts and examples: Permian Basin Section SEPM, Publication 96-38, p. 51-59.

Harms, J.C. and C.R Williamson, 1988, Deep-water density current deposits of Delaware Mountain Group (Permian), Delaware Basin, Texas and New Mexico: AAPG Bulletin, v.72, p. 299-317.

Hills, J.M., 1984, Sedimentation, tectonism, and hydrocarbon generation in Delaware Basin, West Texas and Southeastern New Mexico: AAPG Bulletin, v.68, no.3, p. 250-267.

Hull, J.P.D., 1957 Petrogenesis of Permian Delaware Mountain sandstone, Texas and New Mexico: AAPG Bulletin v.41, p. 153-182.

Jacka, A.D., R.H. Beck, L.C. Germain, and Harrison, 1968, Permian deep-sea fans of the Delaware Mountain Group (Guadalupian), Delaware Basin, *in* B. Silver, ed., Guadalupian Facies, Apache Mountains Area, West Texas: Permian Basin Section SEPM Publication 68-11, p. 49-90.

Justman, H.A., 2001 Petroleum source rocks in the Brushy Canyon Formation (Permian) Delaware Basin, Southeastern New Mexico: Unpublished Masters Thesis, New Mexico Tech, Socorro NM 87801. 106p.

Kerans, C. and W.M. Fitchen, 1996, Stratigraphic constraints on the origin of the Brushy Canyon Formation, *in* W. D. DeMiss and A. G. Cole, eds., The Brushy Canyon in outcrop and subsurface: concepts and examples: Permian Basin Section SEPM, Publication 96-38, p. 61-68.

King, P.B., 1948, Geology of the Southern Guadalupe Mountains, Texas: USGS Professional Paper 215, 183p.

Miall, A.D., 1997, The geology of stratigraphic sequences: Springer-Verlag, Berlin, 433p.

Mitchum, R.M., Jr., P.R. Vail, and S. Thompson III, 1977, Seismic stratigraphy and global changes of sea level, part 2: the depositional sequences as a basic unit for stratigraphic analysis, *in* C.E. Payton, ed., Seismic Stratigraphy- applications for hydrocarbon exploration: AAPG Memoir 26, p. 53-62.

Montgomery, S.L. J. Worrall, and D. Hamilton, 1999, Delaware Mountain Group, west Texas and southern New Mexico, a case of re-found opportunity: part 1 – Brushy Canyon: AAPG Bulletin, v.83, no.12, p. 1901-1926.

North, F.K., 1985, Petroleum Geology: Allen and Unwin, Boston, 607p.

Pettijohn, F.J and P.E. Potter, 1964, Atlas and glossary of sedimentary structures: Springer-Verlag, New York, 370p.

Pettijohn, F.J., P.E. Potter, and R. Siever, 1973, Sand and sandstones: Springer-Verlag, New York, 618p.

Read, A., R.F. Broadhead, A. Lopez, E. Flemming, and J. Watrous, 2000, New Mexico oil and gas pools: New Mexico Bureau of Mines & Mineral Resources Circular 209, CD-Rom.

Spain, D.R., 1992, Petrophysical evaluation of a slope fan/ basin floor fan complex: Cherry Canyon Formation, Ward County, Texas: AAPG Bulletin, v.76, p. 805-827.

Thomerson, M.D. and L.E. Catalano, 1996, Depositional regimes and reservoir characteristics of the Brushy Canyon sandstones: East Livingston Ridge Delaware Field Lea County, New Mexico, *in* W. D. DeMiss and A. G. Cole, eds., The Brushy Canyon in outcrop and subsurface: concepts and examples: Permian Basin Section SEPM, Publication 96-38, p. 103-111.

Wilson, M.D. and E.D. Pittman, 1977, Authigenic clays in sandstones: Recognition and influence on reservoir properties and paleoenvironmental analysis: Journal of Sedimentary Petrology, v.47, no.1, p. 3-31.

APPENDIX I

CORE DESCRIPTIONS

R B Operating 1 Amoco Federal 11-T23S-R28E

Depths (feet)	**Description**
6167-6166	Very fine grained light grey color at top larg shale clasts ~ 2 in across.
6166-6165	Thinly interbedded siltstone and shale flame structure at lower contact.
6165-6153	Very fine grained siltstone greyish color occssionally thin shale beds about 2cm thick from 6158.7-6158.5. Siltstone grades to shale then very abrupt change to siltstone curved contact.
6153-6152	Finely interbedded siltstone and shale. Shale increasing turbidities upwards then abrupt change to siltstone.
6152-6147	Very fine grained siltstone, grey color. 6150-6149-interbedded shale and siltstone, higher shale with depth-then more siltstone.
6147-6138	Very fine grained siltstone, darker grey color. Higher amounts of shale, wavy and even parallel shale laminae. At 6142-6141- flow structure.
6138-6129	Very fine grained siltstone grey color. Occassionally thin bedded siltstone and shale < 2in. Wavy, parallel shale laminae.
6129-6113	Very fine grained siltstone grey color. Occassionally interbedded units of shale and siltstone. Basically an increase in shale content. Small amounts ofshale can be seen in siltstone. Just fragments, no laminae.
6113-6110	Darker grey siltstone with higher shale. Even parallel laminae of shale. Also some interbedded siltstone and shale higher siltstone samples.
6110-6092	Missing intervals.
6092-6083	Interbedded siltstone and shale. Very Thinly interbedded turbities.
	*Note--Depths are unsure, due to miss labeling of core.

STRATA PRODUCTION NASH DRAW UNIT 23 13-T23S-R29E

Depths (feet)	**Description**
6650-6651	Very fine interbedded shale and siltstone. Grey siltstone, black shale. Laminar bedding with thicknesses ranging from 1-8mm. At 6650.5 Turbidities. Siltstone whirled around in shale. No reaction to acid. But mostly shale.
6651-6654.5	Quartz siltstone. Very fine grained, tannish grey. 6651.3-6651.5 increases in shale content, also occassional shale stringers ~ 1 cm thick. Shale sontacts sharp not graded. Siltstone reacts to acid, shale does not, indicates calcite cement. Some shale is siltstone but vey little.
6654.5-6658.3	Very fine interbedded shale and siltstone. Mostly siltstone, grey in color. Shale in black in color. Laminar bedding ranging from 1-8mm thick. At 6657.5 turbidities are about 2 cm thick, caped by a 0.4cm shale layer. This is underlayed by a 5cm thick siltstone (mostly) layer. Slow reaction is most obvious in thicker siltstone sets.
6658.3-6658.8	All sand unit. Quartz siltstone, topped by 0.5cm thick shale. Some crossbedding structures present. Small scale. Two very faint shale layers about 1 cm apart, mark the bottom of crossbedding. Crossbedding from 6658.4-6658.6.
6658.8-6660.2	Interbedded siltstone and shale same as 6654.5-6658.3. Several thin turbidities~1cm thick. A thick shale unit is at the bottom.
6660.2-6660.8	Siltstone unit, mostly quartz some shale, grey in color. No structures. Darker than most siltstone layers, indicating higher shale.
6660.8-6661.2	Interbedded shale and siltstone, mostly thin beds about < 1mm thick. Dark grey.
6661.2-6677.1	Massive quartz and siltstone unit. Little to no acid reactions. Occassional shale units throughout, about 2-15cm thick. Light tannish grey color of siltstone. Shale contacts are sharp for the most part. Occassionally upper contact is slight graded.
6677.1-6684	Massive quartz and siltstone unit. Little to no acid reactions. Ocassional shale units throughout, about 2-15cm thick. Light tannish grey color of siltstone. Shale contacts are sharp for the most part. Occassionally upper contact is slight graded. Now shale units are interbedded in laminar layers.
6684-	Massive siltstone units are structured less and have occassional darker units,

6710	indicating higher shale percent. Out still a shalely sandstone. Contacts between shale rich zones are very sharp but don't appear to folow any bedding pattern. Probably more lenticular, indicated at 6707.9, where edge of shale lens is cut. Siltstone is grey-tannich color. Shale rich units are dark grey-black. All units react rapidly to acid.
6710-6712.5	Poor samples, very broken up. Quartz, siltstone are very fine grained. No structures. One noticable thin scale layer at 6711.3, tannish-grey. Rapid to acid reaction.
6712.5-6713.5	At top a finely bedded siltstone and shale horizon for ~6cm. Then a grey fragment siltstone below that at 6713.3- a shaley siltstone lens. Then a 1cm thick grey/ tan siltstone. All very fine grained. Acid reaction.
6713.5-6715.9	Very finely interbedded siltstone and shale about >80% shale is a black color. Very fine grained. No acid reaction. At 6715.8 a 1 cm laminated shale horizon, solid black. Below fine quartz (yellow/tan) structures appear to be crushed. Below more interbedded siltstone and shale.
6715.9-6729.9	Interbedded siltstone and shale. About 50/50 at 6716.2, a thick shale layer all black. Then at 6716.3 mostly siltstone with a little shale. At 6716.4, an increase in amount of shale but still no bedding structure. At 6716.5, mostly siltstone with a little shale. At 6716.8, interbedded siltstone and shale again. At 6717.3, a shaley siltstone with no bedding decreases downwards to 6717.7. The interbedded shale and siltstone at 6719.6, structures appear to be siltstone lens with clay stringers about 6cm thick, then interbedding again. Occassional increases in amount of shale but stays interbedded. At 6728.1, increase in amount in shale until a solid black shale at 6729.9.
6729.9-6730.6	Silstone with shale component. Increase in shale with depth, appears that lower shale was incorporated into the siltstone. Siltstone is very fine. Reacts to acid quickly.
6730.6-6735.5	A quartz siltstone with shale rich lenses. Generally seeing some increase in shale with depth towards the lenses but lower contacts are sharp. Siltstone is grey-tannish grey with some shale components. Quick reaction to acid.
6735.5-6736.5	Turbidities sequence with a decrease of shale with depth. Topped by a thick black shale. Shale pieces can be up to 1cm long. Yes to acid.
6736.5-6737.5	Quartz siltstone unit, with increase in shale in middle and decrease at bottom. Very fine grained. No structure; reacts sto acid.
6737.5-6739.5	Black shale unit, with fine siltstone interbedded. The siltstone is finely layered ~0.25mm. At 6738.5 turbidite sequence is increasing siltstone with

	depth. Little to no acid. There are some siltstone chunks in some of the shale.
6739.5-6742.6	Siltstone unit with a shaley siltstone lens from 6739.9-6741. Mostly quartz siltstone with a 5-10% shale content. Slow reaction to acid.
6742.6-6743.6	Massive shale unit, black. Some siltstone stringers but few and very thin. No acid reaction. Slight increase in siltstone towards the bottom.
6743.6-6748	Interbedded siltstone and shale, very finely bedded. Percentage of shale increases with depth at 6744.5 and at 6746.8-6747.2, bedding stops for a shaley siltstone lens. Below both lenses is a grey siltstone with no bedding features, then laminar bedding begins again. At the bottom, a 1cm thick shale. Little to no acid reaction.
6748-6749	Siltstone- quartz, very fine grained. Few balck shale stringers at top. Greyish in color. About 10% shale.
6749-6752.4	Dark shale layer with some fine sand stringers. At 6749.7-6749.9, turbidities with increase in sand. At 6750.4-6750.6, a sand unit with shale stringers (possibly a lens?) and then back to shale with fine sand stringers. No reaction to acid.
6752.4-6753.3	Quartz siltstone unit with a high shale component and some shale stringers. Very high shale in middle of interval and possibly turbidite.
6753.3-6760	Interbedded shale and siltstone, fairly equal amounts at 6754-6754.9. Bedding haults and a massive shaley siltstone. Then bedding resumes. Some small shale lenses throughout, just a few about 4cm long and 2cm wide.
6760-6763.4	Black shale unit with some laminar siltstone beds. 1cm thick siltstone bed from 6761-6761.3. No acid reaction.
6763.4-6764.7	Quartz siltstone unit. Slow to acid reaction. Very little shale, light grey color.
6747.7-6767	Turbidities mixed up siltstone and shale, rather than course grain clasts of each. < 1 cm are a few larger grains, still mostly a shale matrix with siltstone clasts. Fast to react to acid.
6767-6778.1	Interbedded siltstone and shale, about even amounts. Occassionally bedding stops for a shaley siltstone-massive or amounts of shale increases with depth. Then forms a thick shale and below the process restarts itself. No acid reaction.
6778.1-6780	Quartz siltstone has no bedding. Shaley siltstone has lots of shale. Fast to react with acid.

	* Note—end of slabs, beginning of core.
6780-6783	Intrbedded siltstone and shale, mostly shale layers. Occassionally bedding stops for massive siltstone units. No reaction to acid.
6783-6784.1	Shaley siltstone no bedding, Quartz sand. Slow to react with acid. Tannish grey in color.
6784.1-6786	Siltstone grades into a brown shale. Rapid reaction to acid. No bedding-grades to a sandy brown shade.
6786-6788.8	Interbedded siltstone and black shale at 6786.8. Small turbidite then becomes siltstone below then bedding resumes, at 6787.8. No reaction to acid.
6788.8-6792	Fine grained quartz-siltstone, shale component increases and drecreases in a lens shape (shale rich lenses). Around 6791, shale clasts appear but are very small <1mm (possible turbidite?) Slow reaction to acid, except in shale rich lenses-rapid reaction to acid.
6792-6794	Interbedded shale and siltstone, laminar bedding. No reaction to acid.
6794-6794.8	Turbidite shale (black) and siltstone (grey) are all mixed up. No reaction to acid.
6794.8-6801	Interbedded siltstone and shale, about equal amounts. Occassionally bedding stops and massive shaley quartz siltstone instead. Shale rich lenses within these siltstone. At 6797, a turbidite then sand, then laminar bedding resumes.
6801-6803	Fragments of quartz siltstone with little shale (grey in color). Fast to acid reactions.

Fortson Oil Poker Lake Unit 80 19-T24S-R31E

Depths (feet)	**Description:**
7860-7864	Finely interbedded black shale and white siltstone. Mostly shale with fine silt laminations ~ 1mm thick Flow structure at top of interval slow to acid
7864-7866	Flow structure Small pieces of siltstone (~ 1mm) in a fast reaction to acid. Black shale matrix, at bottom of interval a siltstone matrix with Larger clasts of shale > 7.5cm.
7866-7872 Sample 7870 & 7867	Siltstone tanish color with some rounded oil stained areas. At 7868.5 & 7869.3 grades to a laminar shale unit then grades back to siltstone. Very faint clay laminae-straight, flat, fast to acid.
7872-7873.5	Thick black shale, which grades to siltstone with depth. Some silt strings, which are laminar, also have some rounded globular units with higher silt content. Some pyrite is present. Shale possibly reworked? Silty globs react fast to acid while shale does not.
7873.5-7875	Grey siltstone, lots of shale is present. Also shale lenses small ~0.8cm, fast to acid.
7875-7884.3	Finely interbedded black shale and grey siltstone. The shale laminae are parallel and wavy occassionally bedding haults for a thin laminar. Shale looks like reworked siltstone from below, fast to acid.
7884.3-7885.8	Grey siltstone with very high amounts of shale and high amount of pyrite. Shale laminae are discontinously wavy. Moderate-slow reaction to acid.
7885.8-7886.3	Finely interbedded black shale and grey siltstone. The shale laminae are parallel and way occassionally bedding haults for a thin laminar. Shale looks like reworked siltstone from below, fast to acid. Upper contact is wavy/ flame structures.
7886.3-7887	Flow structure with very high shale. The silt part reacts to acid, shale does not.
7887-7890.5	Series grey siltstone then interbedded siltstone and shale. Laminar shale layer then starts over again. Siltstone units are thickest ~6in. Laminar shale units are only ~ 1in. At 6889.5 siltstone appears more mottled and reworked. More siltstone is with rip-up shale clasts. Siltstone fast to acid,

	shale is slow.
7890.5-7894.2 Sample of 7891 & 7893	Tannish siltstone shale laminae are discontinously wavyand straight. Some oil staining in interval.
7894.2-7895	Flow structure high shale content with siltstone clasts. Slow to acid.
7895-7895.5	Grey siltstone shale is discontinously wavy-drilling mud rimming outer centimeter of core, fast to acid.
7895.5-7897	Flow structure high shale content with siltstone clasts. Slow to acid.
7897-7897.8	Finely interbedded siltsstone and shale. Shale laminae is wavy and parallel. Bottom contact is a centimeter thick. Shale is wavy bottom. No to acid.
7897.8-7899.2 Sample of 7898	Tan siltstone discontinous. Shale laminae is fast to acid.
7899.2-7902	Black shale unit with several flow structures where silt increases. Silty flow structures are fast to acid, shale is slow to acid.
7902-7904.4	Black shale with some silt stringes are parallel and even.
7904.4-7905	Grey shale rich siltstone. Some laminar shale layers, which is discontionusly wavyat very bottom 7905.8. Thick shale layer, fast to acid.
7905-7950	Missing in interval
7950-7954.1	Finely interbedded siltstone and shale at top of unit. Some flow structures at 7951.2, a siltstone rich lens, the shale laminae are wavy, even and parallel. No to acid.
7954.1-7955	Grey siltstone, clay laminae is discontinous. No to acid.
7955-7956	A grey siltstone with high shale and some laminar shale layers. No to acid.
7956-7957.5	Interbedded siltstone and shale laminae are wavy and even and parallel. No to acid.
7957.5-7959.5	Grey siltstone with even parallel, discontinous shale laminae. Fast to acid.
7959.5-7962.5	Interbedded siltstone and shale laminae are wavy and even and parallel. No to acid. At 7960.6-7961.4 a siltstone rich unit. Fast to acid.

7962.5-7965.9 Sample of 7965	Tan siltstone, clay laminae is discontinously wavy and non-parallel. Fast to acid.
7965.9-7966.5	Interbedded siltstone and shale laminae are wavy and even and parallel. No to acid. Upper contact is flame structure. No to acid.
7966.5-7972.5	Tan siltstone, clay laminae is discontinously wavy and non-parallel. Fast to acid. Oil stained.
7972.5-7973.2	Interbedded siltstone and shale at bottom laminar shale layer. Shale layer are wavy and even and parallel. No to acid.
7973.2-7990.9 Sample of 7980 & 7988	Tannish siltstone with oil stain. See drill mud ring around outer centimeter of core. Clay laminae is wavy, non-parallel. Some small interbedded units, which are based by a laminar shale unit. Then more siltstone. Slow to acid. Very fine shale rich layer at 7783.
7990.9-7993.4	Interbeddes siltstone and shale. Very high shale laminae are even and parallel. Not to acid.
7993.4-7999.3 Sample of 7994	Tan siltstone with several interbedded units. Clay laminae is even, parallel. Fast to acid.
7999.3-8001.9	Flow structures higher shale than siltstone, towards bottom more siltstone. No to acid.
8001.9-8003.4	Black shale with siltstone stringers, even parallel. Not to acid.
8003.4-8005.4 Sample of 8004	Grey siltstone with wavy, curved parallel shale lamainae. Interbedded unit with high shale at 8004.4-8004.6. Fast to acid.
8005.4-8007.6	Interbedded siltstone and shale even parallel, wavy shale laminae. Shale increases with depth. No to acid.
	*Notes—All shale is black in core. --Non-prod sands have laminar shale laminae across, not discontinous, also darker and tends to be in smaller intervals.

R B OPERATING SOUTH CULEBRA BLUFF 5 13-T23S-R28E

Depths (feet)	**Description**
6043-6076	Very fine grained siltstone, tannish grey. Some small shale particles, no laminae. Occasionally very thin interbedded siltstone and shale. Flow structure at 6050-6050.5—with increase in shale.
6076-6079 Sample	Very fine grained siltstone, light grey color Very little shale.
6079-6092	Finely interbedded siltstone and shale turbidities. Lots of silt (silt> shale). But shale increases with depth. At 6091-6092—mostly shale.
6092-6193	Missing Interval.
6193-6199	Very finely interbedded siltstone and shale (turbidities). Amount of shale increases upward.
6199-6201	Very fine grained siltstone, grey, shale particles. Some small wavy discontinous laminations.
6201-6207	Very finely interbedded siltstone and shale. Mostly shale.
6207-6229	Missing Interval.
6229-6232 Sample	Very fine grained siltstone with lots of shale. Dark grey in color.
6232-6238	Black shale with occasional siltstone stringers.

APPENDIX II

THIN SECTION DATA

Well Name: **Amoco Federal** Well #: **1** Location: **11-T23S-R28E**

Depth: 6155

Description:

Very fine grained siltstone with a quartz and feldspar framework. The grains are silt sized and subangular to angular. The grain too grain contacts are point contacts. The matrix is composed of clay and calcite cement, the porosity is good and well interconnected.

	#	%
1) Quartz	36	18
2) Feldspar	64	32
3) Carbonate Grains	1	0.5
4) Fragments	4	2
5) Kerogen	7	3.5
6) Clay Minerals	16	8
7) Calcite Cement	5	2.5
8) Micro Porosity	5	2.5
9) Macro Porosity	62	31

Well Name: **Amoco Federal** Well #: **1** Location: **11-T23S-R28E**

Depth: 6152

Description:

Very fine grained siltstone with a quartz and feldspar framework. The grains are silt sized and subangular to angular, with point contacts. The matrix consists of clay and calcite cement. Some parts of this sample have high amounts of matrix and very low porosity levels. Most of the sample has high porosity and low matrix.

	#	%
1) Quartz	51	25.5
2) Feldspar	58	29
3) Carbonate Grains	1	0.5
4) Fragments	3	1.5
5) Kerogen	7	3.5
6) Clay Minerals	22	11
7) Calcite Cement	6	3
8) Micro Porosity	7	3.5
9) Macro Porosity	45	22.5

Well Name: **Amoco Federal** Well #: **1** Location: **11-T23S-R28E**

Depth: 6152

Description:

Very fine grained siltstone with a quartz and feldspar framework. The grains are silt sized and subangular to angular, with point contacts. The matrix consists of clay and calcite cement. Some parts of this sample have high amounts of matrix and very low porosity levels. Most of the sample has high porosity and low matrix.

	#	%
1) Quartz	51	25.5
2) Feldspar	58	29
3) Carbonate Grains	1	0.5
4) Fragments	3	1.5
5) Kerogen	7	3.5
6) Clay Minerals	22	11
7) Calcite Cement	6	3
8) Micro Porosity	7	3.5
9) Macro Porosity	45	22.5

Well Name: **Amoco Federal** Well #: **1** Location: **11-T23S-R28E**

Depth: 6112

Description:

Very fine grained siltstone with a quartz and feldspar framework. The grains are subangular to angular, silt sized. The grain too grain contacts are concavo-convex. The matrix (high) is clay and calcite cement that fills up the pores, with the porosity being low.

	#	%
1) Quartz	40	20
2) Feldspar	53	26.5
3) Carbonate Grains	6	3
4) Fragments	6	3
5) Kerogen	15	7.5
6) Clay Minerals	34	17
7) Calcite Cement	18	9
8) Micro Porosity	9	4.5
9) Macro Porosity	19	9.5

Well Name: **Nash Draw Unit** Well #: **23** Location: **13-T23S-R29E**

Depth: 6836.5

Description:

Very fine grained siltstone with a quartz and feldspar framework. The grains are very fine silt sized and subangular to angular grains. The grain too grain contacts are concavo-convex. The matrix is composed of clay and calcite cement. There is a lot of matrix therfore the porosity is very low and poorly interconnected.

	#	%
1) Quartz	24	12
2) Feldspar	55	27.5
3) Carbonate Grains	11	5.5
4) Fragments	1	0.5
5) Kerogen	12	6
6) Clay Minerals	42	21
7) Calcite Cement	32	16
8) Micro Porosity	9	4.5
9) Macro Porosity	14	7

Well Name: **Nash Draw Unit** Well #: **23** Location: **13-T23S-R29E**

Depth: 6811.9

Description:

Very fine grained siltstone with a quartz and feldspar framework. The grains are subangular and silt sized. The grain too grain contacts are linear to concavo-convex. The matrix is composed of clay and calcite. The porosity is moderate and fairly well interconnected. The matrix fills in the pores, thus reducing the porosity.

	#	%
1) Quartz	44	22
2) Feldspar	57	28.5
3) Carbonate Grains	1	0.5
4) Fragments	2	1
5) Kerogen	6	3
6) Clay Minerals	25	12.5
7) Calcite Cement	15	7.5
8) Micro Porosity	8	4
9) Macro Porosity	42	21

Well Name: **Nash Draw Unit** Well #: **23** Location: **13-T23S-R29E**

Depth: 6787.6

Description:

Very fine grained quartz and feldspar framework with a clay and calcite matrix, there is a lot of kerogen present in this sample. The kerogen is seen throughout the entire sample but appears to have an area that has very high in kerogen content. This area has very low porosity due to the kerogen, clay and calcite that can be seen reducing the pore space. The clay and calcite matrix is very fine and mixed together. The porosity is high and appears to be moderately interconnected.

	#	%
1) Quartz	34	17
2) Feldspar	48	24
3) Carbonate Grains	3	1.5
4) Fragments	0	0
5) Kerogen	16	8
6) Clay Minerals	27	13
7) Calcite Cement	16	8
8) Micro Porosity	9	4.5
9) Macro Porosity	48	24

Well Name: **Nash Draw Unit** Well #: **23** Location: **13-T23S-R29E**

Depth: 6764

Description:

Very fine grained quartz and feldspar framework. The grains of the framework are subangular and very fine and very low in porosity. The matrix is composed of clay and calcite cement, which fills in the pores reducing pore space.

	#	%
1) Quartz	40	20
2) Feldspar	49	24.5
3) Carbonate Grains	9	4.5
4) Fragments	3	1.5
5) Kerogen	11	5.5
6) Clay Minerals	42	21
7) Calcite Cement	24	12
8) Micro Porosity	7	3.5
9) Macro Porosity	15	7.5

Well Name: **Nash Draw Unit** Well #: **23** Location: **13-T23S-R29E**

Depth: 6752.6

Description:

Very fine grained siltstone with a fine-grained quartz and feldspar matrix. The grains are subangular and fine sand to silt sized. The grain too grain contacts are concavo-convex. The matrix consists of calcite cement and clay, which clogs up pore space and surrounds the grains. Due to the high amount of the matrix, the porosity is very low and poorly interconnected.

	#	%
1) Quartz	31	15.5
2) Feldspar	64	32
3) Carbonate Grains	2	1
4) Fragments	4	2
5) Kerogen	15	7.5
6) Clay Minerals	33	16.5
7) Calcite Cement	25	12.5
8) Micro Porosity	11	5.5
9) Macro Porosity	15	7.5

Well Name: **Nash Draw Unit** Well #: **23** Location: **13-T23S-R29E**

Depth: 6748.3

Description:

Very fine grained sandstone with a quartz and feldspar framework. Some carbonate is also present in the framework. The grains are subangular to angular. Very fine sand to silt sized grains. The grain too grain contacts are planar and concavo-convex. The matrix consists of calcite cement (mainly) and clay. The matrix fills in the pores and surrounds the grains. The porosity is very low and poorly interconnected, due to the clay and calcite matrix. In this sample there is some kerogen present.

	#	%
1) Quartz	29	14.5
2) Feldspar	58	29
3) Carbonate Grains	10	5
4) Fragments	5	2.5
5) Kerogen	13	6.5
6) Clay Minerals	29	14.5
7) Calcite Cement	37	18.5
8) Micro Porosity	10	5
9) Macro Porosity	9	4.5

Well Name: **Nash Draw Unit** Well #: **23** Location: **13-T23S-R29E**

Depth: 6730.9

Description:

Very fine grained sandstone with a quartz and feldspar matrix. The grains are subangular to subround and very fine. The grain too grain contacts are concavo-convex. The matrix is composed of calcite cement and clay. Due to the high amount of matrix, the porosity is very low and poorly interconnected.

	#	%
1) Quartz	37	18.5
2) Feldspar	50	25
3) Carbonate Grains	1	0.5
4) Fragments	4	2
5) Kerogen	7	3.5
6) Clay Minerals	38	19
7) Calcite Cement	59	29.5
8) Micro Porosity	1	0.5
9) Macro Porosity	3	1.5

Well Name: **Nash Draw Unit** Well #: **23** Location: **13-T23S-R29E**

Depth: 6730.5

Description:

The framework is a quartz and feldspar, with a clay and calcite matrix. The framework is subrounded and the grain size is very fine sand to silt. The framework of the clay and calcite is very fine and often mixed together. The matrix is easliy seen surrounding the grains and is filling in some pore spaces. The porosity is high and well interconnected.

	#	%
1) Quartz	40	20
2) Feldspar	36	18
3) Carbonate Grains	1	0.5
4) Fragments	2	1
5) Kerogen	3	1.5
6) Clay Minerals	40	20
7) Calcite Cement	36	18
8) Micro Porosity	3	1.5
9) Macro Porosity	39	19.5

Well Name: **Nash Draw Unit** Well #: **23** Location: **13-T23S-R29E**

Depth: 6701

Description:

Very fine grained quartz and feldspar with a clay and calcite matrix. The matrix fills in some pores but the porosity is high and well interconnected. Some kerogen is present and also fills in some pores. The grain too grain contacts are linear to concavo-convex and subrounded to subangular.

	#	%
1) Quartz	35	17.5
2) Feldspar	54	27
3) Carbonate Grains	2	1
4) Fragments	3	1.5
5) Kerogen	8	4
6) Clay Minerals	24	12
7) Calcite Cement	20	10
8) Micro Porosity	9	4.5
9) Macro Porosity	45	22.5

Well Name: **Nash Draw Unit** Well #: **23** Location: **13-T23S-R29E**

Depth: 6697.1

Description:

Very fine grained siltstone with a quartz and feldspar framework. The grains are silt sized and subrounded to subangular. The grain too grain contacts are concavo-convex to point. The matrix (very little) is composed of clay and calcite cement with high porosity and well interconneted. This sample contains very little kerogen.

	#	%
1) Quartz	40	20
2) Feldspar	70	35
3) Carbonate Grains	0	0
4) Fragments	1	0.5
5) Kerogen	4	2
6) Clay Minerals	24	12
7) Calcite Cement	5	2.5
8) Micro Porosity	5	2.5
9) Macro Porosity	51	25.5

Well Name: **Nash Draw Unit** Well #: **23** Location: **13-T23S-R29E**

Depth: 6662.9

Description:

Very fine grained siltstone with a quartz and feldspar framework. The grains are very fine sand sized and are subangular to subrounded. The matrix consists of clay and some calcite cement. The porosity is high and fairly well interconnected. The grain too grain contacts are convaco-convex to linear. This sample contains very little kerogen. Note—some small areas are rich in calcite and some clay, but in the pores.

	#	%
1) Quartz	57	28.5
2) Feldspar	47	23.5
3) Carbonate Grains	3	1.5
4) Fragments	2	1
5) Kerogen	1	0.5
6) Clay Minerals	25	12.5
7) Calcite Cement	12	6
8) Micro Porosity	7	3.5
9) Macro Porosity	46	23

Well Name: **Nash Draw Unit** Well #: **23** Location: **13-T23S-R29E**

Depth: 6661.5

Description:

Very fine grained siltstone with a quartz and feldspar framework. The grains are silt sized subangular and the grain too grain contacts are concavo-convex. The matrix is composed of calcite cement and clay. There is not a lot of matrix therfore, the porosity is moderately high but does not appear to be well connected. There is very little kerogen present in this sample.

	#	%
1) Quartz	38	19
2) Feldspar	82	41
3) Carbonate Grains	1	0.5
4) Fragments	2	1
5) Kerogen	1	0.5
6) Clay Minerals	32	16
7) Calcite Cement	12	6
8) Micro Porosity	0	0
9) Macro Porosity	32	16

Well Name: **Poker Lake Unit** Well #: **80** Location: **19-T24S-R31E**

Depth: 8004.9

Description:

Very fine grained siltstone with a quartz and feldspar matrix, with silt sized and subangular to subrounded grains. The grain too grain contacts are concavo-convex. The matrix (very high amounts) is composed of clay and calcite cement and the porosity (very little).

	#	%
1) Quartz	25	12.5
2) Feldspar	72	36
3) Carbonate Grains	3	1.5
4) Fragments	3	1.5
5) Kerogen	14	7
6) Clay Minerals	31	15.5
7) Calcite Cement	43	21.5
8) Micro Porosity	1	0.5
9) Macro Porosity	8	4

Well Name: **Poker Lake Unit** Well #: **80** Location: **19-T24S-R31E**

Depth: 7994.6

Description:

Very fine grained siltstone with a quartz and feldspar framework, with silt sized, subrounded grains. The grain too grain contacts are concavo-convex to point. The matrix (low) consists of clay and calcite cement, so the pore spaces are individually small but well interconnected.

	#	%
1) Quartz	38	19
2) Feldspar	73	36.5
3) Carbonate Grains	3	1.5
4) Fragments	2	1
5) Kerogen	4	2
6) Clay Minerals	25	12.5
7) Calcite Cement	11	5.5
8) Micro Porosity	3	1.5
9) Macro Porosity	41	20.5

Well Name: **Poker Lake Unit** Well #: **80** Location: **19-T24S-R31E**

Depth: 7988

Description:

Very fine grained siltstone with a quartz and feldspar framework, with silt sized subangular grains. The grain too grain contacts are concavo-convex and the matrix consists of calcite cement and clay.

	#	%
1) Quartz	34	17
2) Feldspar	80	40
3) Carbonate Grains	6	3
4) Fragments	2	1
5) Kerogen	3	1.5
6) Clay Minerals	15	7.5
7) Calcite Cement	45	22.5
8) Micro Porosity	6	3
9) Macro Porosity	9	4.5

Well Name: **Poker Lake Unit** Well #: **80** Location: **19-T24S-R31E**

Depth: 7979.9

Description:

Very fine grained siltstone with a quartz and feldspar framework, with silt sized and subrounded grains. The grain too grain contacts are concavo-convex to point. The matrix (low) consists of clay and calcite cement, so the pore spaces are individually small but well interconnected.

	#	%
1) Quartz	46	23
2) Feldspar	69	34.5
3) Carbonate Grains	8	4
4) Fragments	2	1
5) Kerogen	2	1
6) Clay Minerals	20	10
7) Calcite Cement	9	4.5
8) Micro Porosity	2	1
9) Macro Porosity	42	21

Well Name: **Poker Lake Unit** Well #: **80** Location: **19-T24S-R31E**

Depth: 7964.9

Description:

Very fine grained siltstone with a quartz and feldspar framework. The grains are silt sized, subangular to sub rounded. The grain too grain contacts are point to concavo-convex. The matrix (high) composed of clay and calcite cement, the porosity (high) is moderately well interconnected.

	#	%
1) Quartz	31	15.5
2) Feldspar	65	32.5
3) Carbonate Grains	4	2
4) Fragments	3	1.5
5) Kerogen	8	4
6) Clay Minerals	10	5
7) Calcite Cement	19	9.5
8) Micro Porosity	1	0.5
9) Macro Porosity	59	29.5

Well Name: **Poker Lake Unit** Well #: **80** Location: **19-T24S-R31E**

Depth: 7898.5

Description:

Very fine grained siltstone with a quartz and feldspar matrix, silt sized grains that are subrounded and point at grain too grain contacts. The matrix (very little) consists of clay to calcite cement. The porosity (high) is well interconnected.

	#	%
1) Quartz	45	22.5
2) Feldspar	72	36
3) Carbonate Grains	5	2.5
4) Fragments	1	0.5
5) Kerogen	9	4.5
6) Clay Minerals	11	5.5
7) Calcite Cement	7	3.5
8) Micro Porosity	1	0.5
9) Macro Porosity	49	24.5

Well Name: **Poker Lake Unit** Well #: **80** Location: **19-T24S-R31E**

Depth: 7891.6

Description:

Very fine grained siltstone with a quartz and feldspar framework, with subrounded to subangular grains. The grain too grain contacts are point to concavo-convex. The matrix (low) consists of clay and calcite cement, porosity (high) is well interconnected.

	#	%
1) Quartz	32	16
2) Feldspar	72	36
3) Carbonate Grains	4	2
4) Fragments	0	0
5) Kerogen	8	4
6) Clay Minerals	17	8.5
7) Calcite Cement	9	4.5
8) Micro Porosity	6	3
9) Macro Porosity	52	26

Well Name: **Poker Lake Unit** Well #: **80** Location: **19-T24S-R31E**

Depth: 7870

Description:

Very fine grained siltstone with quartz and feldspar framework, the grains are silt sized and subrounded. The grain too grain contacts are point. The matrix (little) consists of clay and calcite cement, the porosity (high) is large and interconnected pores.

	#	%
1) Quartz	50	25
2) Feldspar	59	29.5
3) Carbonate Grains	1	0.5
4) Fragments	4	2
5) Kerogen	1	0.5
6) Clay Minerals	23	11.5
7) Calcite Cement	5	2.5
8) Micro Porosity	2	1
9) Macro Porosity	55	27.5

Well Name: **Poker Lake Unit** Well #: **80** Location: **19-T24S-R31E**

Depth: 7867

Description:

Very fine grained siltstone with a quartz and feldspar framework. The grains are silt sized and subrounded. The grain too grain contacts are concavo-convex to point. The matrix (low) is composed of clay and calcite cement, the porosity (high) is well interconnected but the pore spaces are fairly small.

	#	%
1) Quartz	50	25
2) Feldspar	62	31
3) Carbonate Grains	5	2.5
4) Fragments	0	0
5) Kerogen	11	5.5
6) Clay Minerals	20	10
7) Calcite Cement	6	3
8) Micro Porosity	7	3.5
9) Macro Porosity	39	19.5

Well Name: **South Culebra Bluff** Well #: **5** Location: **13-T23S-R28E**

Depth: 6229

Description:

Very fine grained siltstone with a quartz and feldspar framework. The grains are fine silt sized and subangular, with contacts concavo-convex. The matrix (very high) is composed of clay and calcite cement, with the porosity very low. In this sample fossil is present.

	#	%
1) Quartz	39	19.5
2) Feldspar	60	30
3) Carbonate Grains	5	2.5
4) Fragments	0	0
5) Kerogen	7	3.5
6) Clay Minerals	23	11.5
7) Calcite Cement	55	27.5
8) Micro Porosity	5	2.5
9) Macro Porosity	6	3

Well Name: **South Culebra Bluff** Well #: **5** Location: **13-T23S-R28E**

Depth: 6068

Description:

Very fine grained siltstone with a quartz and feldspar framework. The grains are silt sized and subangular to subrounded. The grain too grain contacts are point contacts. The matrix (low) is composed of clay and calcite cement, the porosity (high) is well interconnected.

	#	%
1) Quartz	27	13.5
2) Feldspar	56	28
3) Carbonate Grains	8	2
4) Fragments	3	1.5
5) Kerogen	5	2.5
6) Clay Minerals	20	10
7) Calcite Cement	12	6
8) Micro Porosity	2	1
9) Macro Porosity	67	33.5

Well Name: **South Culebra Bluff** Well #: **5** Location: **13-T23S-R28E**

Depth: 6058

Description:

Very fine grained siltstone with a quartz and feldspar framework. The grains are silt sized and subangular. The grain too grain contacts are point and concavo-convex contacts. The matrix (little) is composed of clay and carbonate, with the porosity (high) well interconnected.

	#	%
1) Quartz	47	23.5
2) Feldspar	53	26.5
3) Carbonate Grains	2	1
4) Fragments	2	1
5) Kerogen	4	2
6) Clay Minerals	18	9
7) Calcite Cement	12	6
8) Micro Porosity	3	1.5
9) Macro Porosity	59	29.5

APPENDIX III

MAPS

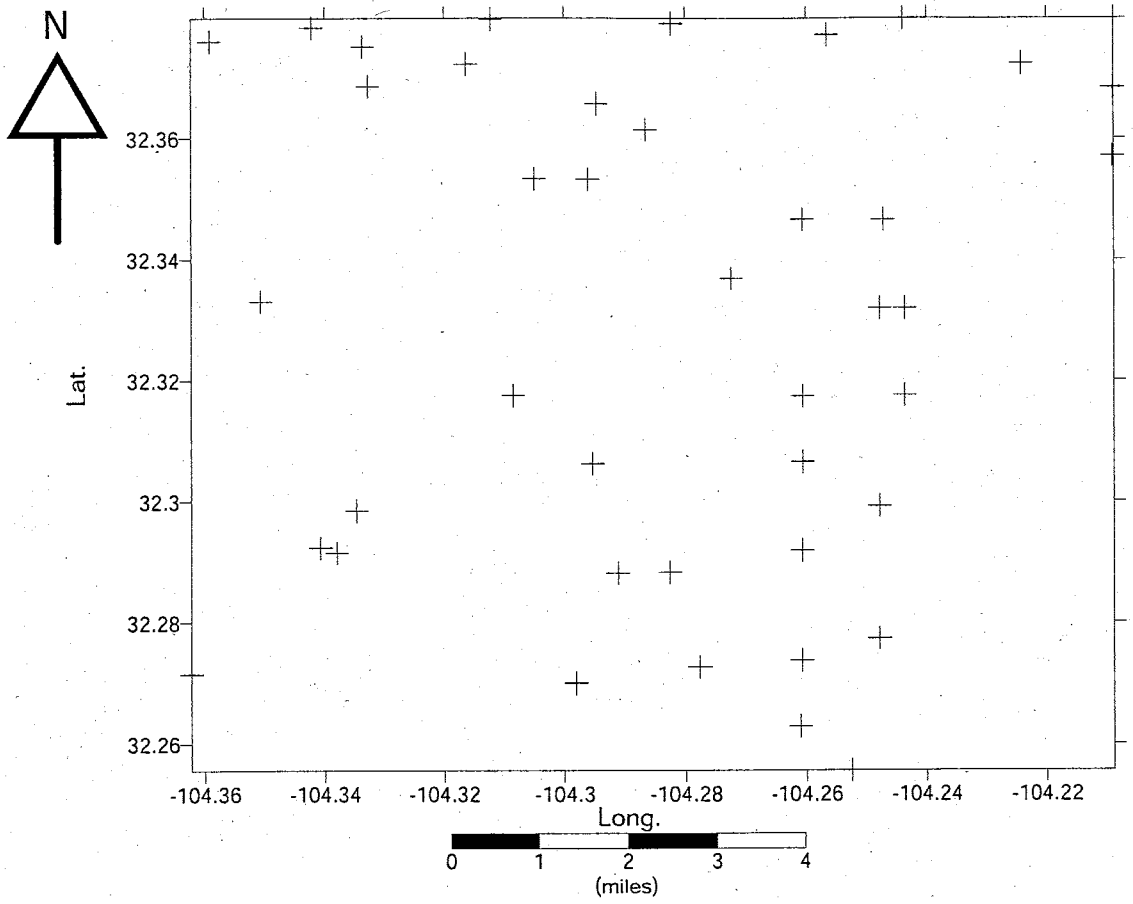

Western area well locations for structure and isopach maps.

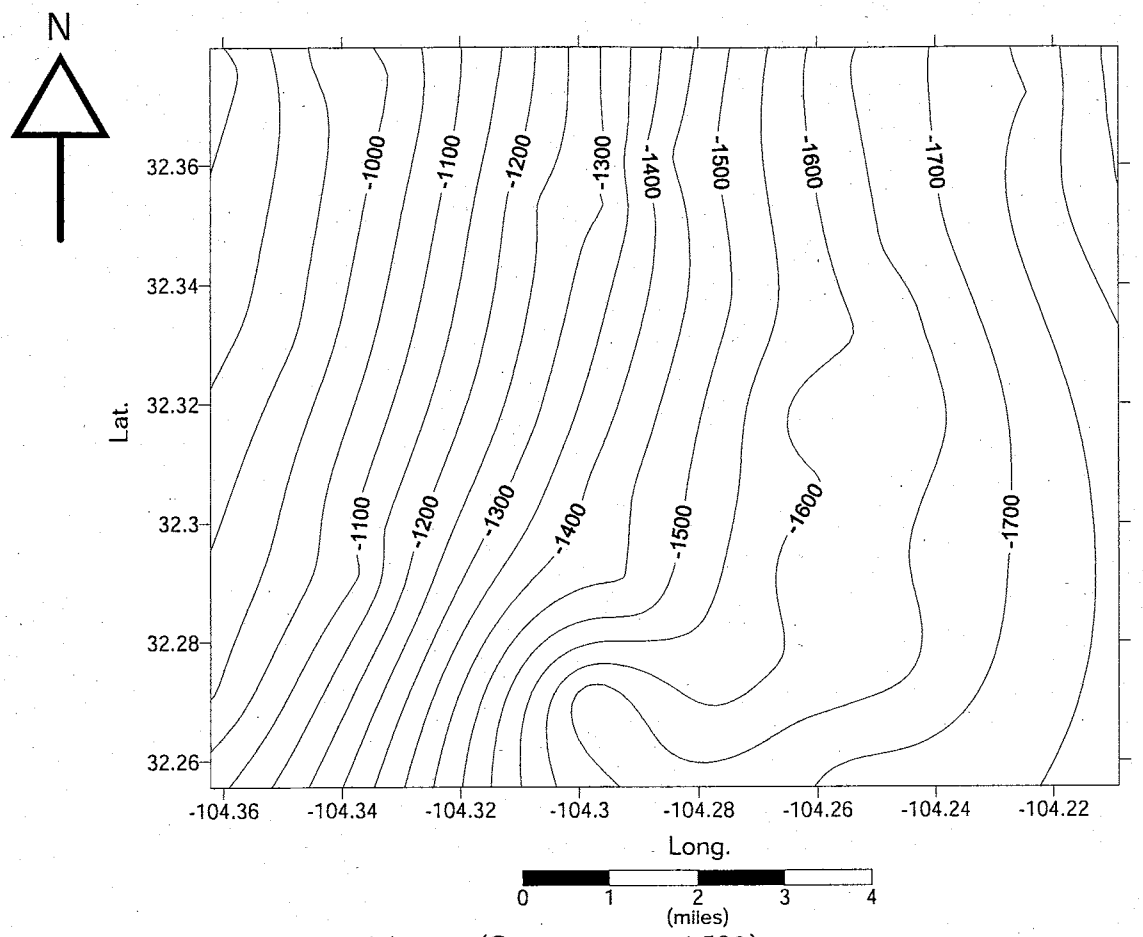

Western area structure top of A unit. (Contour interval 50ft)

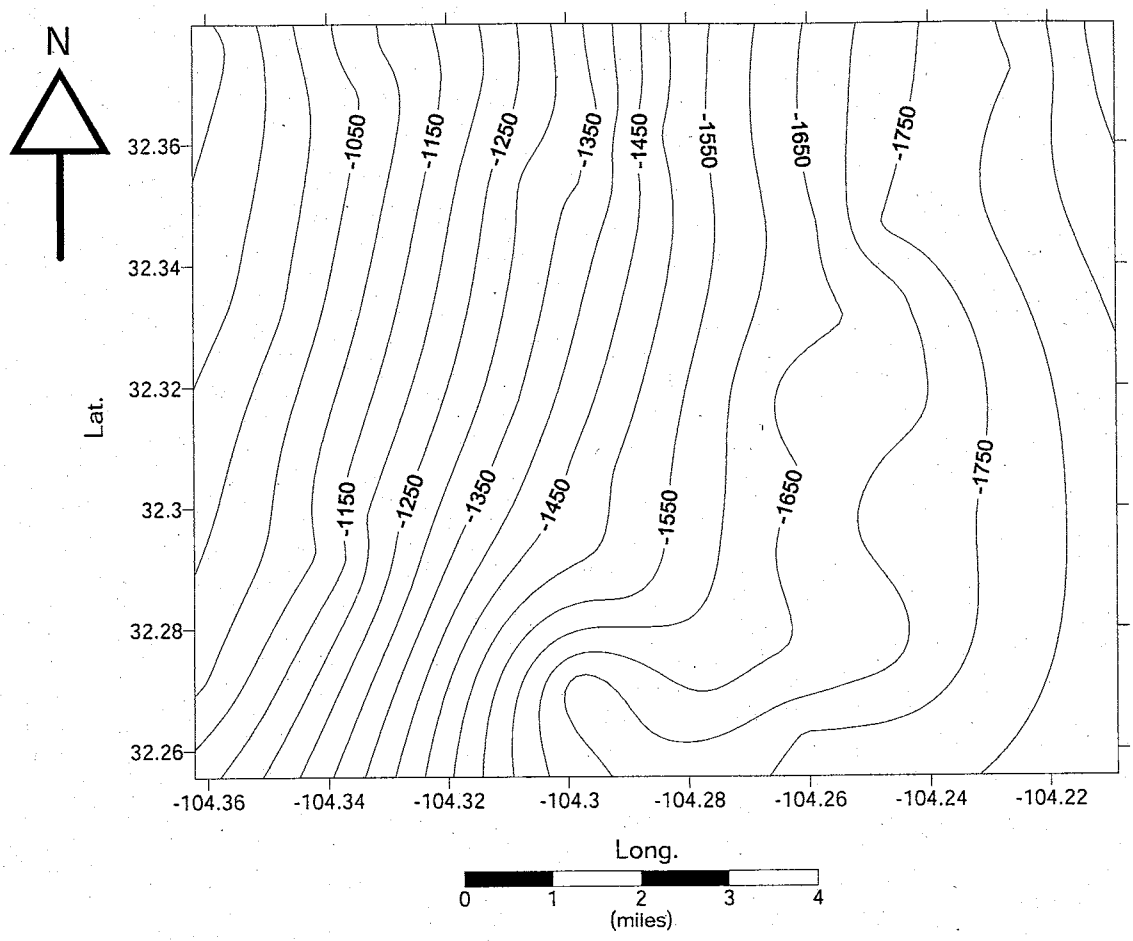

Western area structure, top of B unit. (Contour interval 50ft)

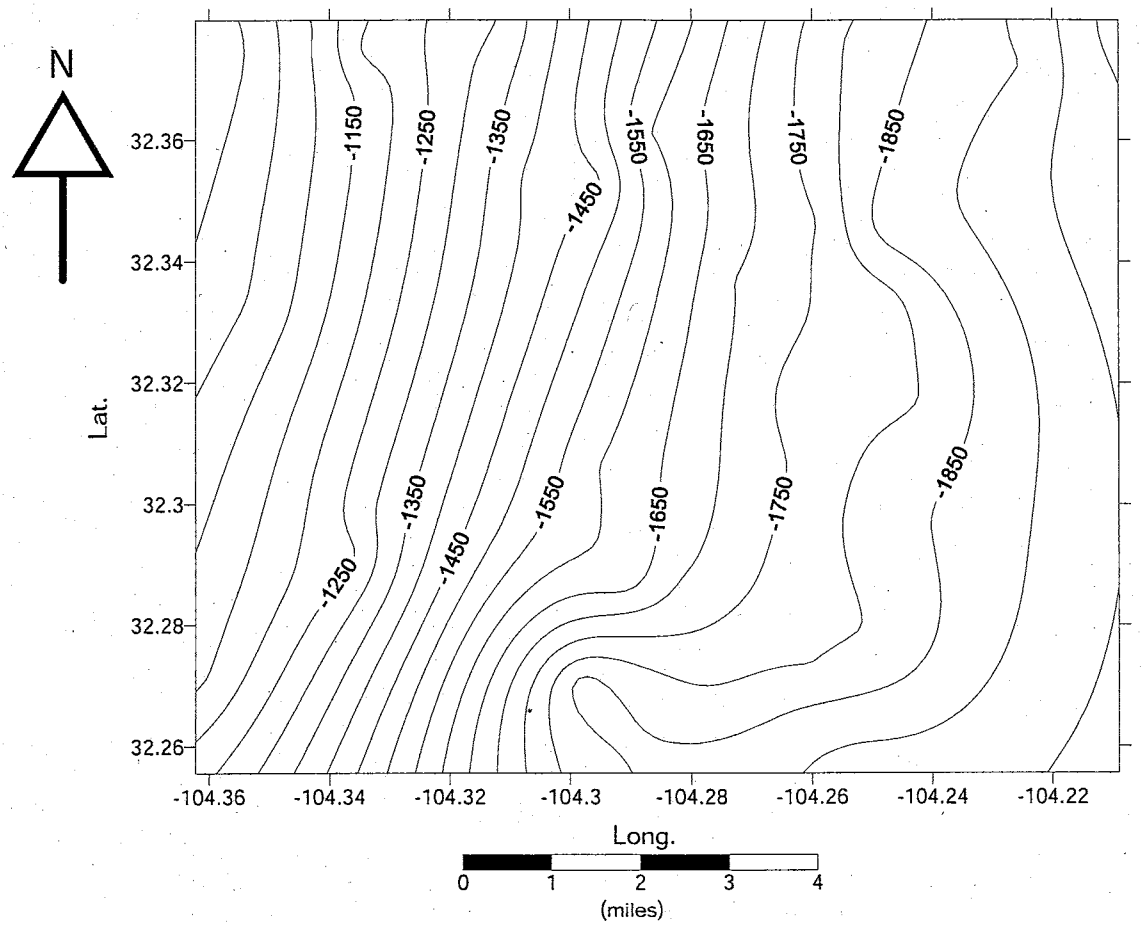

Western area structure, top of C unit. (Contour interval 50ft)

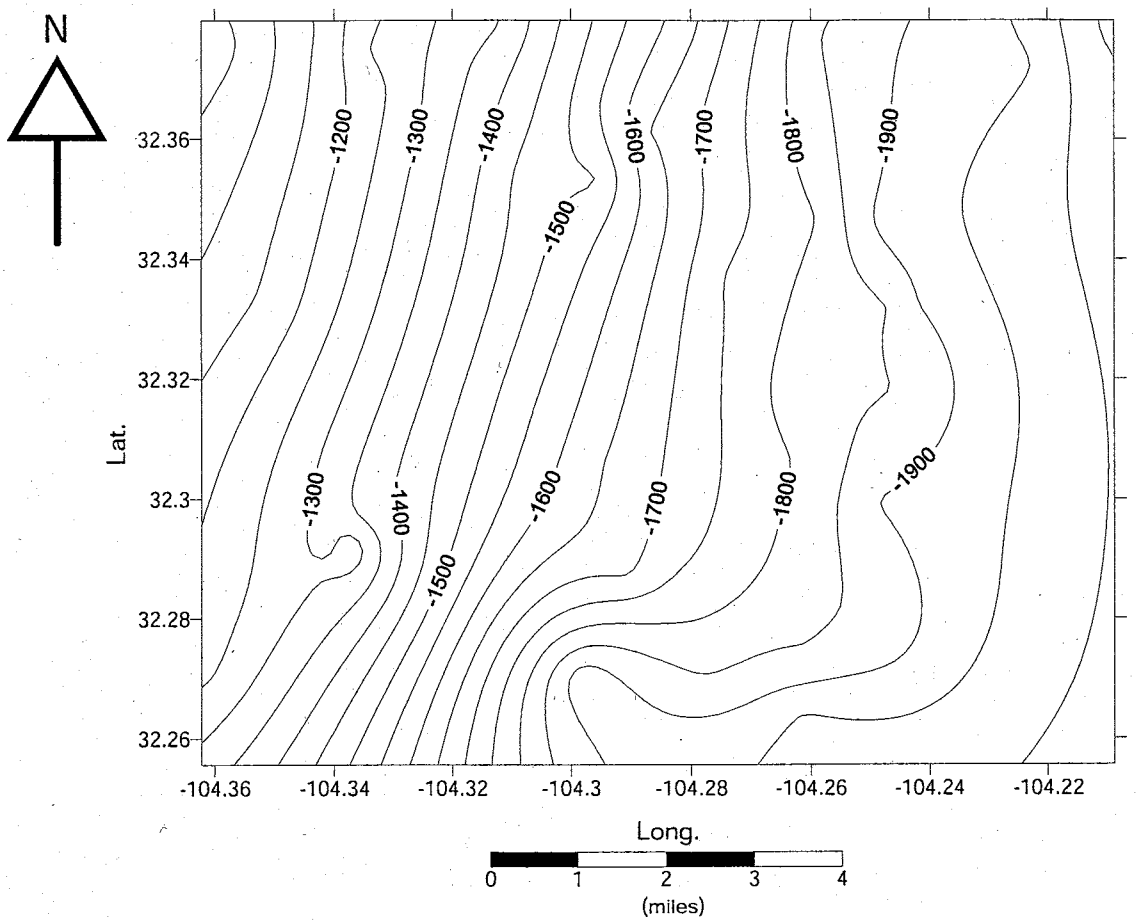

Western area structure, top of D unit. (Contour interval 50ft)

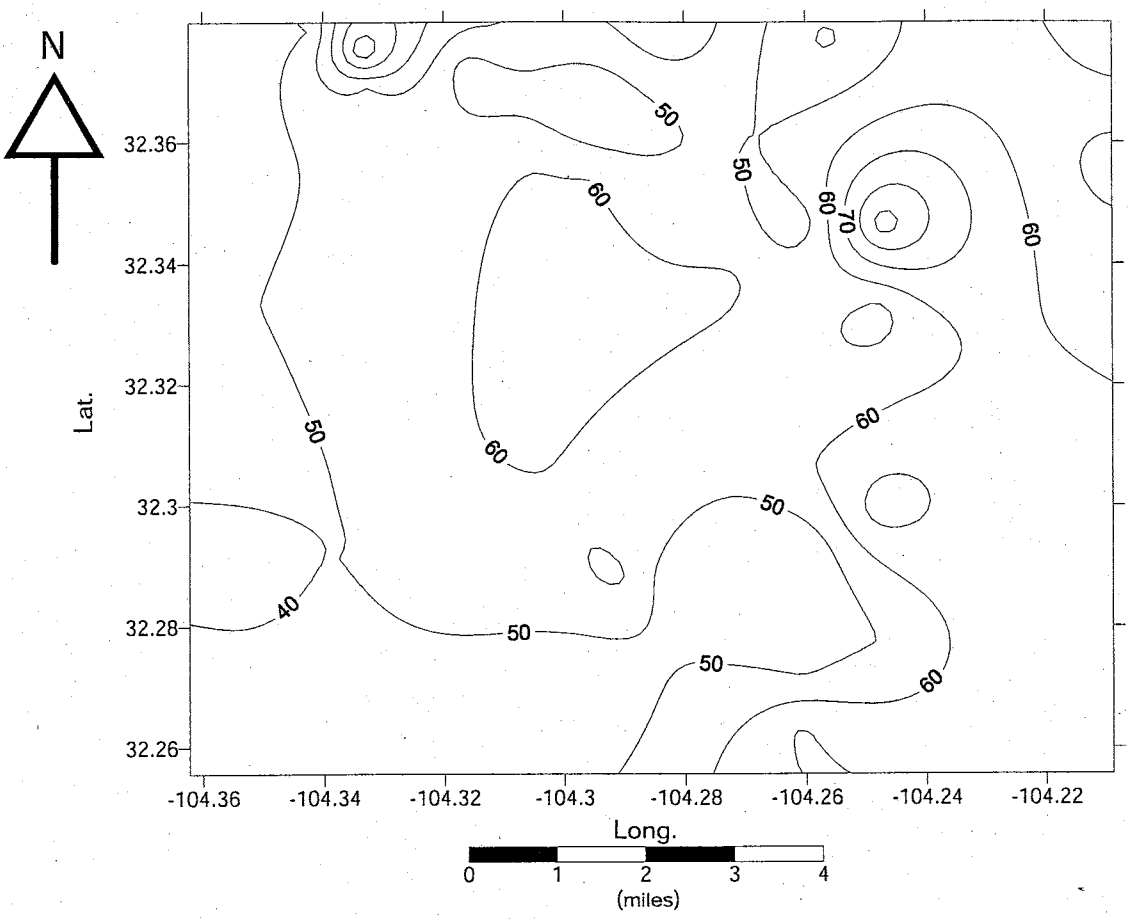

Western area isopach, A unit. (Contour interval 10ft)

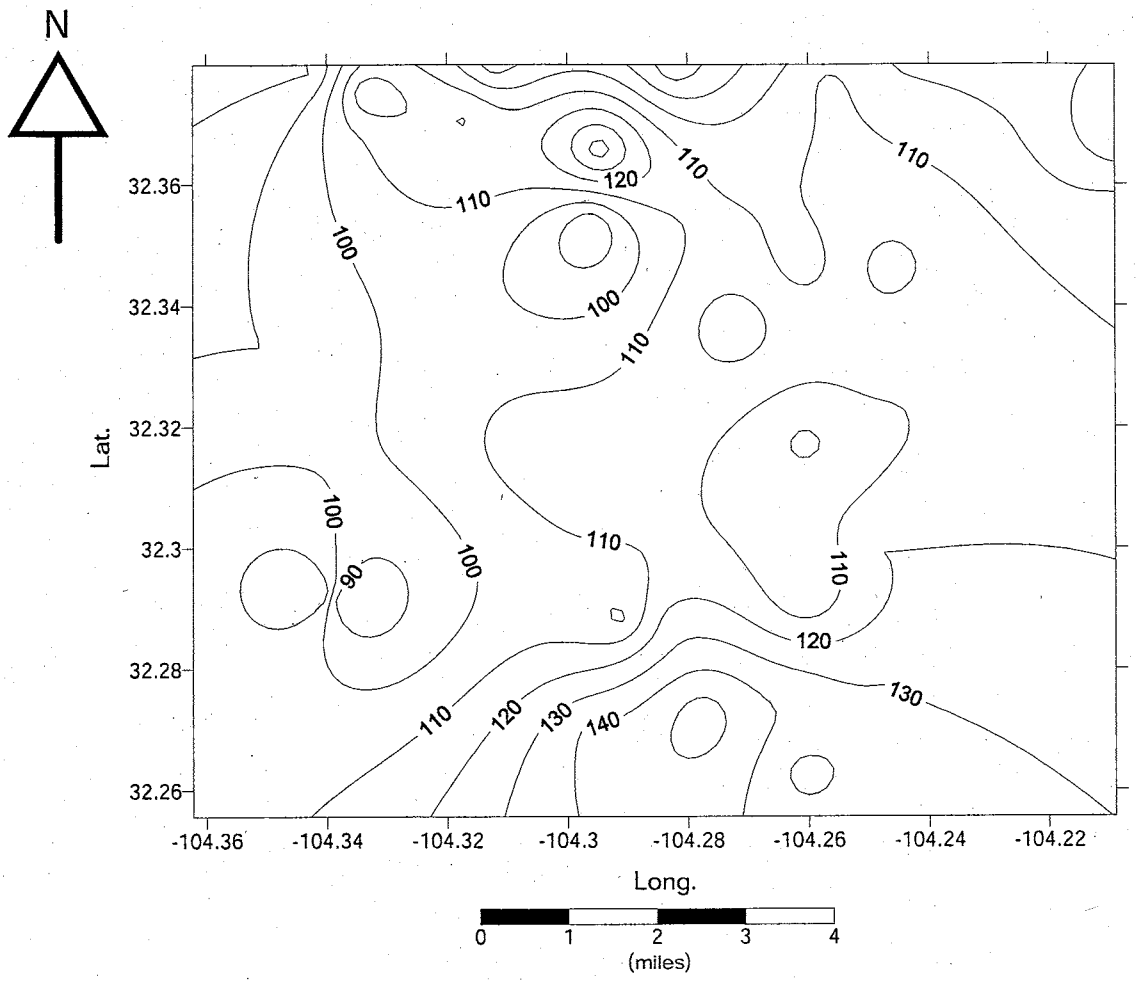

Western area isopach B unit. (Contour interval 10ft)

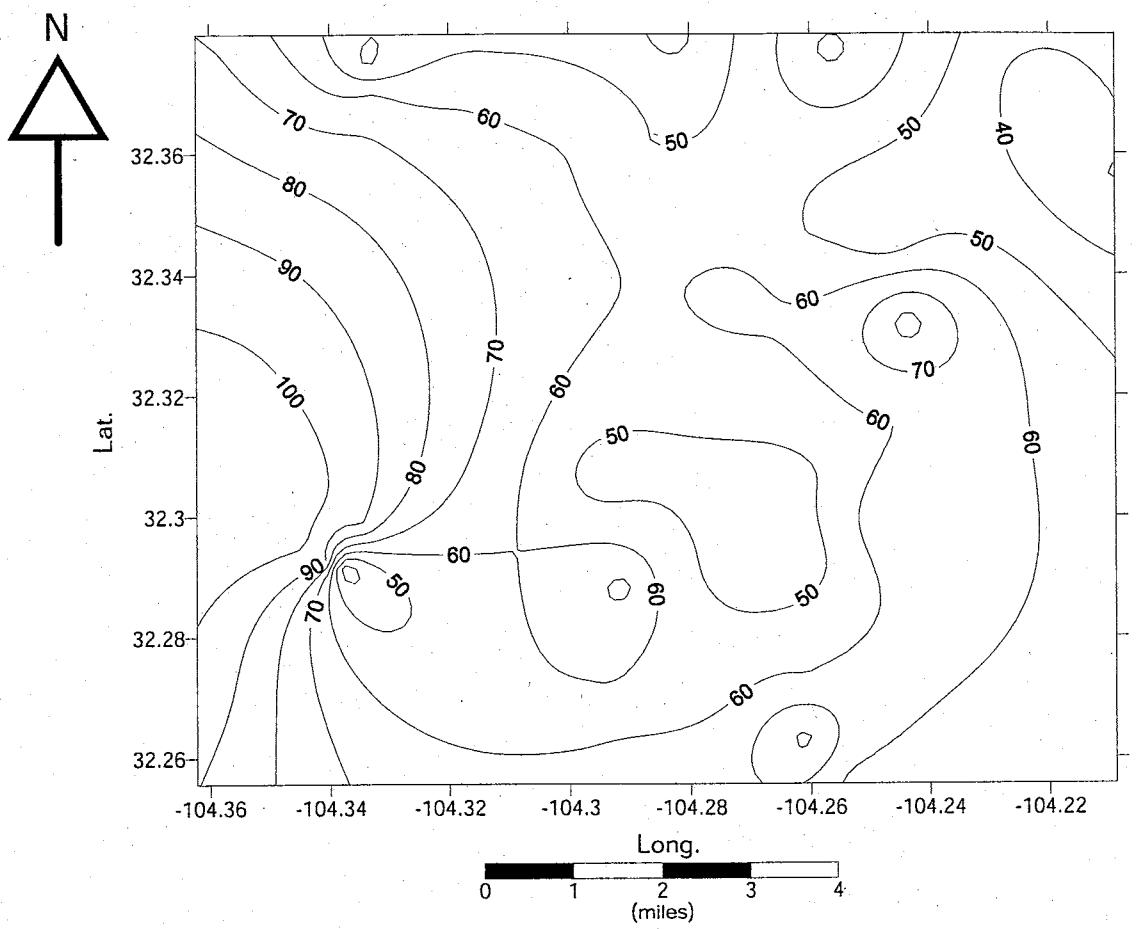

Western area isopach C unit. (Contour interval 10ft)

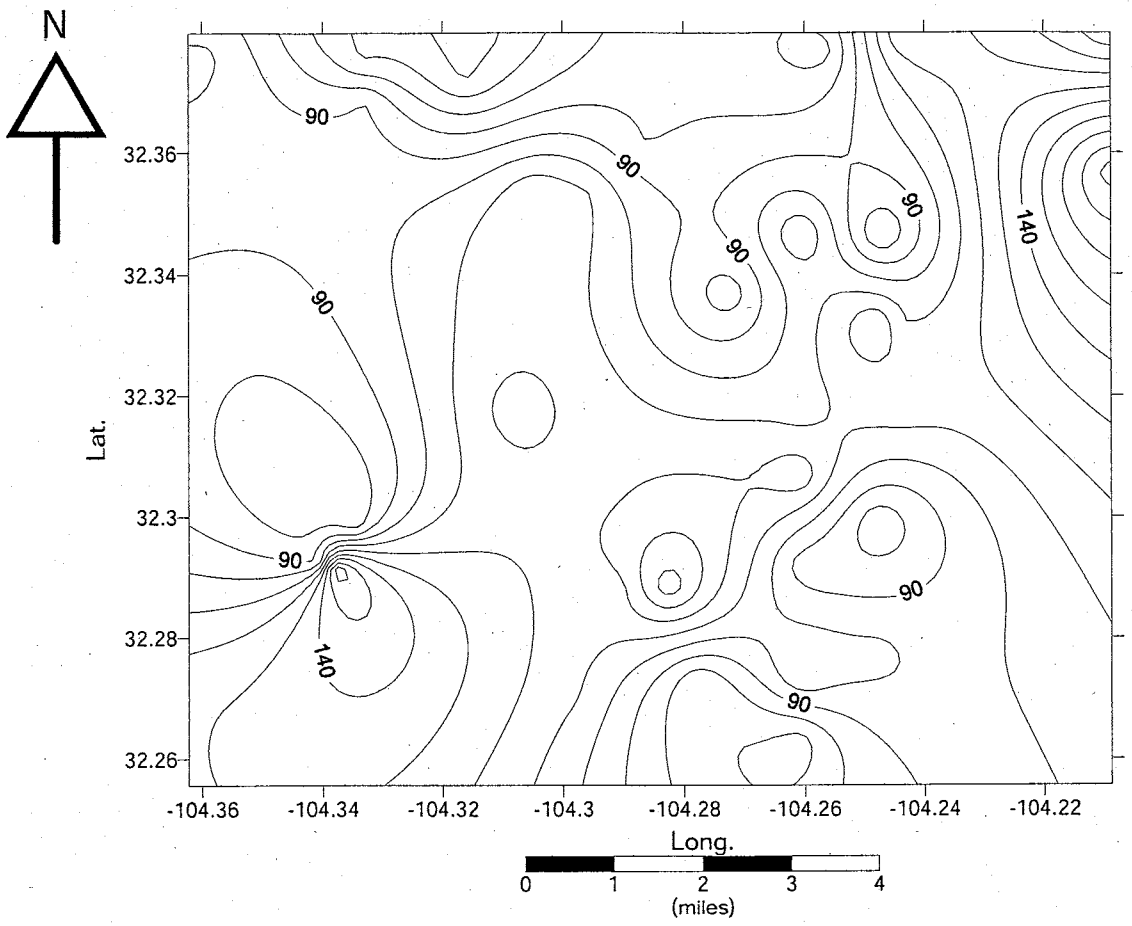

Western area isopach D unit. (Contour interval 10ft)

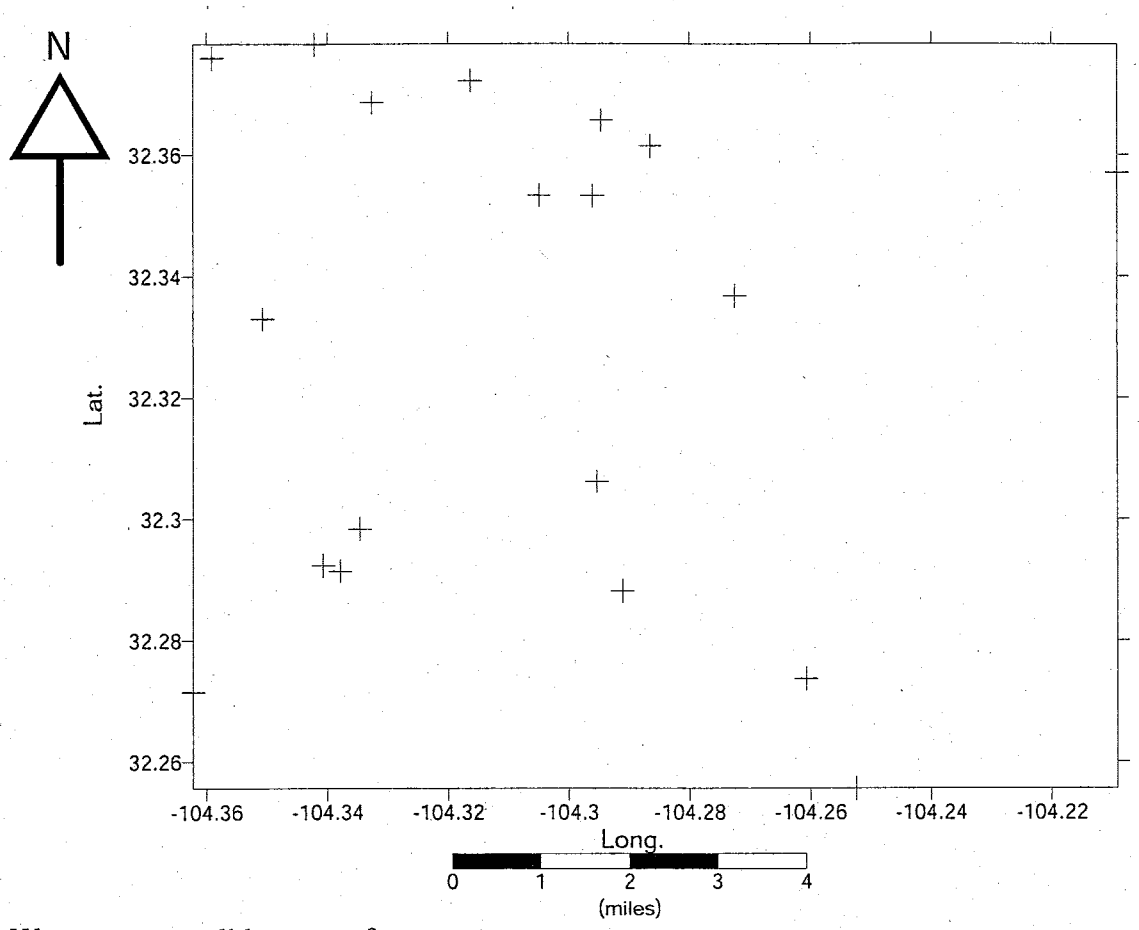

Western area well locations for porosity maps.

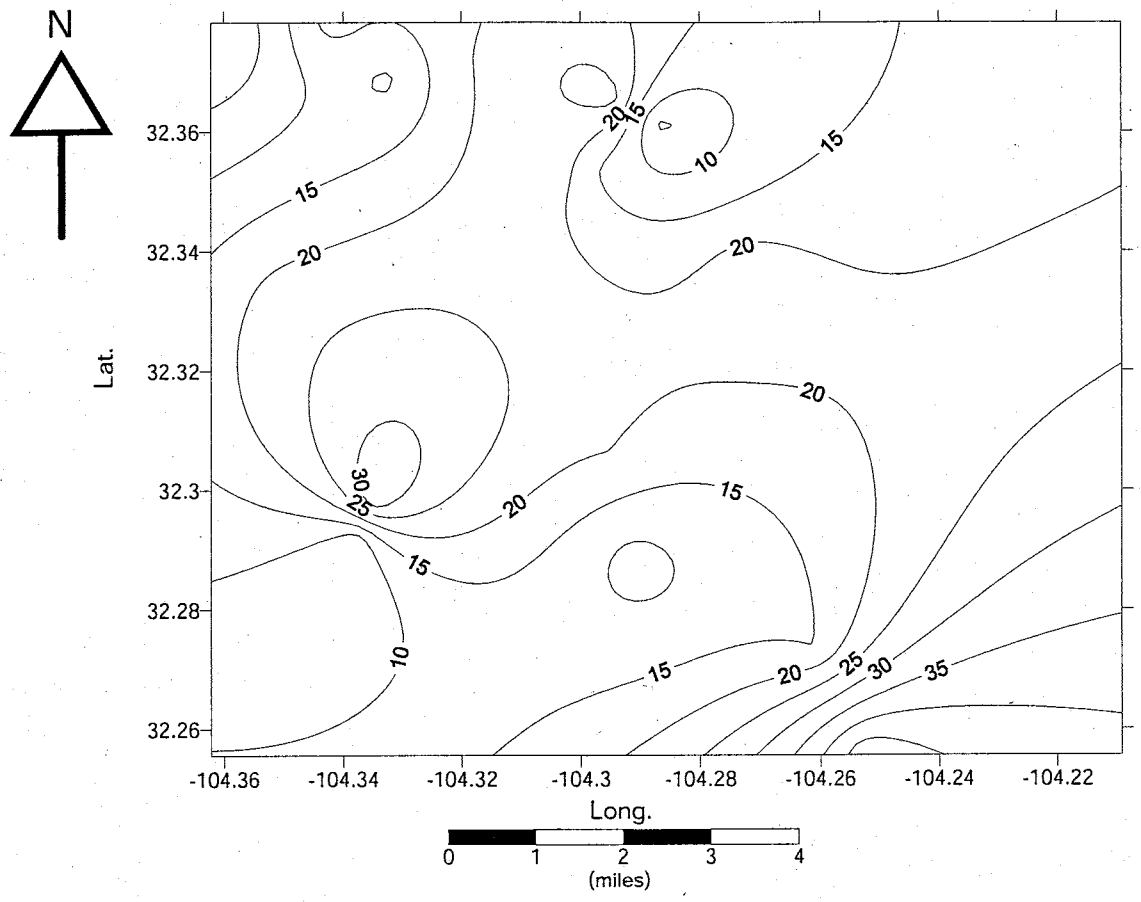

Western area isopach of sands with over 10% porosity, A unit. (Contour interval 5ft)

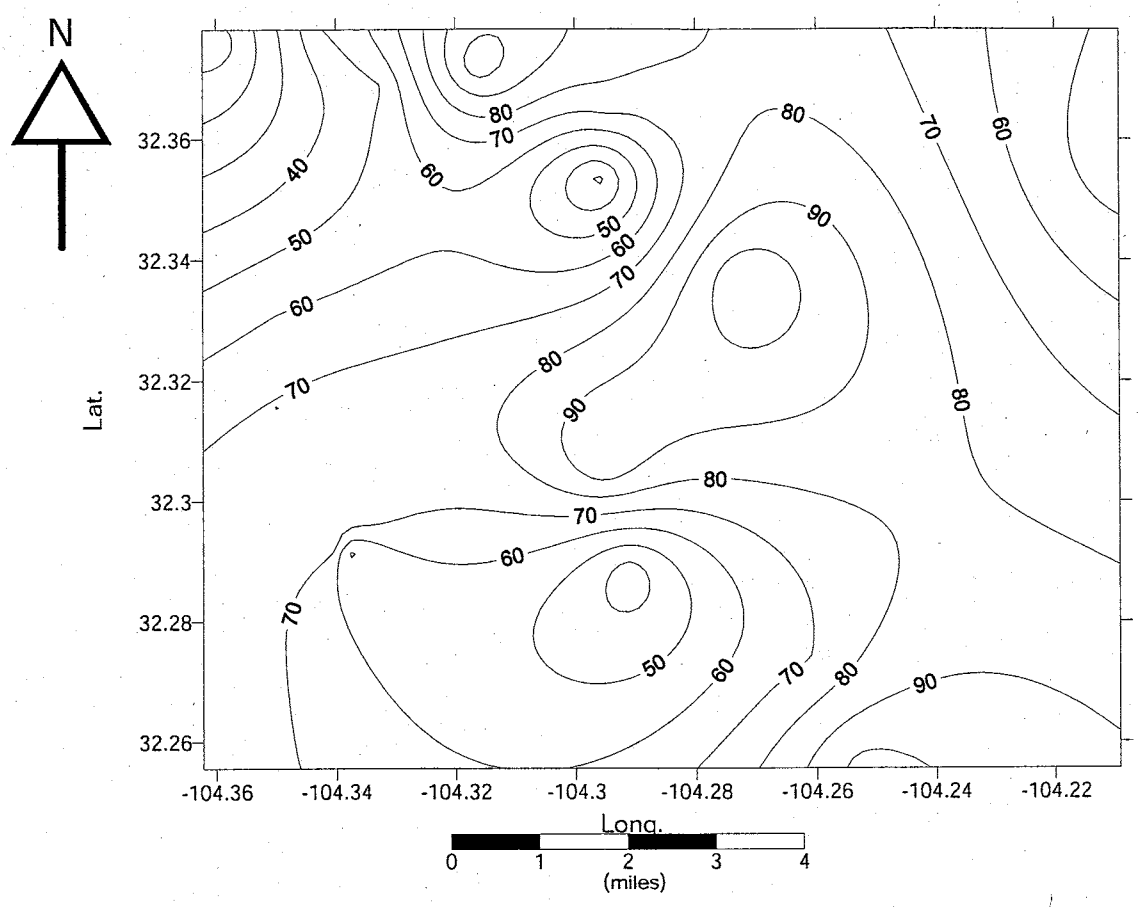

Western area isopach of sands with over 10% porosity, B unit. (Contour interval 10ft)

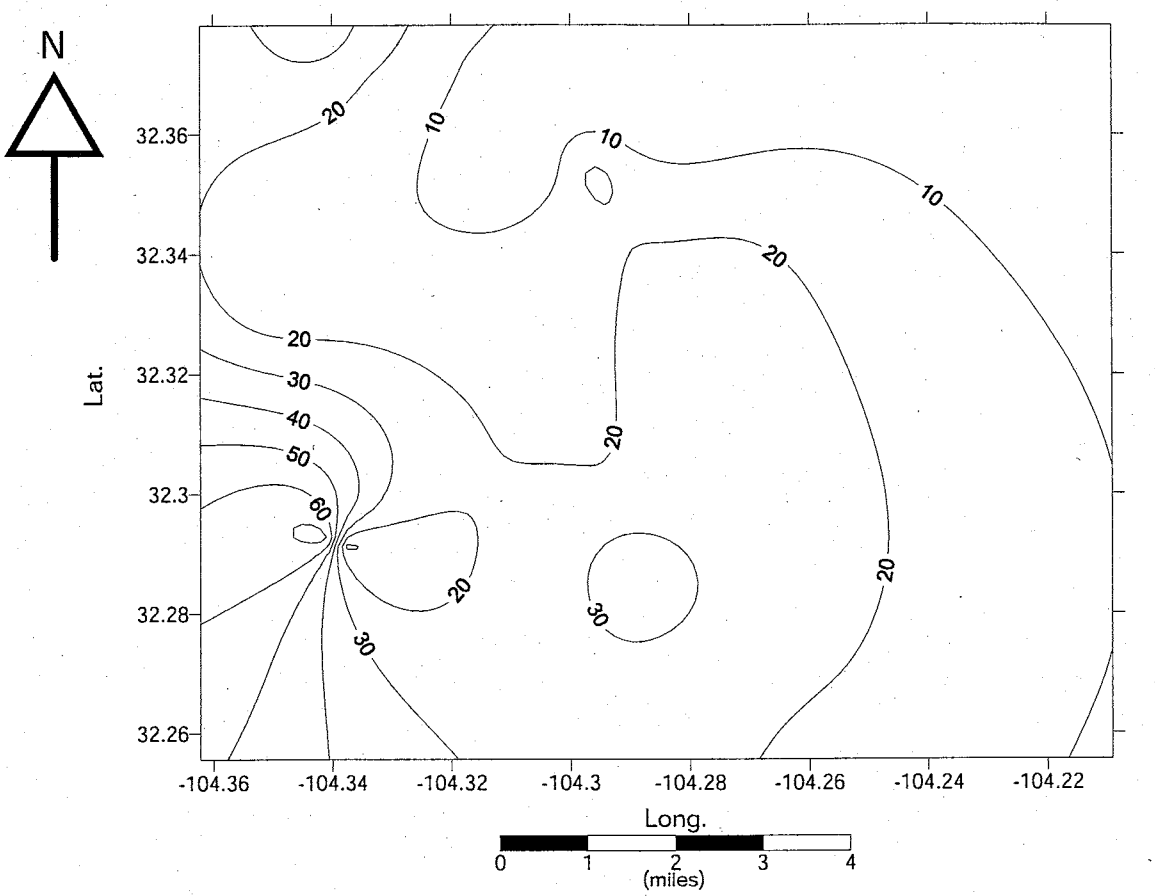

Western area isopach of sands with over 10% porosity, C unit. (Contour interval 10ft)

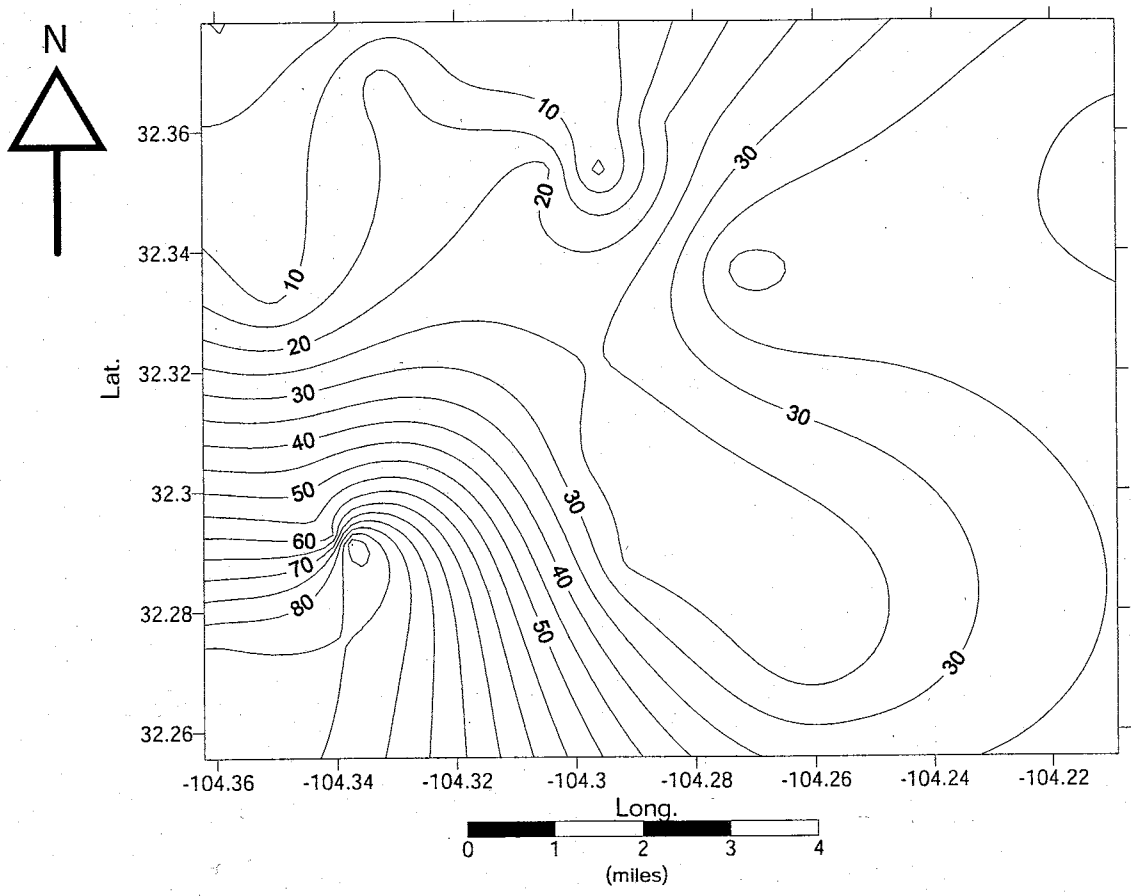

Western area isopach of sand with over 10% porosity, D unit. (Contour interval 5ft)

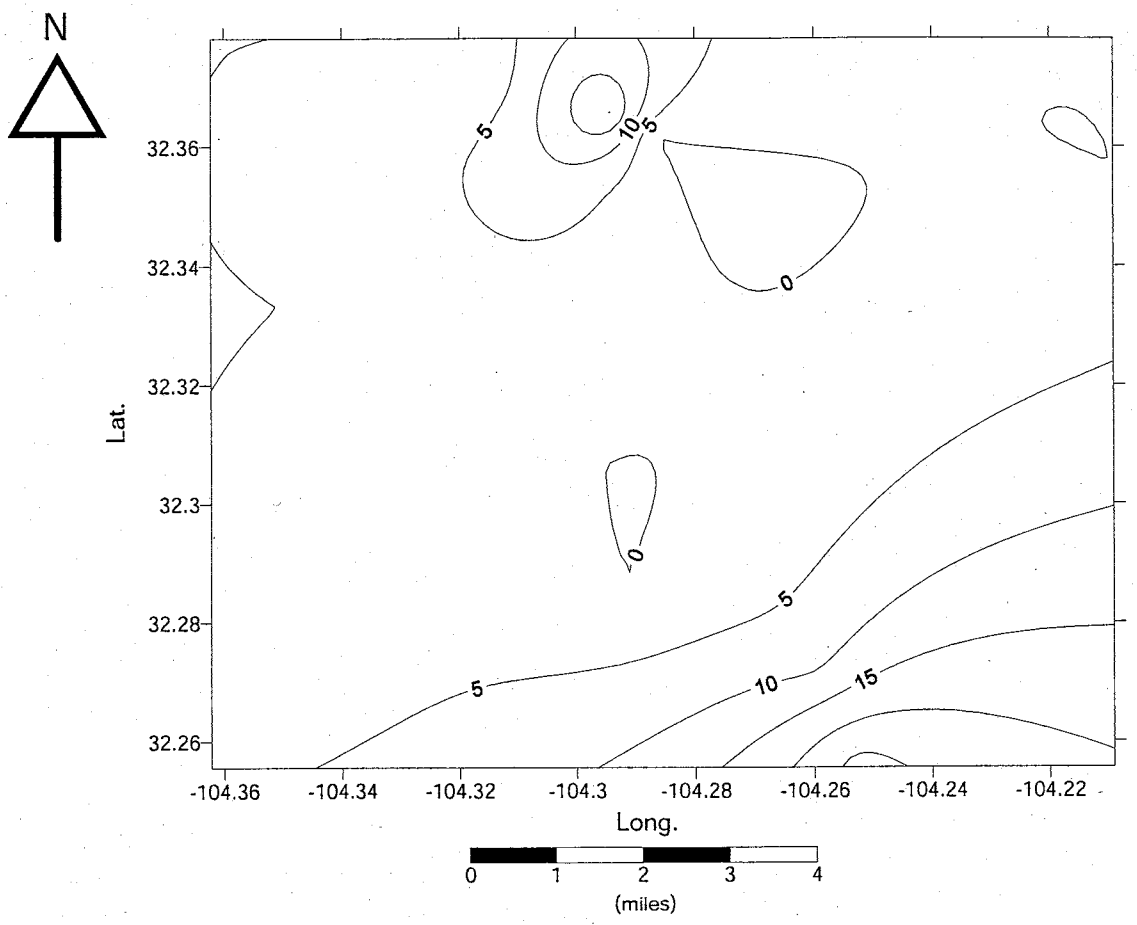

Western area isopach of sands with over 15% porosity, A unit. (Contour interval 5ft)

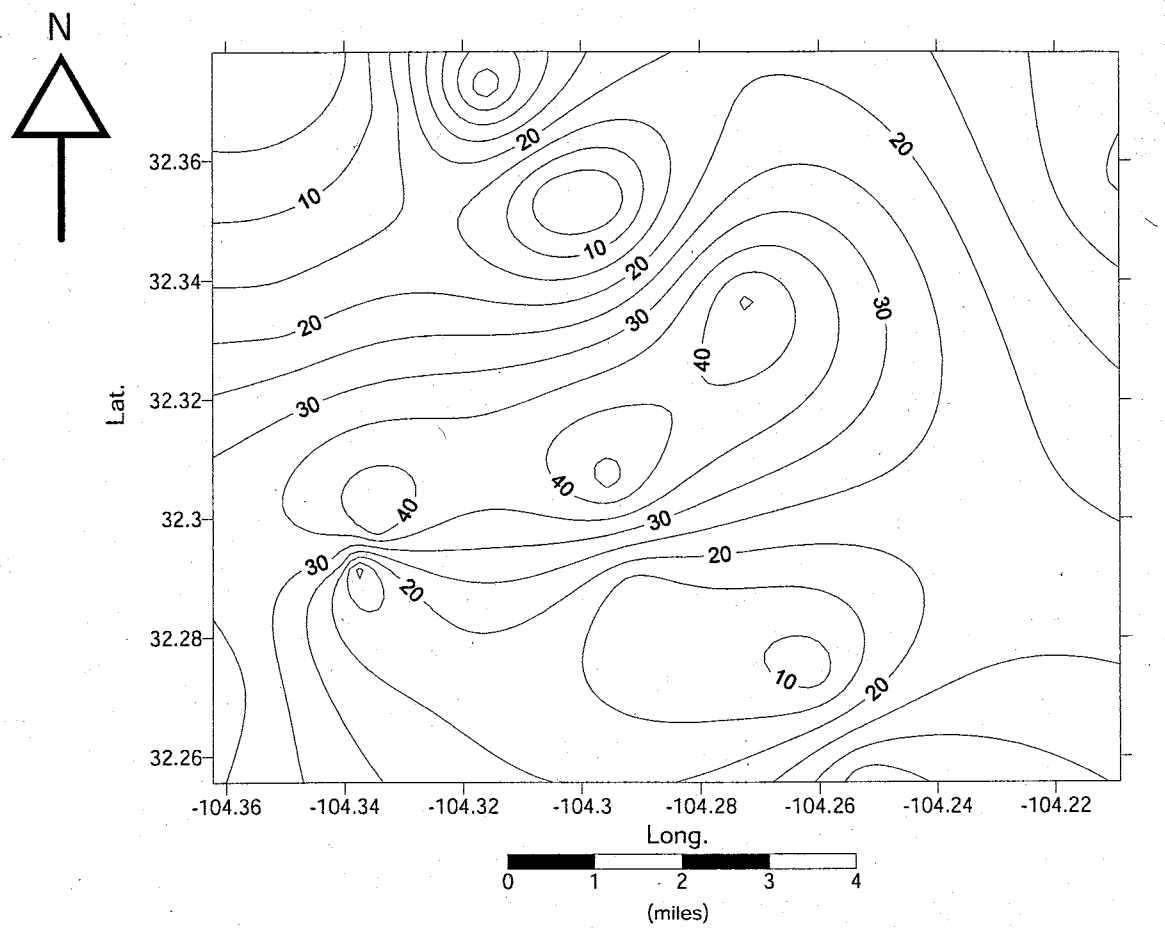

Western area isopach of sands with over 15% porosity, B unit. (Contour interval 5ft)

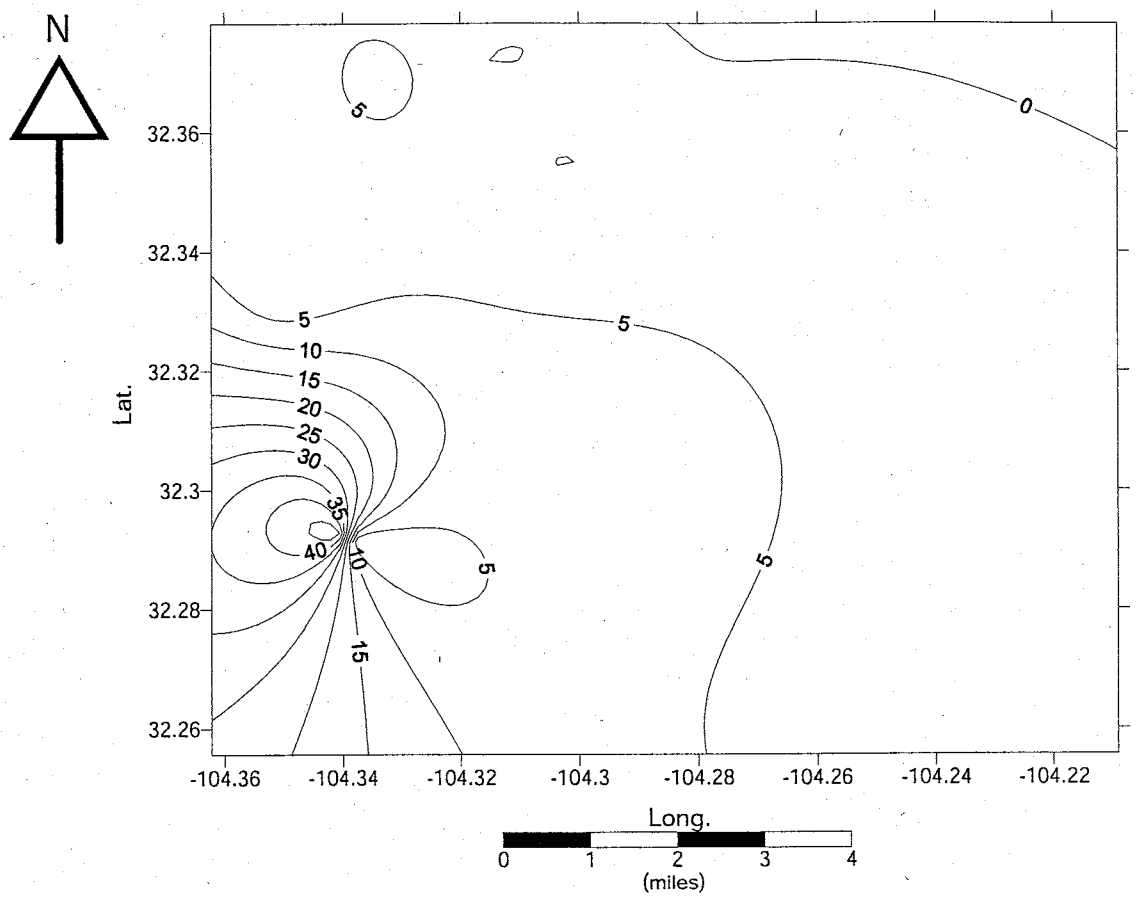

Western area isopach of sands with over 15% porosity, C unit. (Contour interval 5ft)

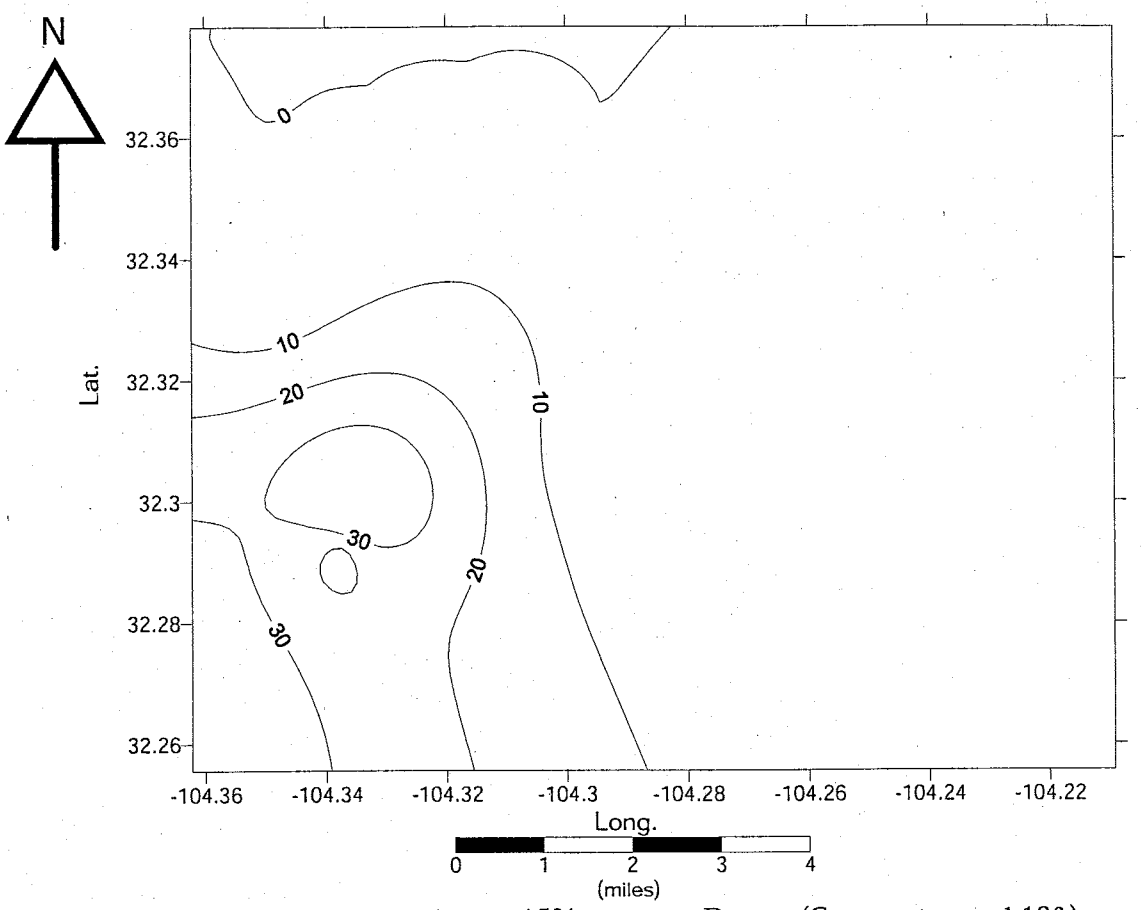

Western area isopach of sands with over 15% porosity, D unit. (Contour interval 10ft)

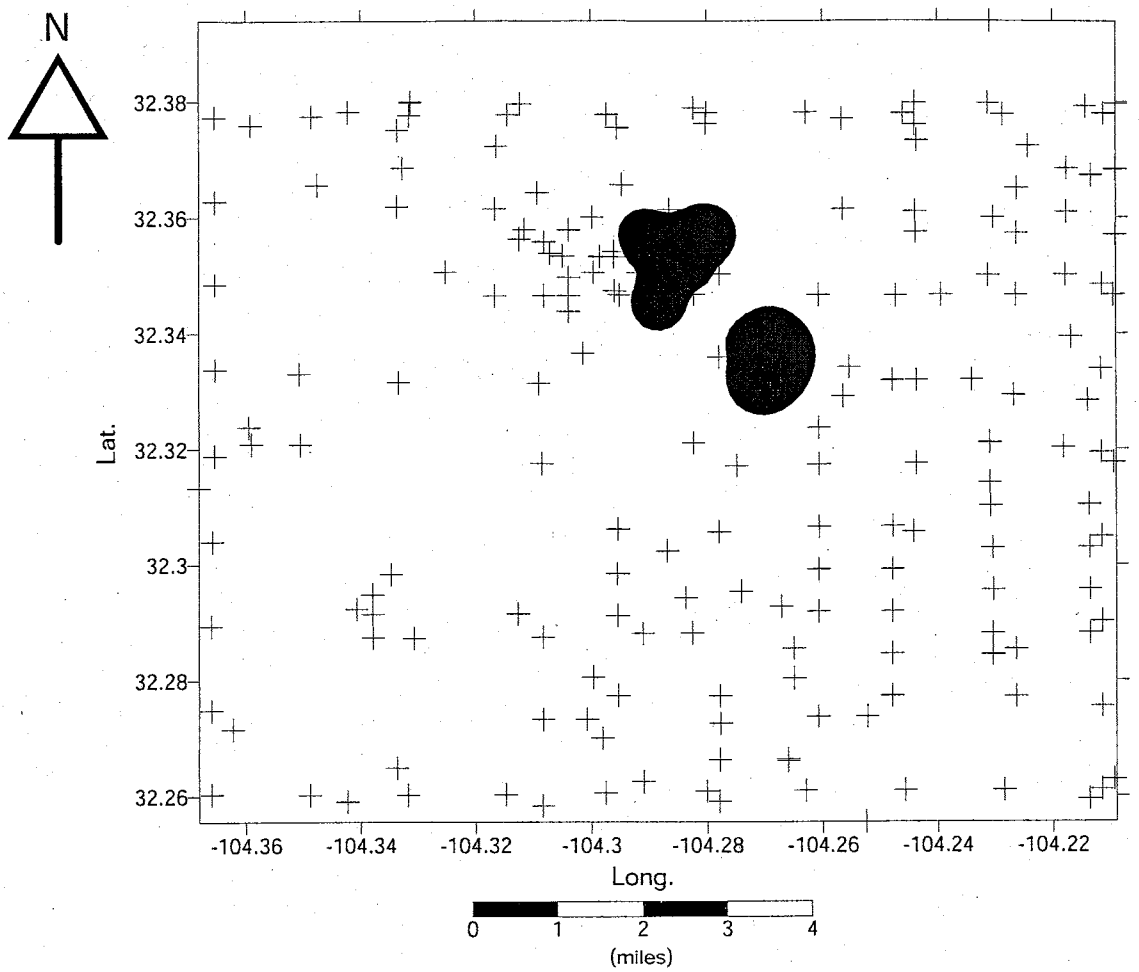

Western area hydrocarbon production with well locations.

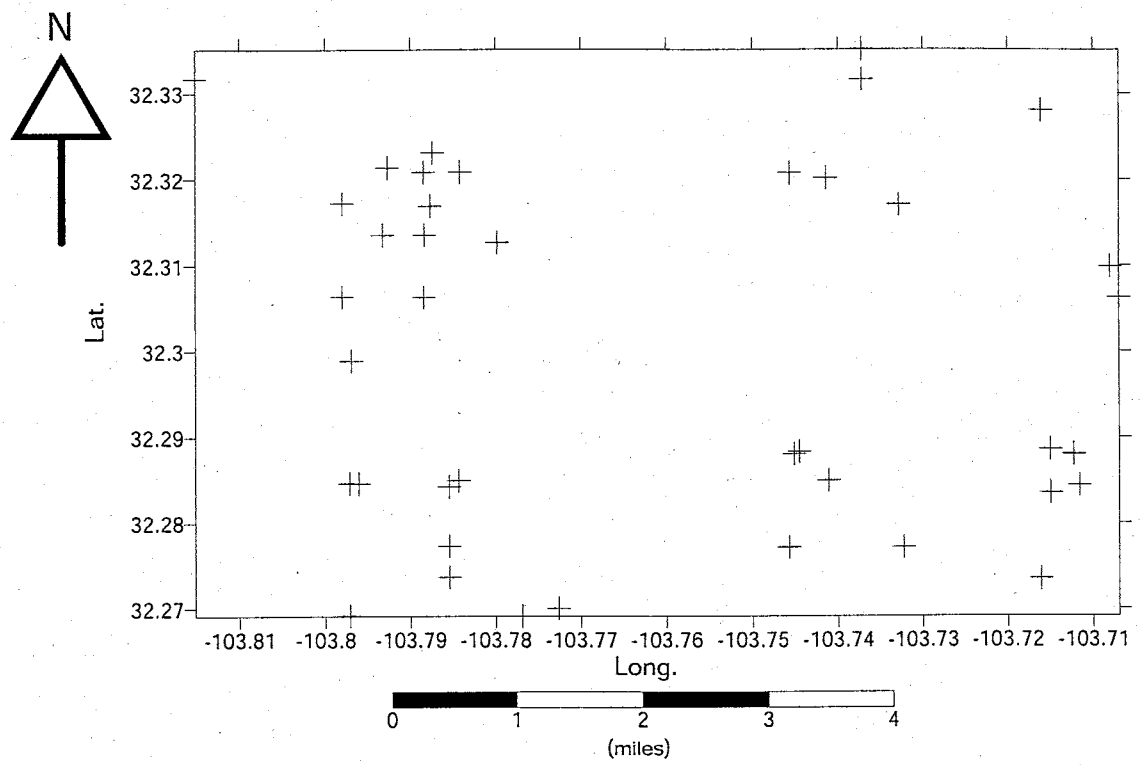

Eastern area well locations for structure and isopach maps.

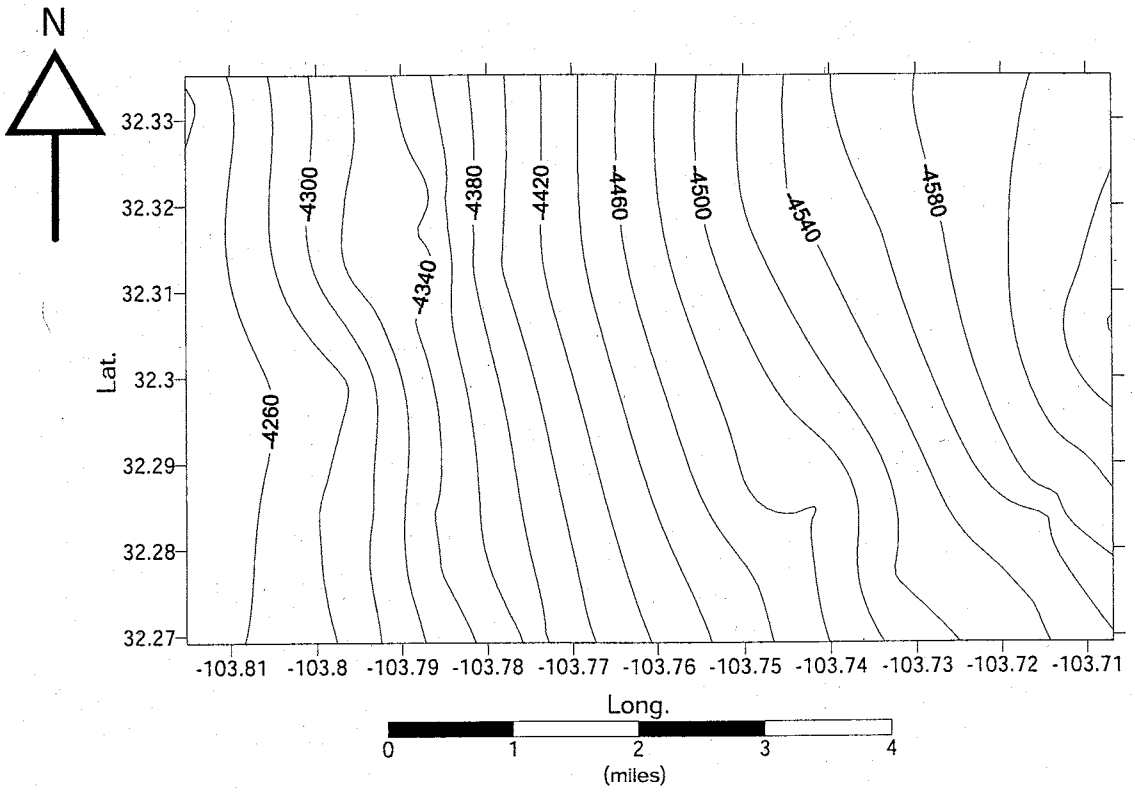

Eastern area structure, top of A unit (Contour interval 20ft.)

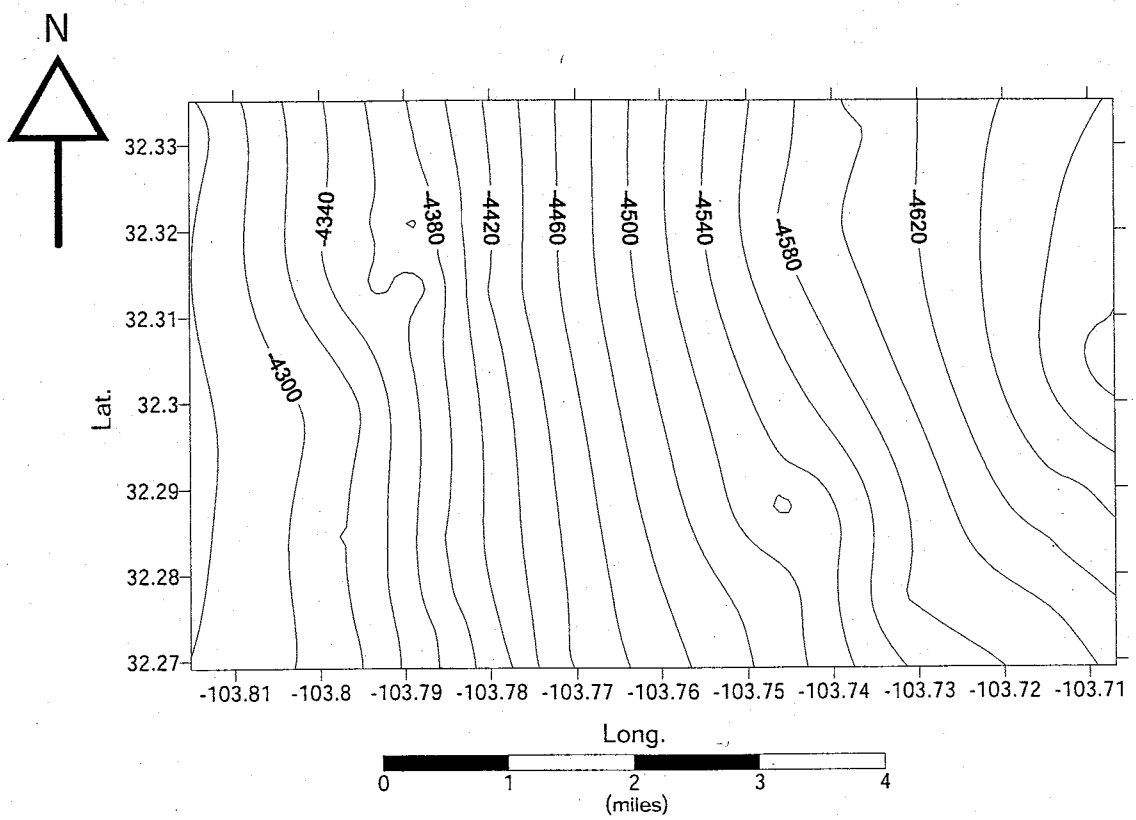

Eastern area structure, top of B unit. (Contour interval 20ft)

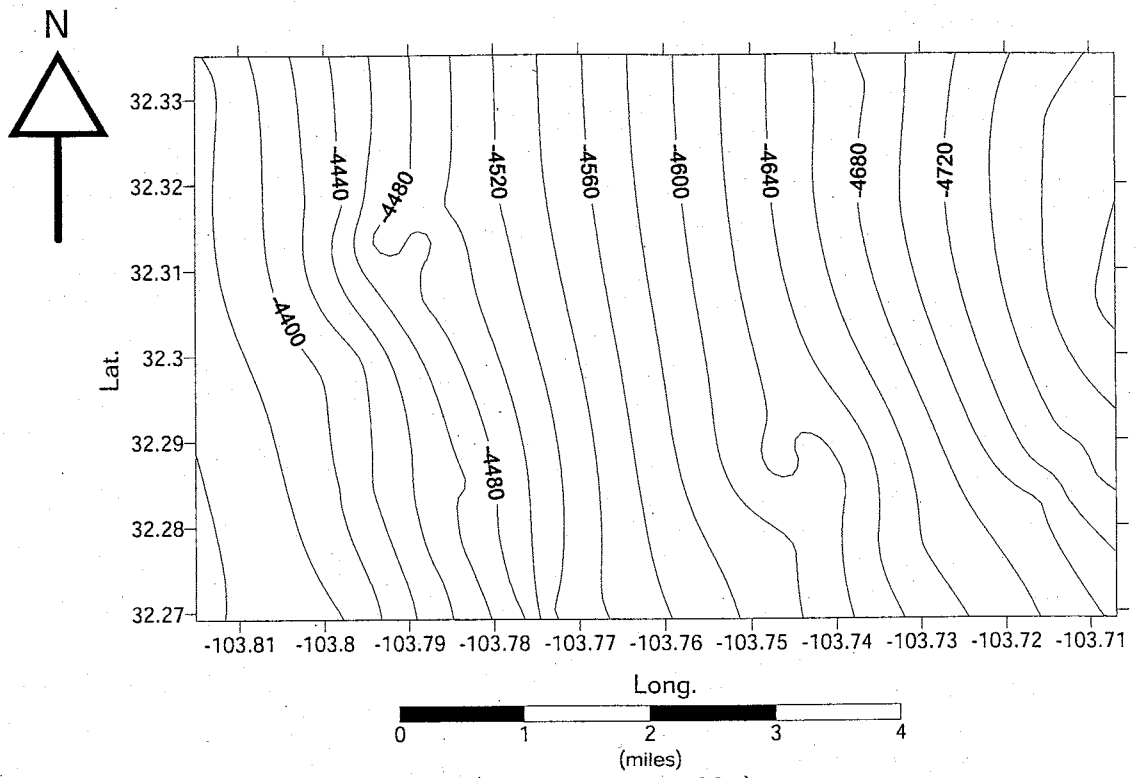

Eastern area structure, top of C unit. (Contour interval 20ft)

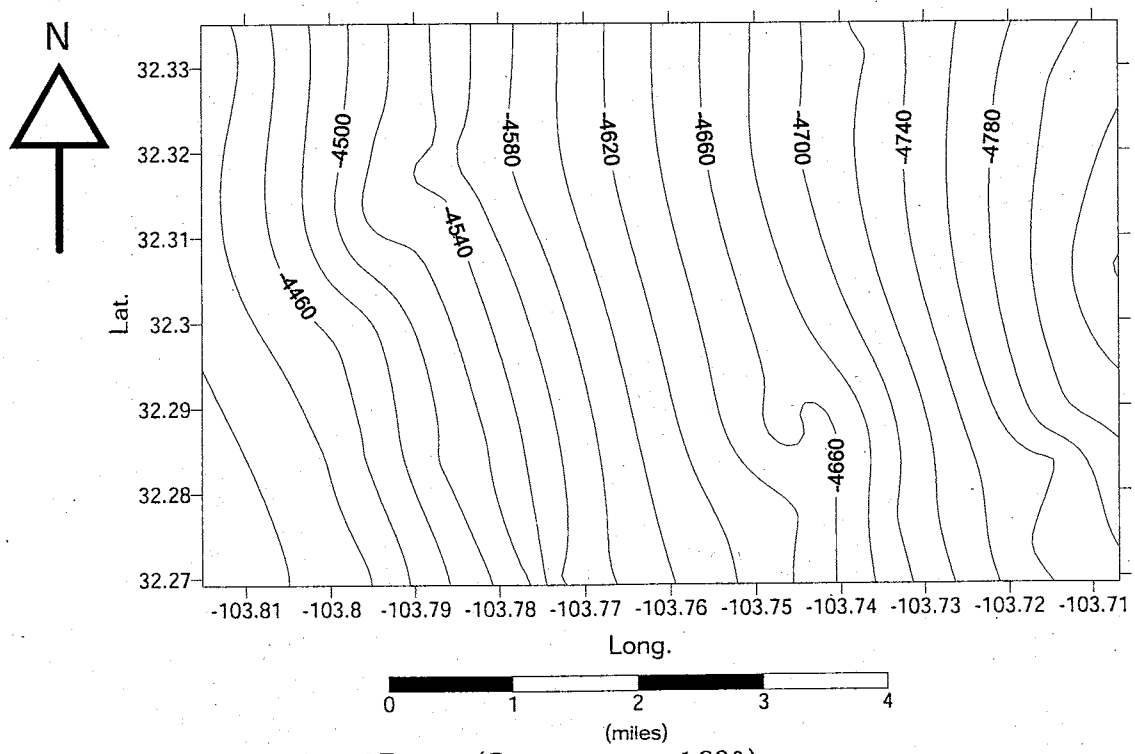

Eastern area structure, top of D unit. (Contour interval 20ft)

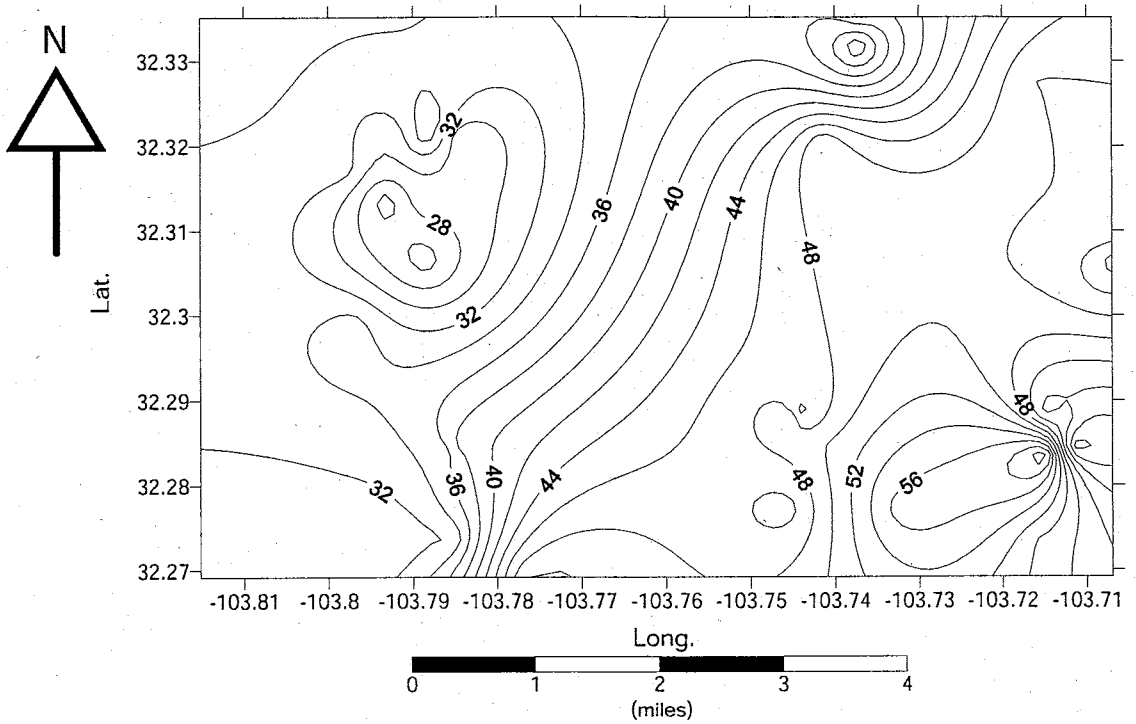

Eastern area isopach, A unit. (Contour interval 2ft)

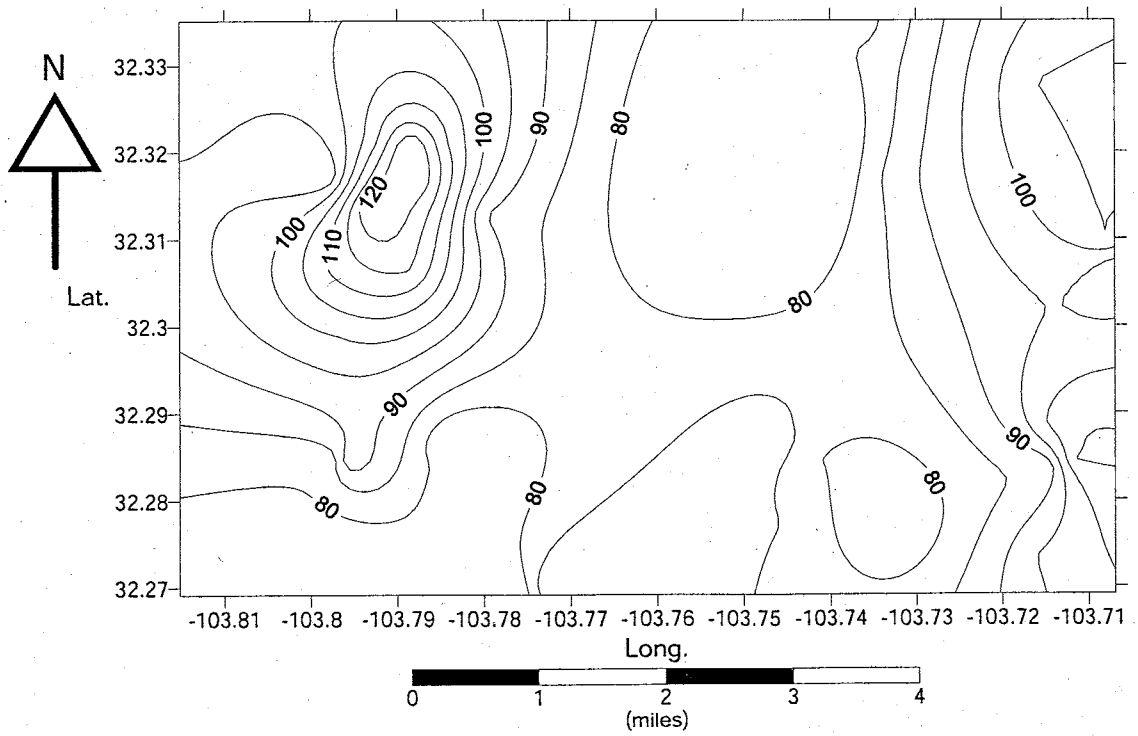

Eastern area isopach, B unit. (Contour interval 5ft)

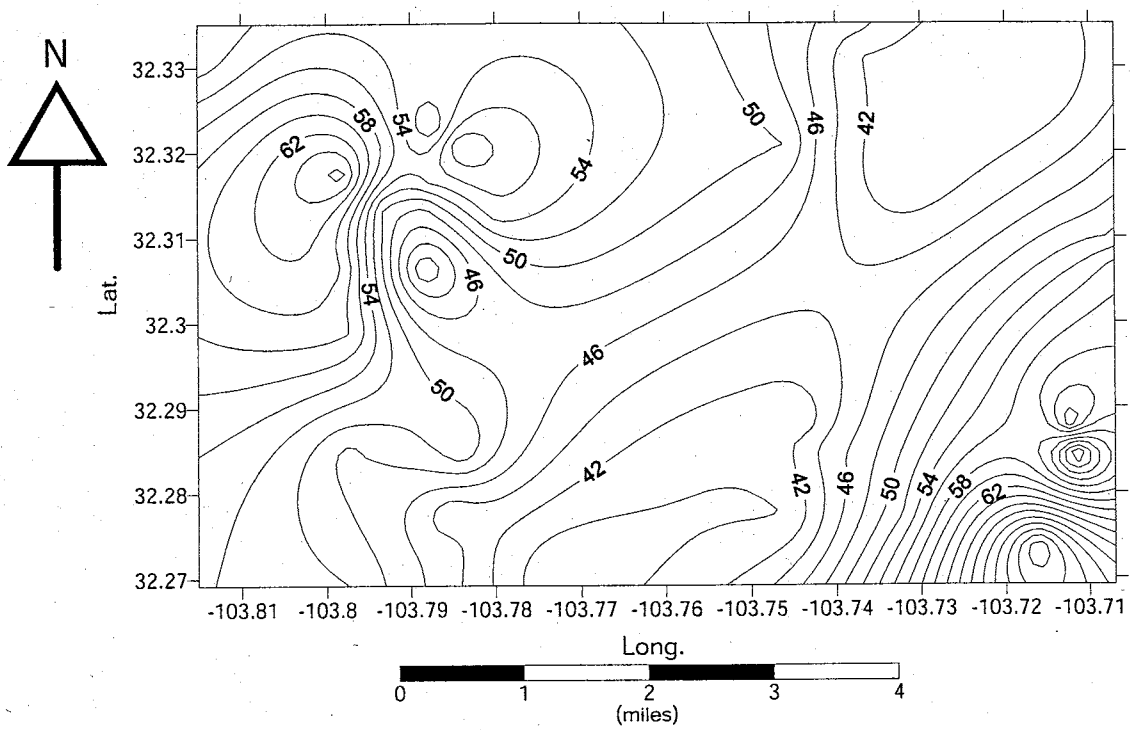

Eastern area isopach, C unit. (Contour interval 2ft)

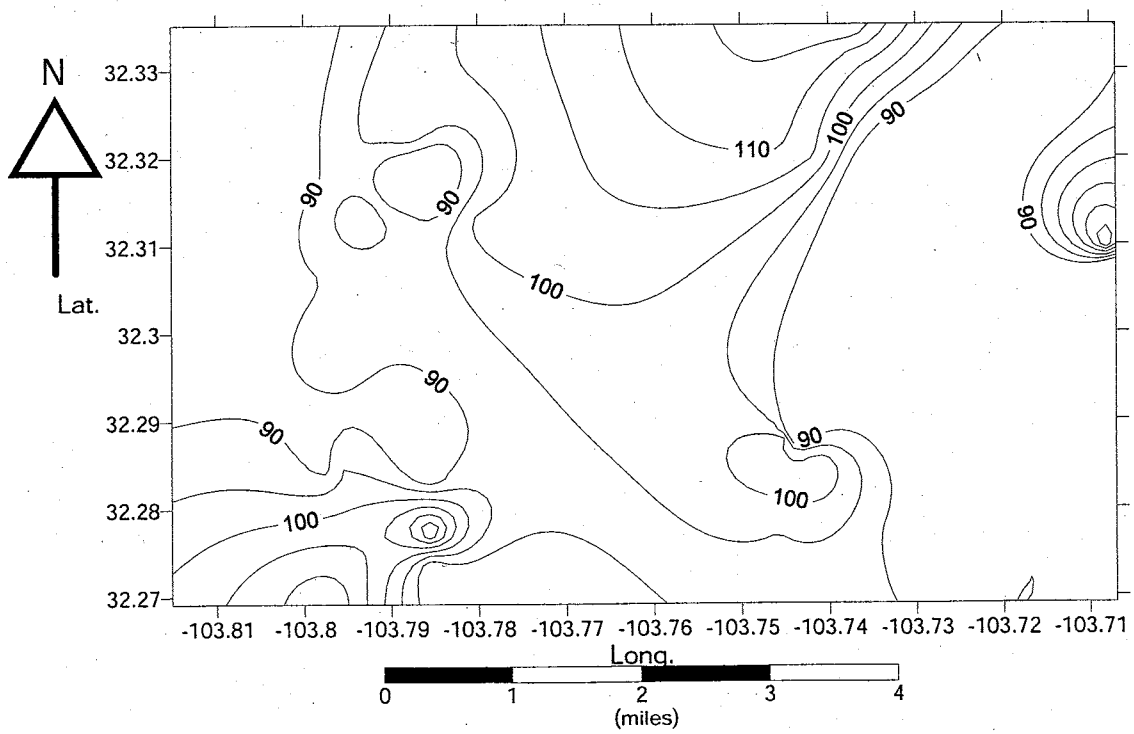

Eastern area isopach, D unit. (Contour interval 5ft)

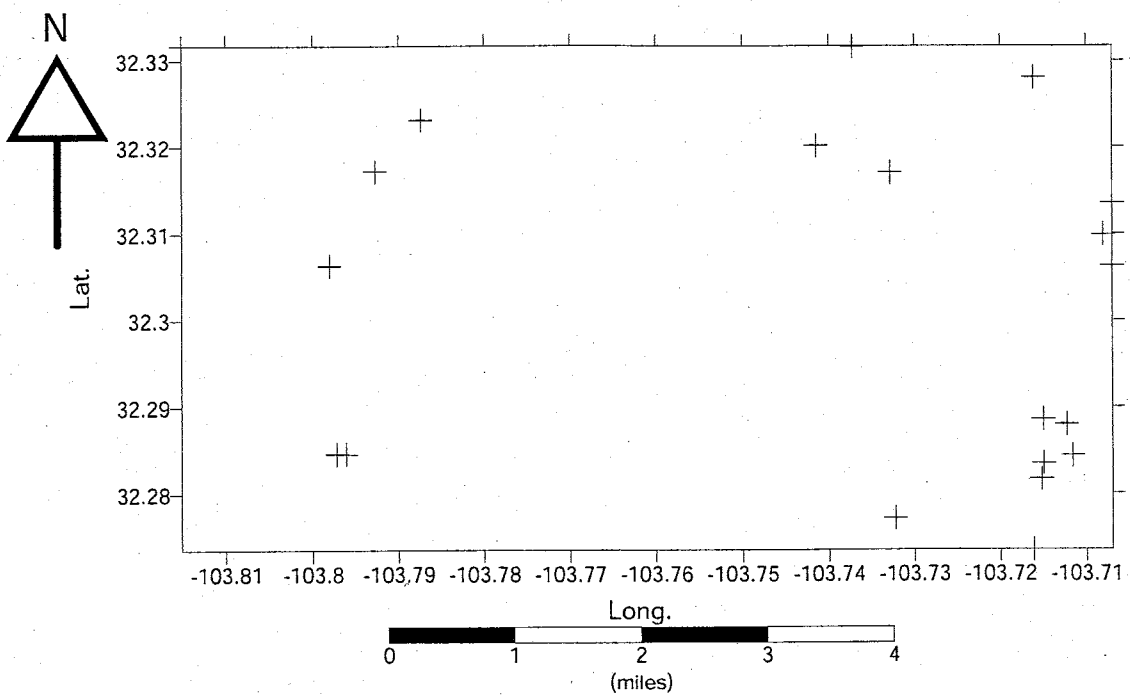

Eastern area well locations for porosity maps.

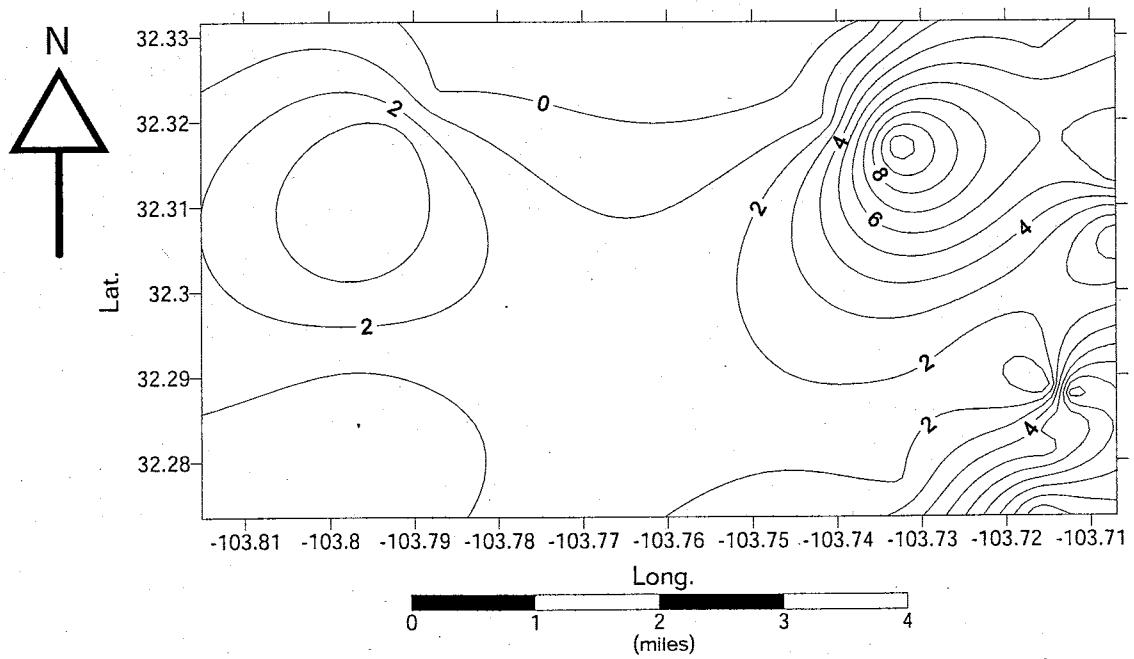

Eastern area isopach of sands with over 15% porosity, A unit. (Contour interval 1ft)

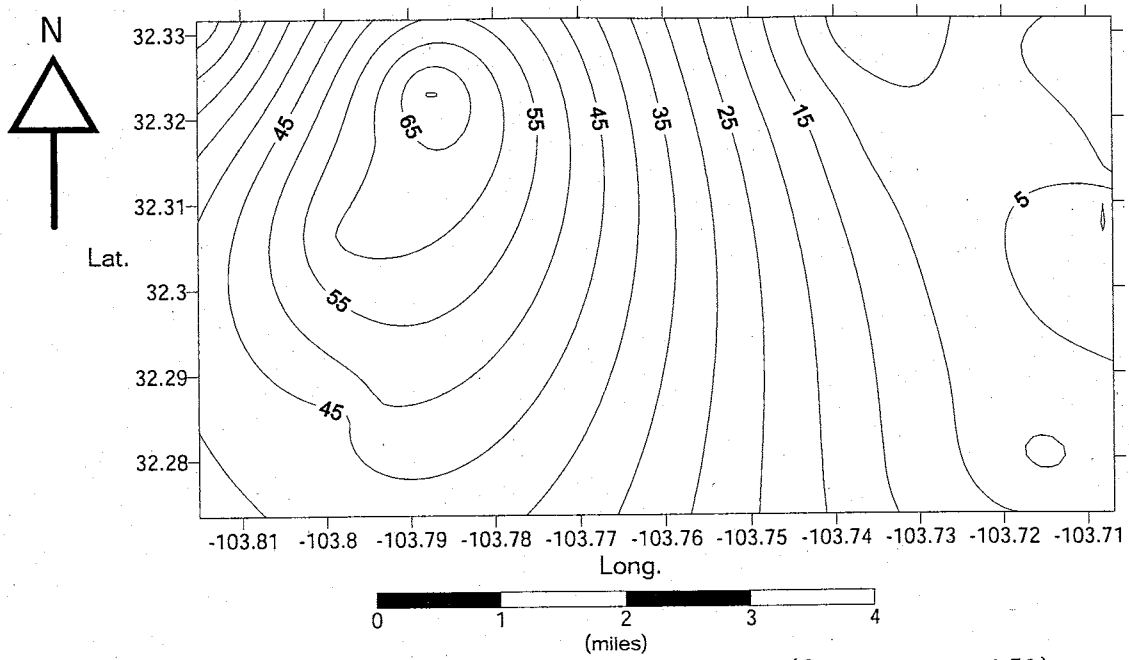

Eastern area isopach of sands with over 15% porosity, B unit. (Contour interval 5ft)

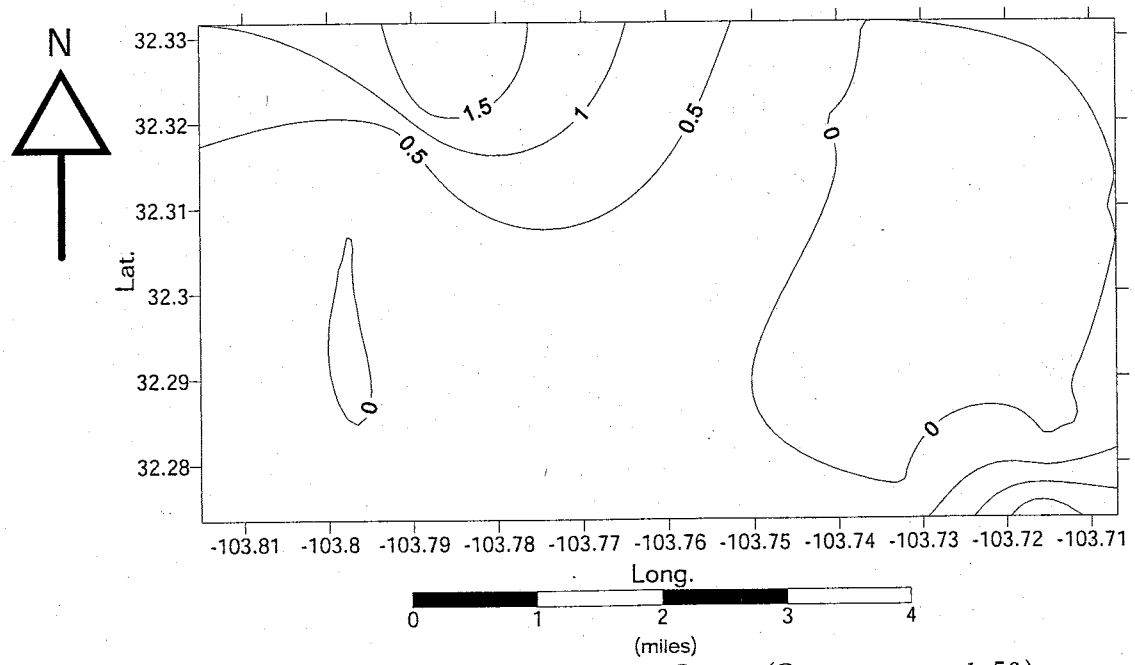

Easter area isopach of sand with over 15% porosity, C unit. (Contour interval .5ft)

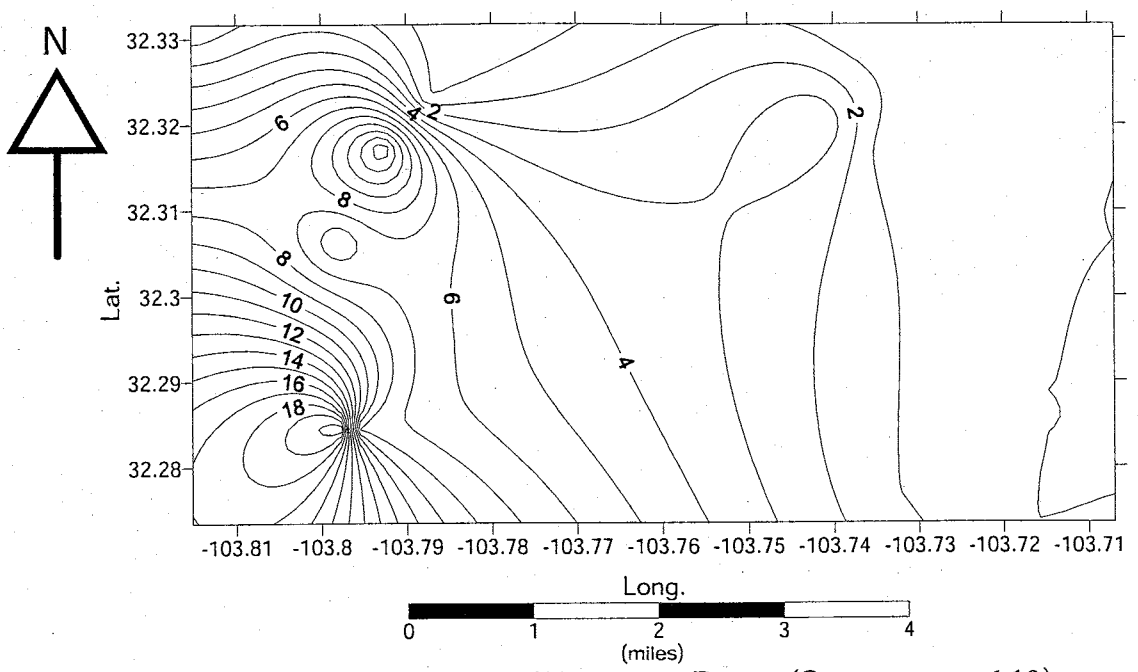

Eastern area isopach of sands with over 15% porosity, D unit. (Contour interval 1ft)

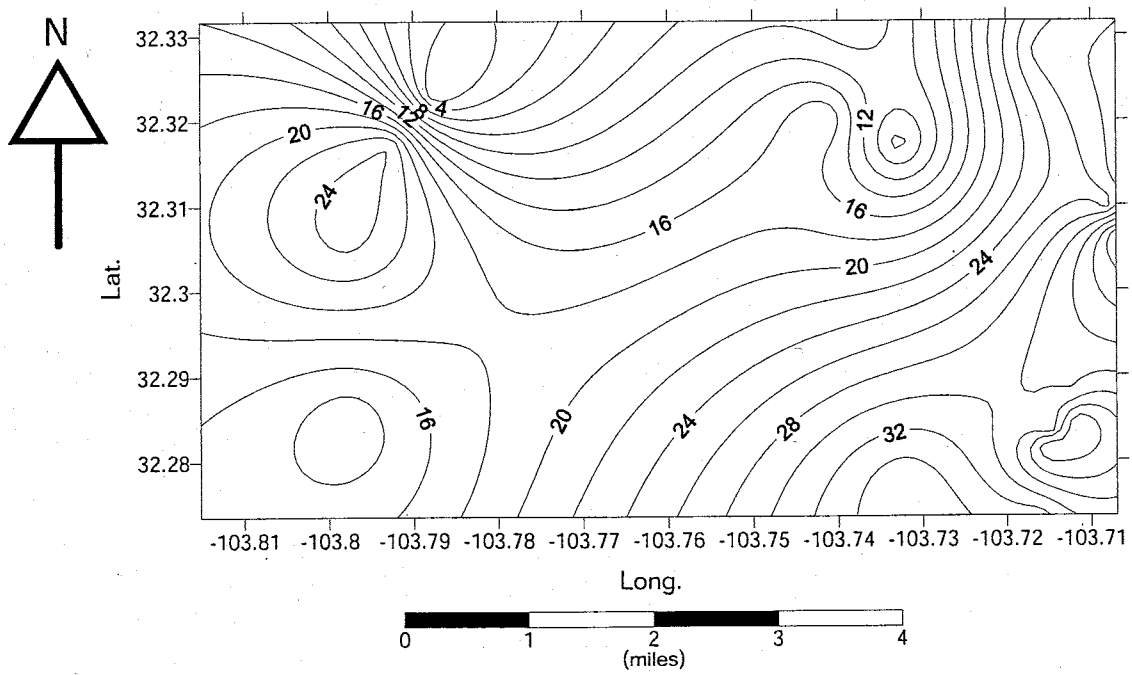

Eastern area net sand thickness, A unit. (Contour interval 2ft)

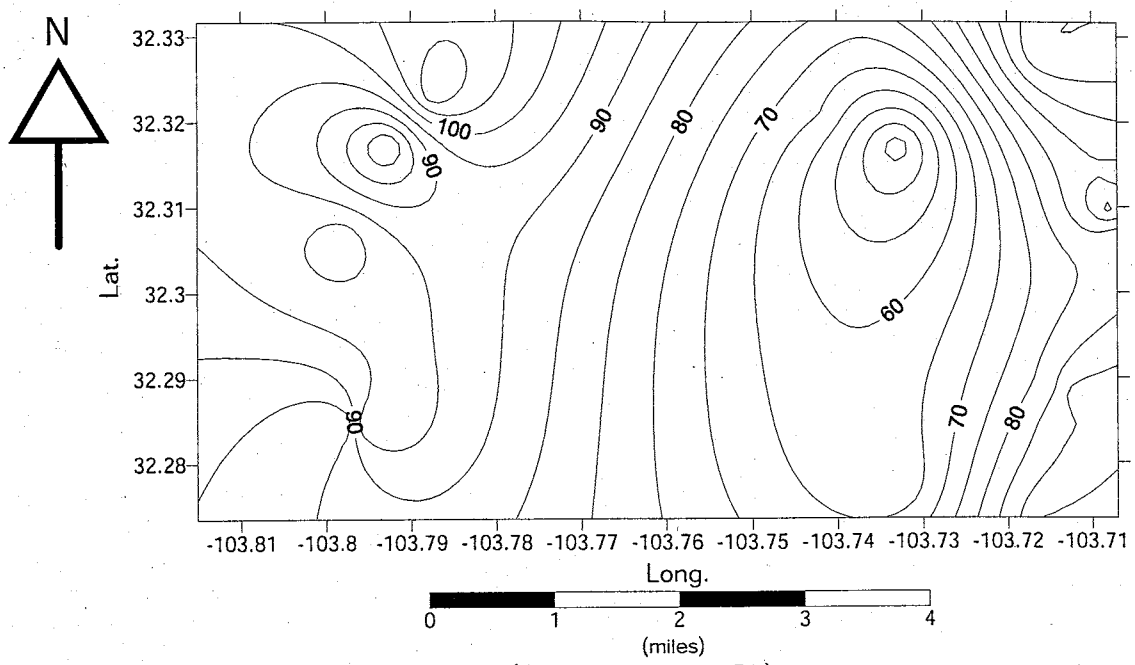

Eastern area net sand thickness, B unit. (Contour interval 5ft)

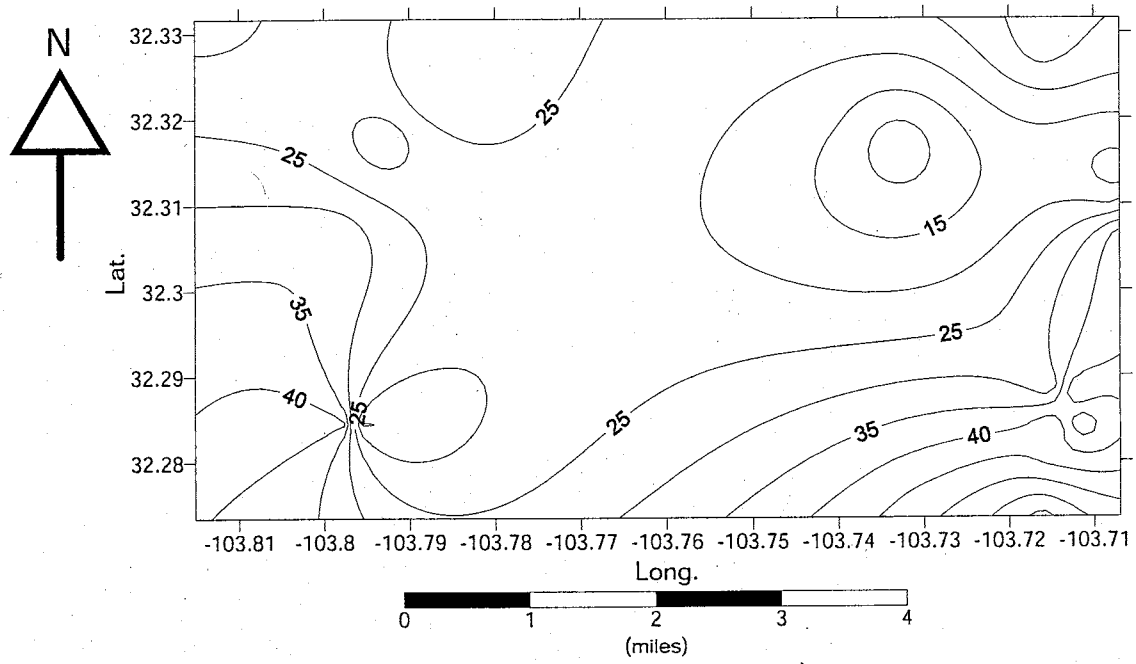

Eastern area net thickness of sand, C unit. (Contour interval 5ft)

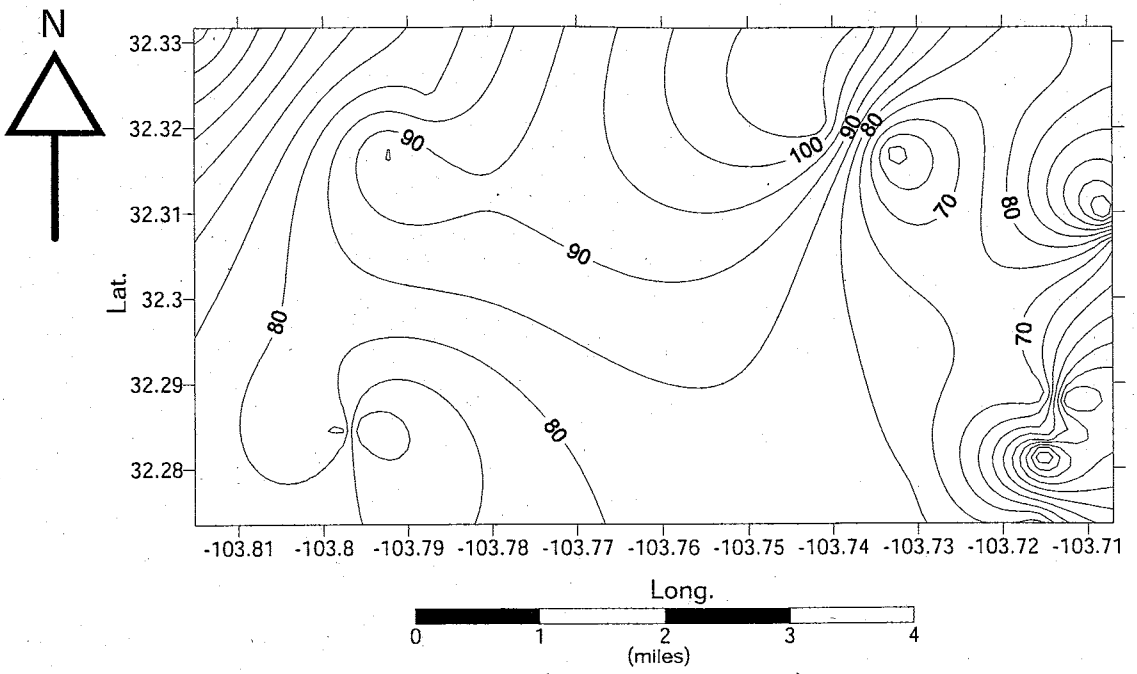

Eastern area net thickness of sand, D unit. (Contour interval 5ft)

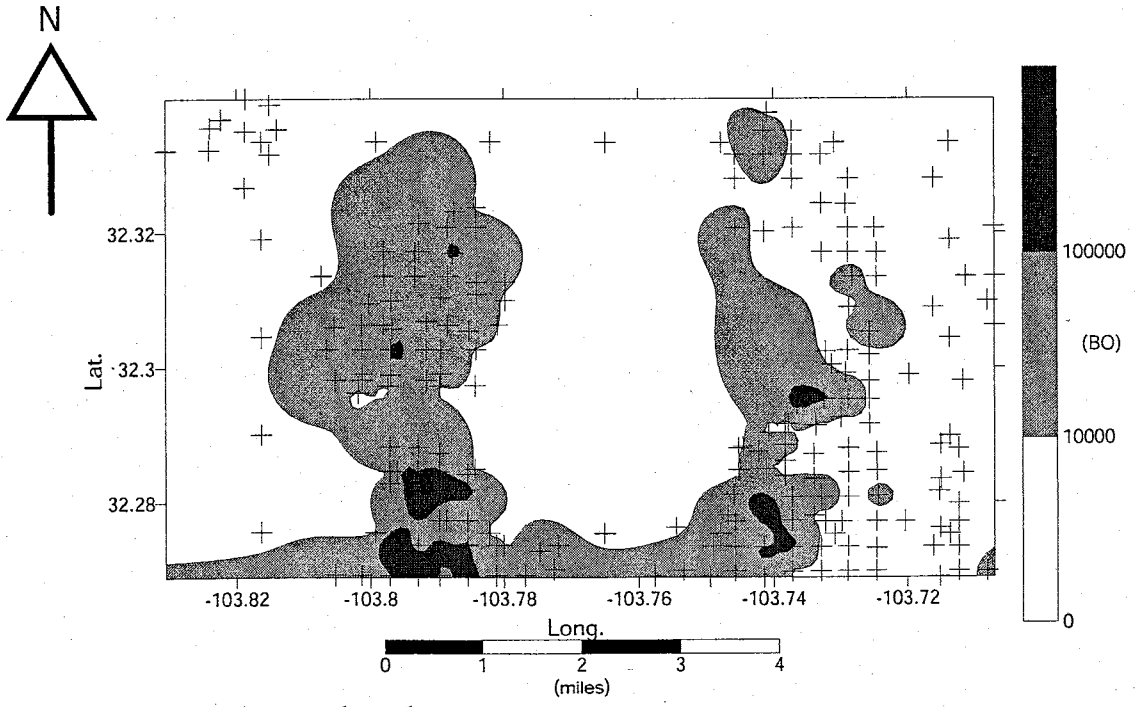

Eastern area cumulative oil production

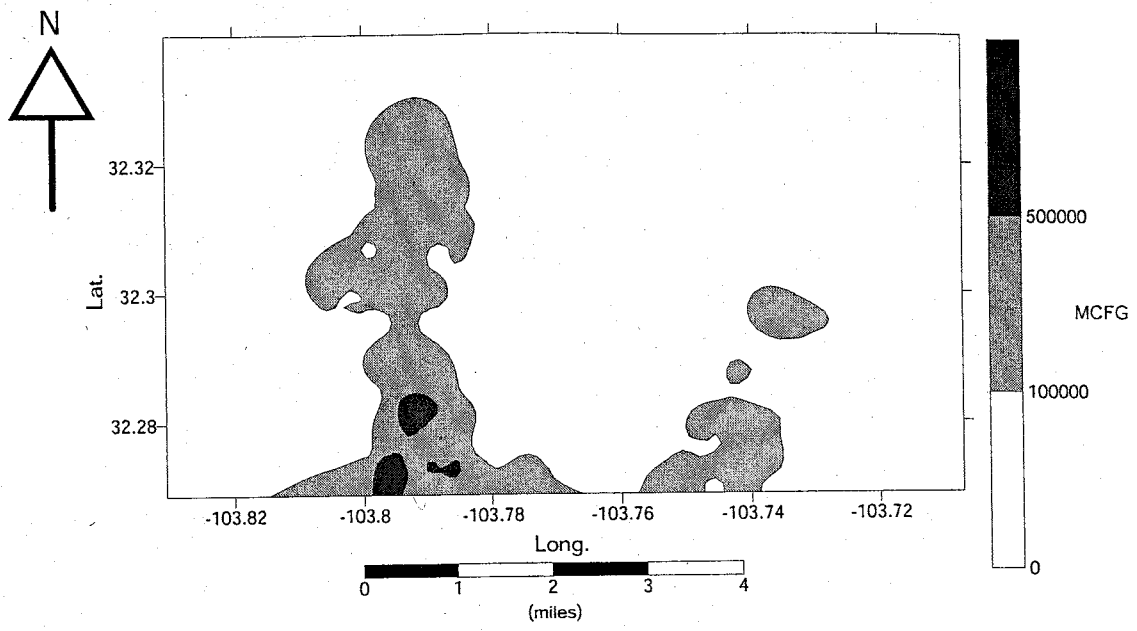

Eastern area cumulative gas production

APPENDIX IV

POROSITY AND PERMEABILITY IN SANDSTONES

Porosity refers to the void space within a rock. In sandstones porosity refers to the space between individual grains, and the pore throats connecting these spaces together. Permeability is described as a measure of the ability of a rock to transmit fluids from one point to another. Permeability is primarily controlled by how well individual pores are in contact with each other. In many cases porosity and permeability compliment each other, high porosity yields high permeability. In certain cases this is not true, for example, clay has very high porosity often up to 60% but its permeability is very small 10^{-6} -10^{-3} darcys. However in sandstones permeability tends to increase with porosity (Fetter, 1994). Porosity and permeability play a very important role in the trapping, accumulation, and eventual production of hydrocarbons.

Reduction of porosity and permeability greatly affects a rocks ability to produce hydrocarbons. Porosity and permeability of sandstones can be reduced in several ways. In general the most common of these is the cementation of the sand grains most often by carbonates, or by clay minerals. Both types of cements may be either detrital or authogenic, however carbonate cements tend to be authogenic. According to North, (1985) clay minerals greatly affect the porosity of a sandstone by their ability to adsorb and retain water, thus lowering the permeability and therefore not enabling hydrocarbons to migrate into the pores. Clay minerals also reduce pore space by filling in pore throats and "choking" the rock. This not only decreases pore size but also greatly reduces permeability two fold. The "choking" of the pore throats increases the sinuosity of the

pores and increases the capillary pressures within the pores. This effect could render the pores useless; any hydrocarbons that may be present would not be able to be produced.

Carbonate cements also have a large role in the reduction of porosity and permeability. These cements, which include carbonate mud, and calcite often precipitate within the pores. This reduces the amount of pore space available and therefore reduces the permeability as well (North, 1985).

Another method of reducing porosity in sandstone is through compaction. This is generally related to deep burial of the rock and the size, shape and composition of the sandstone. More immature sandstones that have a high amount of ductile grains such as shale, glauconite, and feldspar tend to loose porosity at shallower depths with compaction than those composed mainly of quartz. The ductile minerals tend to flow into the pore spaces during compaction (North, 1985).

This thesis is accepted on behalf of the
Faculty of the Institute by the following committee:

Advisor

11/18/02
Date

I release this document to the New Mexico Institute of Mining and Technology.

Student's Signature

12/6/02
Date